Theme 4. New materials for use in mixed structures

THEME 4

New Materials for Use in Mixed Structures

Nouveaux matériaux utilisés dans la construction mixte

Neue Baustoffe für Misch- und Verbundbauweisen

Leere Seite
Blank page
Page vide

Fiber Reinforced Plastic Bridges in Chongqing

Passerelles renforcées de fibres à Chongqing

Glasfaserverstärkte Brücken in Chongqing

Robert BRUCE
Boh Professor
Tulane University
New Orleans, LA, USA

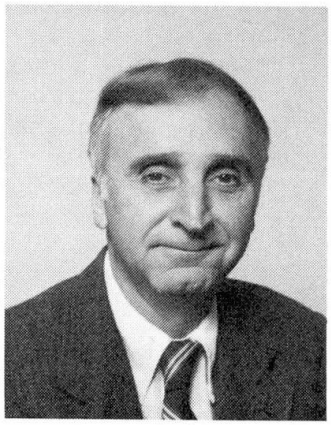

Robert Bruce, born in 1930, earned the PhD. at the University of Illinois, and is the Chairman of the ACI-ASCE Committee on Prestressed Concrete.

SUMMARY

The Pedestrian Cable-Stayed Bridge and the Guanyinqiao Pedestrian Bridge in Chongqing are a unique combination of high strength steel and reinforced concrete with glass reinforced plastic. This paper is a brief report in which the physical characteristics of the bridges are described.

RÉSUMÉ

La passerelle piétonne haubanée et la passerrelle piétonne du Guanyinqiao à Chongqing offrent un exemple unique d'emploi d'acier à haute résistance combiné au béton armé avec apport de matière plastique renforcée par fibres de verre. Cet article vise a décrire les caractéristiques techniques de ces passerelles.

ZUSAMMENFASSUNG

Die Schrägseilfussgängerbrücke und die Guanyinqiao-Fussgängerbrücke in Chongqing sind einzigartige Kombinationen von hochfestem Stahl und glasfaserverstärktem Beton. Dieser Bericht beschreibt die physikalischen Eigenschaften dieser Brücken.

1. INTRODUCTION

Through the efforts of Mr. Chen Kesheng, Senior Engineer, and Madame Cheng Liping, Deputy Chief Engineer of the China Highway and Transportation Society; the author was invited to inspect two of the three fiber reinforced plastic bridges in Chongqing. Both of the bridges were conceived and built by The Research Institute of Composite Material Bridges of the Chongqing Institute of Transportation.

It is noted that this paper pertains to work done by others, and that the author did not participate in the projects reported. The paper is a "trip report" which provides information on an innovative use of FRP (GRP) material in bridges. Much information pertaining to mechanical properties of the materials, technical details of the design, and methods of fabrication and erection, were not available to the author; and thus the paper is limited to the brief descriptions provided. In the case of the first bridge described, some technical information was provided by Mr. Tang Guodong of the Composite Material Bridge Institute in Chongqing.

2. GRP PEDESTRIAN CABLE-STAYED BRIDGE

The first bridge visited was the GRP Pedestrian Cable-Stayed Bridge joining two parts of the campus of the Chongqing Institute of Transportation. The bridge was completed in 1986, and is shown in Fig. 1.

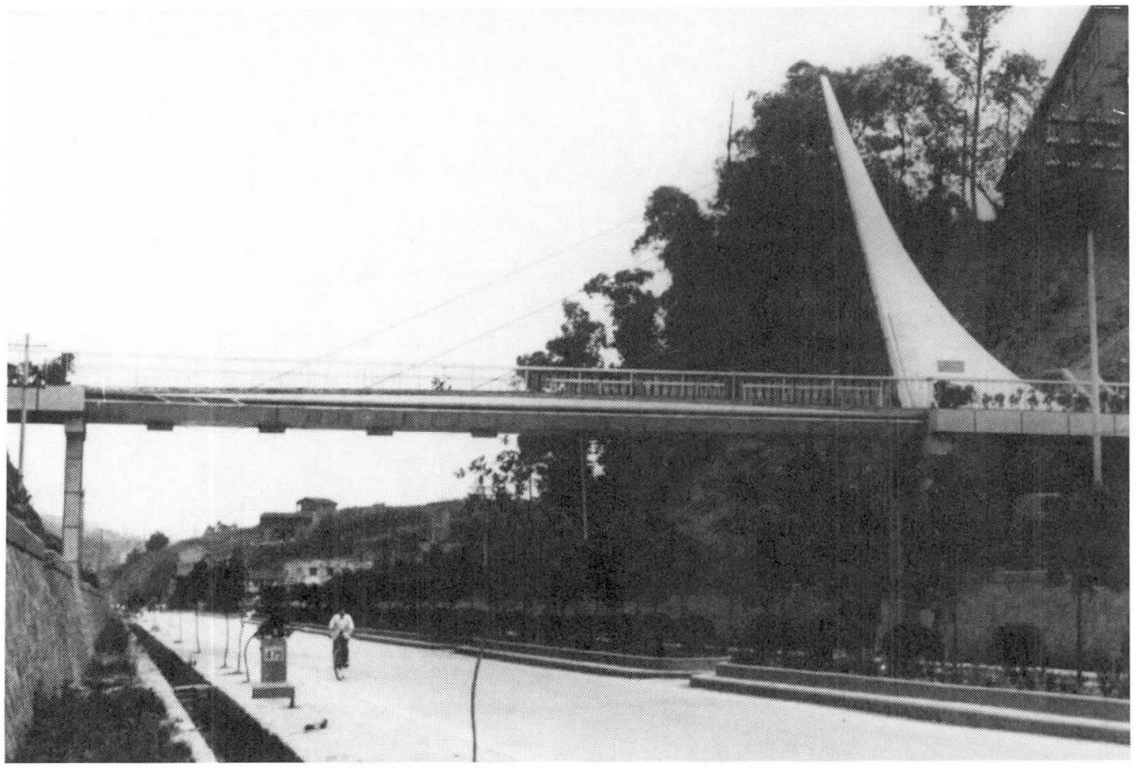

Fig. 1 GRP Pedestrian Cable Stayed Bridge

The layout of the bridge is an unsymmetrical system having a single tower and a single harped array of cable stays. The side spans and the tower are of reinforced concrete, with the tower having a height of 11m and an inclination of 15^{o} from the vertical. Each of the seven cable stays consists of 19 No. 5 steel wires encased in a polyethylene tube.

The entire length of the bridge is 50m which includes a non-continuous main span and two side spans. The main span consists of a single FRP box girder with cover plates. The FRP girder is 27.4m long, and 4.3m wide. The weight of the FRP girder is approximately 8 tons. The cost of the single FRP box girder was 120,000 yuan, or approximately 45% of the total cost of the project. The total cost of the completed structure, including a test program, was 260,000 yuan for a unit cost of 1,000 yuan per square meter. To translate the unit cost into dollars would result in a range between $25 per square foot and $13 per square foot, depending on the exchange rate used.

Complete technical information regarding bridge design, materials, and con struction, was not available at the time of inspection; however, limited information has been provided related to the glass fiber reinforced plastic, and related to design criteria.

The GRP is composed of high strength plastic reinforced with glass fiber. The bond between the fiber and the plastic is enhanced by the use of a resin. The high strength plastic is referred to as a plastic resin. Some of the physical properties of the GRP were provided.

The structural stiffness (EI and GI) is dependent on material parameters and member cross-section. Although the physical stiffness of the material (E, G) is less than that for concrete or steel, the stiffness of individual structural members can be increased by increasing the geometric stiffness in terms of moment of inertia of the cross-section. Values of elastic modulus (E, G) can be increased by the proper choice of fiber orientation.

The FRP box girder used in the GRP Pedestrian Cable-Stayed Bridge consisted of a top and bottom flange, and five vertical webs. The arrangement of fiber reinforcement in the webs could be placed at an angle of 45^{o} in order to provide increased shear resistance to shear stresses, thus improving the strength and stiffness of the laminated sections used in the box girder. This predetermined arrangement of the fiber reinforcement can result in a material having anisotropic properties. These anisotropic properties must be considered in design. In the case of fiber reinforcement placed in a longitudinal direction only, physical properties may be determined.

The elastic modulus of the GRP in tension and compression are given, respectively, in equation (1) and (2).

$$E_o = E_f \cdot V_f + E_m \cdot V_m \qquad (1)$$

$$E_o = E_f \cdot V_f + E_m (1 - V_f) \qquad (2)$$

where

E_o = modulus of GRP

E_m = modulus of plastic resin

E_f = modulus of glass fiber

V_m = percentage content of resin

V_f = percentage content of fiber

The specific gravity of the GFP is between 1.4 - 2.2. For the GRP reinforced in a longitudinal direction only, the tensile strength is 10,000 kg/cm^2.

Design criteria included a design live load of 350 kg/cm^2; with a factor of safety of 10 for direct stress, and a F.S. between 3 and 6 for shear stress. The allowable deflection is L/600. The highest design temperature under service conditions is 70^{o}C.

The FRP box girder was fabricated in the New Material Factory of Wuhan Industry University. The box girder was transported and erected in one piece. The bridge was tested under combinations of dead load and live load. The completed bridge was reviewed by the PRC Ministry of Communications, the agency responsible for transportation. About 40 experts of highway, railway, material and urban construction took part in the review.

The review indicated that the cost of the FRP bridge is less than the cost of the same bridge in steel, and that the FRP bridge is maintenance free. This GRP Pedestrian Cable-Stayed Bridge is the first in the world, and the design may be used for the pedestrian bridges of cities in China

3. GUANYINQIAO PEDESTRAIN BRIDGE IN CHONG QING

The second bridge visited was the Guanyinqiao Pedestrain Bridge of Jiangbei District in Chongqing. The bridge was completed in May of 1988. The bridge is described as a space frame, with FRP deck griders suspended from reinforced concrete rigid frames. The model of the bridge is shown in Fig. 2.

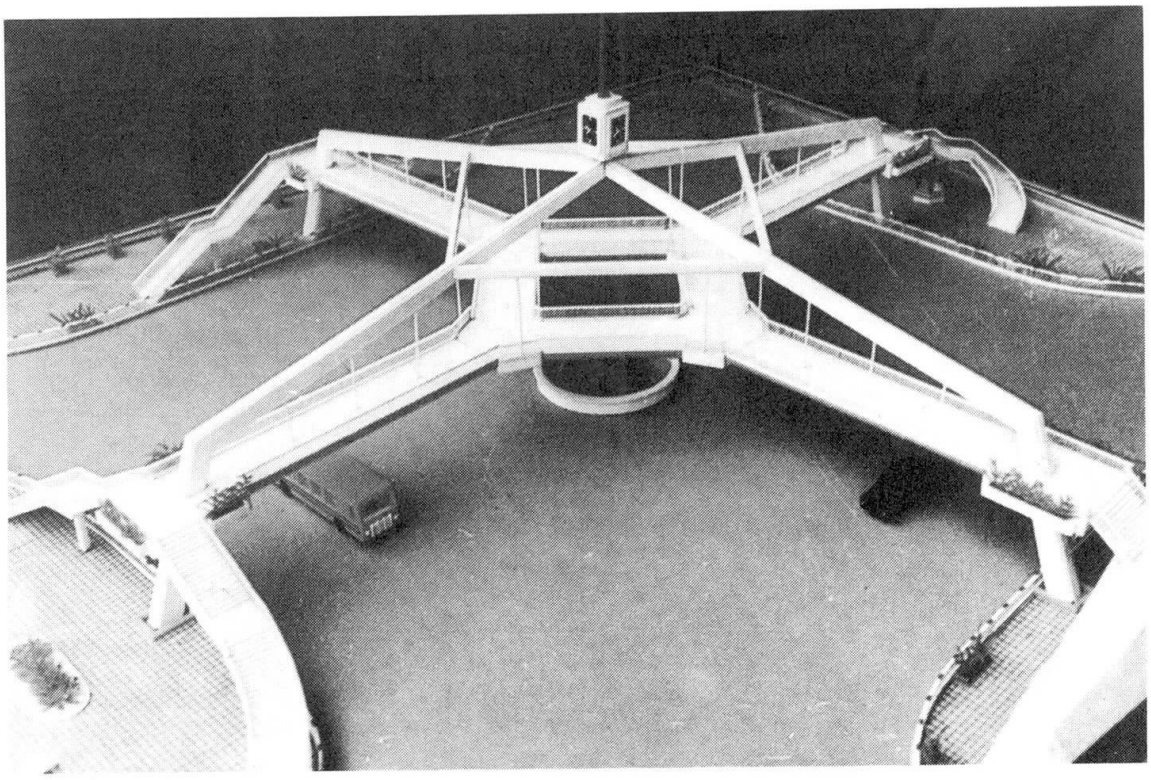

Fig. 2 Model of Guanyinqiao Pedestrian Bridge

The bridge crosses an intersection of two main streets in downtown Chongqing. The structural layout is in the shape of an ancient Chinese coin. The span of the rigid frame is 70m, with the overall total length of the bridge equal to 157 m. The four long FRP girders are 19 m long. The four FRP girders forming the central geometry are 9m long. All eight FRP girders are 4.3m wide, and 0.9m deep. All girders are hung from the space frames by

high strength wire. Total weight of the FRP girders was 43 tons, with the 19m girders each weighing 7.29 tons and 9m girders each weighing 3.46 tons. The cost of the FRP girders in place represented 42% of the total cost of the completed project. The total cost of the project was 1,700,000 yuan. This amount converts to $485,000 to $243,000 depending on the exchange rate used.

The complete bridge in service is shown in Fig. 3.

Fig. 3 Guanyinqiao Bridge in Service

The FRP girders were fabricated in Chongqing Glass Fiber Product Factory then transported and erected in single pieces. Those responsible for the design and construction of the FRP bridges in Chongqing have indicated certain characteristics of FRP bridges as follows:

1. Cost of FRP bridges is less than steel bridges of same type.
2. There is no rusting problem, and maintenance is minimized.
3. Tests indicate that the FRP structure is maintenance free for 40 years, except in especially bad environment. Tests indicate that is it unnecessary to worry about the problem of life span for FRP bridges.
4. FRP has good properties for resisting fatigue and low energy impact.
5. FRP is easy to form and to color.

Attempts are being made to obtain additional technical information on the GRP bridges in China, including the vehicular bridge in Beijing. When such information is received, it will be incorporated into an expanded version of this report.

REFERENCES

1. Guodong, Tang, Analytical and Experimental Work of GRP Cable-Stayed Pedestrian Bridge. Composite Material Bridge Institute, Chongqing, China.

Polymer Impregnated-Steel Fiber Reinforced Concrete

Béton renforcé de fibres d'acier imprégnées et polymérisées

Imprägnierter und polymerisierter stahlfaserbewehrter Beton

Corneliu BOB
Assoc. Professor
Polytechnical Inst.
Timisoara, Romania

Corneliu Bob, born 1939, received his Civil Engineering degree and doctorate at the Polytechnical Institute of Timisoara, Romania. He has been involved in research on new special concrete types and reinforced concrete as well as in design and analysis of building structures.

Maria ROSU
Lecturer
Polytechnical Inst.
Timisoara, Romania

Maria Rosu, born 1938, received her graduate in chemistry at the Polytechnical Institute of Timisoara, Romania. She has been principally involved in research and development on building materials.

Iosif BUCHMAN
Lecturer
Polytechnical Inst.
Timisoara, Romania

Iosif Buchman, born 1948, received his Civil Engineering degree and doctorate at the Polytechnical Institute of Timisoara, Romania. He has been primarily involved in research on concrete structures.

SUMMARY

The investigation reported in this paper had the goal of developing the new composite material "polymer impregnated-steel fiber reinforced concrete". The mechanical properties, ductility and relative impermeability of this material suggest the possibility for its use in bridge deck and pavements.

RÉSUMÉ

Les recherches présentées dans cette étude ont pour but d'étudier un nouveau matériau de construction « Béton renforcé de fibres d'acier imprégnées et polymérisées ». Les propriétés mécaniques, la ductilité, ainsi que la relative imperméabilité de ce matériau le rend apte à la construction des tabliers de ponts et pour les surfaces de roulement.

ZUSAMMENFASSUNG

Der Zweck dieser Arbeit ist die Untersuchung eines neuen imprägnierten und polymerisierten stahlbewehrten Betons. Die mechanischen Eigenschaften, die Duktilität und relative Wasserdichte dieses Materials, unterstreichen die Möglichkeit der Verwendung für die Fahrbahn von Brücken und als Strassenbelag im Allgemeinen.

1. INTRODUCTION

Fiber reinforced concrete is essentially a composite system in which, unlike conventional reinforced concrete, the material as a whole carries the tensile and compressive stresses due to load. In the composite material discussed in this paper, short discrete steel fibers are randomly distributed throughout the concrete mass.

Polymer impregnated concrete (PIC) is a precast and cured hydrated cement concrete which has been impregnated with a low viscosity monomer and polymerized in-situ. The significant improvement in structural and durability properties have been obtained with PIC comparated to ordinary concrete.

The investigation reported in this paper had the goal of developing the new composite material "polymer impregnated - steel fiber reinforced concrete". The mechanical properties, ductility and relative impermeability of this material suggest the possibility of using for bridge deck and pavement.

2. LABORATORY INVESTIGATIONS

2.1. Steel fiber reinforced concrete (SFRC)

This investigation was made to determine the influence of the randomly oriented fiber on the mechanical properties and ductility of SFRC. Both plain and fiber reinforced concrete were tested. The concrete mixture consisted of : Portland cement (P40; Pa35); regular tap water; sand (0...10 mm); Romanian additive DISAN (0,3% of cement). The fiber used for the investigations were of 0.28 mm diameter, 30 mm length (aspect ratio is 107) and manufactured from low-carbon steel wire by a chopping process. The concrete specimens were reinforced with 1-1.5 % by volume. All mixings were done in a rotary mixer : sand and cement were first dry mixed (30 sec.), then the fiber were added slowly to insure random distribution; the water was then addet and all components were mixed (30 sec.).

Main characteristics of SFRC are presented in Table 1. For a wide spectrum of mechanical properties, the improvement imported by fibers is mainly dependent on fiber concentration μ (μ represent the volume reinforcement coefficient) and aspect ratio L/D (L and D are the length and the diameter of the fiber).

On the basis of the large amount of data for flexural strength analysed in [1], it was found :

$$r_1 = 1 + 0.57\mu\frac{L}{D} - 0.018\left(\mu\frac{L}{D}\right)^3 \qquad (1)$$

where r_1 is the ratio of the flexural strength of SFRC members to that of plain concrete members.

2.2. Polymer impregnated concrete (PIC)

The main steps of process techniques for producing PIC has been : fabrication of precast concrete specimens in similar way with conventional concrete; oven-drying for 24 h at 105°; saturation with monomer by immersion in methyl-methacrylate (MMA) at normal pressure and temperature; in-situ polymerization by thermal-cata-

lytic techniques at 75°C for 2 h.

Characteristics		Plain concrete	Steel fibre reinforced concrete	
			Value of characteristics	μ (%)
Flexural strength	MPa	1.98	3.38	2
Impact resistance	MPa	6.9	17.25	1
			19.12	1.5
			16.90	2
Freeze-thaw (200 cycles)	Loss of flexural strength %	18.3	4	1.5
Flexure toughness	Area under load-deflexion curve	1	14.8-23.5	2

Table 1 Main characteristics of steel fibre reinforced concretes

Main mechanical and physical properties are given Table 2 for unimpregnated and MMA-impregnated concrete polymerized by thermal -catalytic means.

Characteristics			Unimpregnated Concrete	Polymer Impregnated Concrete
Compressive strength	(R_c)	MPa	25.00	68.00
Tensile strength	(R_t^c)	MPa	2.60	11.50
Flexural strength	(R_{ti})	MPa	4.42	19.55
Modulus of elasticity	(E^t)	MPa	$3.5 \cdot 10^4$	$4.28 \cdot 10^4$
Abrasion loss	(U)	(mm)	1.00	0.48
Water absorption	(W_m)	(%)	3.0	0.40
Density	(ρ_b^m)	kg/m^3	2400	2416

Table 2 Main characteristics of polymer impregnated concrete

The efficiency of impregnation on compressive strength of PIC is defined as the difference between compressive strength of PIC and unimpregnated concrete - ΔR_c [3]. It was found [2] [3] that the efficiency of impregnation ΔR_c is an exponential relation with the polymer loading p_g (in %), as (Fig. 1) :

$$\Delta R_c = \alpha p_g^{3/2} \qquad (2)$$

where α is a numerical parameter ($\alpha_{min} = 4$; $\alpha_{midd} = 6$; $\alpha_{max} = 8$). The dependence between the efficiency of impregnation ΔR_c and the polymer loading p_v (in % by volume) is an exponential relation too :

$$\Delta R_c = 2.5\, p_v^{3/2} \qquad (3)$$

2.3. Polymer impregnated - steel fiber reinforced concrete

The data in Table 3 give some characteristics of the new composite

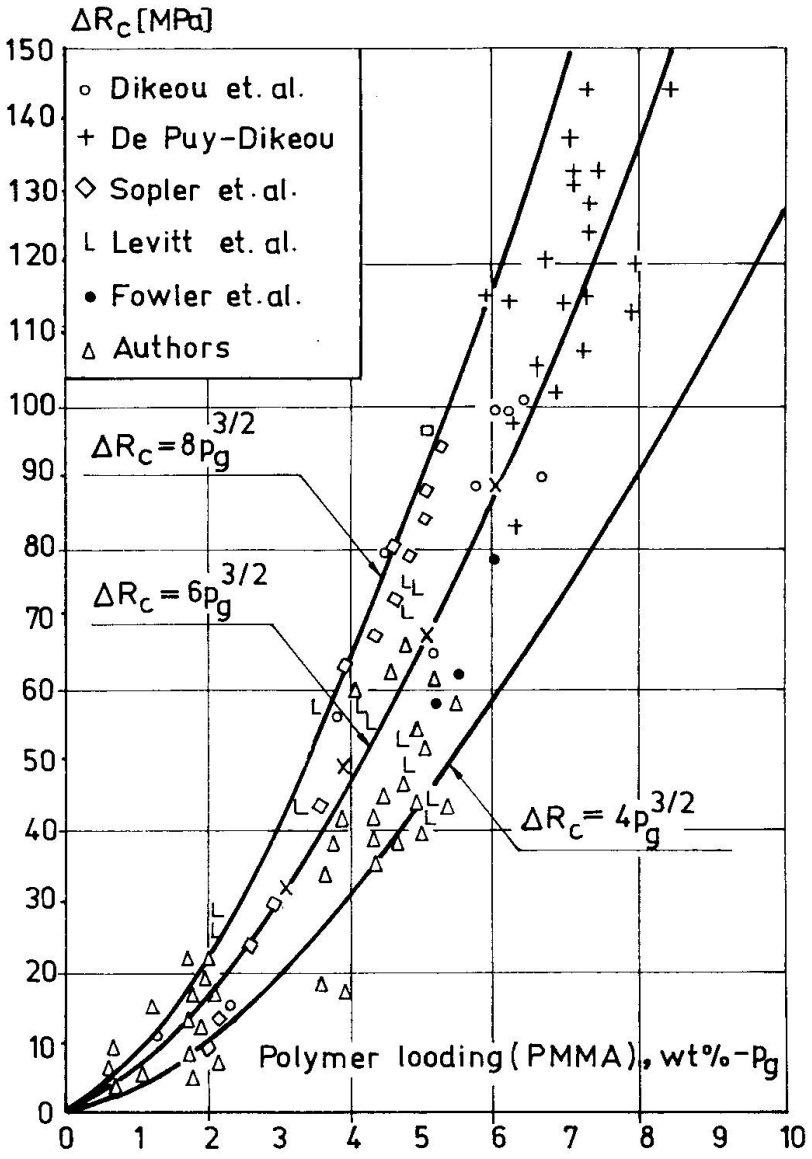

Fig.1 The dependence between the efficiency of impregnation and the polymer loading

material : monomer MMA and steel fiber loadings as well as flexural strength. It was found the efficiency of polymer impregnation on flexural strength and the influence of the reinforcement with steel fiber on the nature of failure : it become more ductile.

	Plain concrete composition		
Specimen size, mm	Cement, Pa35, kg/m^3	Water/cement	Sand 0-3 mm, kg/m^3
40 x 40 x 160	445	0.47	1570
Characteristics of :		Flexural strength , MPa	
Monomer MMA p_g, %	Steel fiber (L=20 mm;D=0.29 mm) μ, %	Plain concrete	Polymer impregnated steel fiber concrete
4-5	1.25	4.02	15.36

Table 3 Polymer impregnated - steel fiber reinforced concrete characteristics

3. APPLICATIONS

The applications of SFRC have been in the areas of pavements, over lays, refractories, patching, mine tunnel lining etc.; in Romanian it was used as an experimental section of a road from prefabricated slabs and for repairing of a rigid overlays. Numerous applications of PIC are under development which indicates a large potential for this material : bridge deck, vessels used in varied applications, tunnel linings, sewer pressure pipes, panels etc. The authors tested a PIC anchorage for prestressed concrete elements.

Polymer impregnated - steel fiber reinforced concrete was used by the authors for two bridge decks. In order to provide an efficient solution, a steel fiber reinforced concrete layer of 5 cm in depth was performed. The compositions of steel fiber reinforced concrete used is given in Table 4.

Experimental section	Cement, Pa35, kg/m^3	Water/Cement	Sand kg/m^3		Steel fiber				Additive DISAN (20 %)
			0-3 mm	3-7 mm	L mm	D mm	μ %	Batch kg/m^3	
DN 59 B km 35+050	520	0.55	900	653	30	0.28	1.5	120	1.5 l for 100 kg cement
DN 59 B km 43+320					22	0.24			

Table 4 Compositions of steel fiber reinforced concrete

The application of the monomer system for field applications to bridge decks consisted of :
(1) cleaning the concrete surface by simply swept and scrubbed

with hard brushes;
(2) drying the surface with ceramic bulbs at 105°C for 1-4 hours or by solar heating for 5-7 days;
(3) applying of the monomer with a watering can in many layers;
(4) covering the surface with polyethylene to retard evaporation;
(5) applying heat by ceramic bulbs for 2 hours (70-75°C) to polymerize the monomer.
The total monomer required was of p_g = 4 % for 2.5 cm depth.

4. CONCLUSIONS

4.1. Application of SFRC for rigid overlays and bridge decks leads to the following : significant increases in mechanical properties and ductility; the mixing of the concrete is carried out with similar equipment as for plain concrete; the depth of the fiber reinforced concrete layer shold be no less than 5 cm and the minimum volume percent of reinforcement should be 1.5.

4.2. Polymer - impregnated concrete surface treatment indicated very good freeze - thaw durability and resistance to water penetration before and after freeze - thaw as well as increases in flexural and compressive strengths, modulus of elasticity and resistance to acid attack.

REFERENCES

1. AVRAM C. and BOB C., New special concrete types (in Romanian), Editura Tehnică, Bucureşti, 1980.
2. AVRAM C., BOB C. and ROSU M., Some properties of polymer impregnated concrete. ICP/RILEM/IBK International Symposium, Prague, June, 1981.
3. BOB C. and ROSU M., The efficiency of PIC (in Romanian), Bul. St. şi Teh. al IPT, Nr. 32, Fasc. 1, Timişoara, 1975.
4. BOB C., BUCHMAN I., NICOARA L. and IONESCU N., Steel fiber reinforced concrete. 2nd International Conference on Bearing Capacity of Roads and Airfields. Proceedings, Plymouth, England, September, 1986.
5. ACI Polymers in Concrete. Proceedings of the International Symposium, Publication SP-40, Detroit, 1973.
6. ACI Fiber Reinforced Concrete. Proceedings of the International Symposium, Publication SP-44, Detroit, 1974.

Fiber Reinforced Plastics Grid Reinforcement for Concrete Structures

Grillage en matière plastique renforcé de fibres pour les structures en béton

Faserarmierte Plastiknetze als Betonbewehrung

Kenzo SEKIJIMA
Senior Res. Eng.
Shimizu Corp.
Tokyo, Japan

Kenzo Sekijima, born in 1951, received his M.Eng. degree from the University of Tokyo in 1976. He has been engaged in research and design of concrete structures with new materials in the Shimizu Corporation.

Hisao HIRAGA
Exec. Managing Dir.
Dainihon Glass Ind.
Kanagawa, Japan

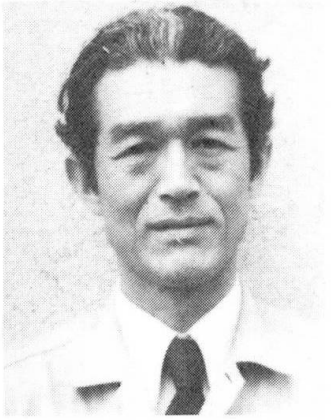

Hisao Hiraga, born in 1927, received his B.S. degree from the University of Yamagata in 1949. He is an authority on fiber reinforced plastics and an executive managing director of the Dainihon Glass Industry Co., Ltd.

SUMMARY

Fiber-reinforced plastic grid reinforcement is a new composite material for reinforcing concrete, which is composed of high strength continuous fibers impregnated with resin and formed in grid shapes. It has many excellent characteristics such as non-corrosive, light-weight, non-magnetic. In this paper, the latest application cases of fiber reinforced plastics grid reinforcements to various kinds of concrete structures are described.

RÉSUMÉ

Le grillage d'armature en matière plastique renforcé de fibres est un nouveau matériau composite servant à renforcer le béton; il est composé de fibres continues à haute résistance imprégnées de résine et disposées en forme de grillage. Ce matériau possède les excellentes caractéristiques suivantes: non corrosif, de poids faible et non magnétique, etc. Cette contribution décrit les derniers cas d'applications des grillages d'armature en matière plastique renforcés de fibres dans diverses structures en béton.

ZUSAMMENFASSUNG

Faserverstärkte Plastiknetze sind ein neuer Baustoff, zur Bewehrung von Beton. Sie bestehen aus mit Hartz imprägnierten hochfesten, kontinuierlichen Fasern, die zu Netzen verarbeitet die folgenden Eigenschaften aufweisen: es korrodiert nicht, ist sehr leicht, ist nicht magnetisch usw. In diesem Aufsatz sind die neuesten Anwendungsbeispiele von faserarmierten Plastiknetzen in diversen Betonstrukturen beschrieben.

1. INTRODUCTION

Recently in Japan, reinforced concrete structures have sometimes been seriously deteriorated owing to the corrosion of reinforcing steel bars. This problem is a significant topic of concern. A thick concrete cover to protect steel bars is not economical, because the sections of concrete members become large and the weight of the structure increases.

In order to improve the durability of concrete structures and make them light in weight, we have developed the New Fiber Composite Material for Reinforcing Concrete (NEFMAC), which is composed of fiber reinforced plastics (FRP) and formed in grid shapes. Through various series of experiments [1], the practical application cases of NEFMAC have increased in number. And those to the tunnel supports have already been presented in another paper [2]. The latest application cases of NEFMAC to the other concrete structures are described in this paper.

2. CHARACTERISTICS OF NEFMAC

Table 1 Characteristics of NEFMAC

* Non-corrosive	* Improve durability of concrete structure under severe condition
* Use of continuous fibers	* Effective use of fibers
* Enough strength at cross point of grids	* Sufficient bond and anchorage to concrete
	* Lap splice joint
* Light in weight (specific gravity ≒ 2)	* Improve work productivity in site
* Formed in complicated shapes	
* Non-magnetic	* Applicable to concrete structure required non-magnetic

NEFMAC is a new composite material for reinforcing concrete, which is composed of high strength continuous glass and/or carbon fibers impregnated with non-corrosive resin and formed in flat or curved shapes by the filament winding method [1]. NEFMAC has many excellent characteristics as listed in Table 1. For instance, it has enough strength at the cross point of grids, it provides good bond and anchorage to concrete, therefore lap splice joints are made possible. Furthermore, it is not only light in weight but also non-magnetic.

3. SHOTCRETE FOR LANDSLIDE PROTECTION OF LPG INGROUND STORAGE TANK

NEFMAC has been widely used as reinforcing grids

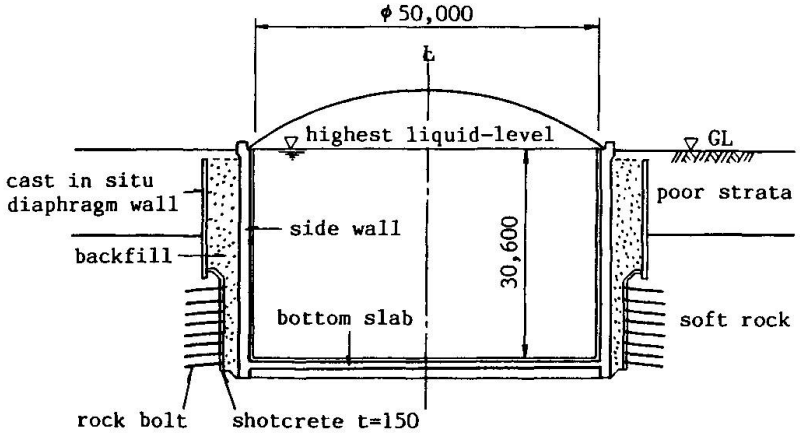

Fig. 1 Cross-section of LPG inground storage tank

for shotcrete of tunnels and slopes, because it can curtail the amount of the secondary shotcrete compared with welded wire fabrics when it secures the same cover from the surface of the secondary shotcrete [2]. Lately, it was adopted as reinforcing grids for shotcrete of landslide protection of a liquid petroleum gas (LPG) inground storage tank in the gas company. Figure 1 shows the vertical cross-section of the tank. The side wall and the bottom slab are made of reinforced concrete as one body. And its capacity is 60,000 m^3.

The soft rock, which is the foundation bed of the tank, was excavated with a backhoe while it was reinforced with shotcrete of 15 cm thick and rock bolts. Approximately 4,300 m^2 of NEFMAC was used for reinforcing the shotcrete. Its dimension was 3.0 m x 1.7 m and it was set between the primary and second layers of the shotcrete (See Fig. 2). NEFMAC was lapped each other with one grid. Since it is light in weight and easy for handling, a large size can be used. Consequently, the setting rate became much higher than that of conventional welded wire fabrics.

4. FENDER PLATES FOR BOATS INSTALLED IN THE FRONT OF PIER

At low tide, boats accidentally went under the pier and damaged it with the wave motion. To prevent this kind of accident, reinforced concrete fender plates had been proposed to be installed in the front of the pier. Since these fender plates should be installed between the high and low tide zone, ordinary reinforcing steel bars would be corroded by the salt attack of sea water. Thus, epoxy coated steel bars had been selected to be used at first.

In order to apply non-corrosive NEFMAC to the fender plates in place of epoxy coated steel bars, the bending test of the concrete beams which were reinforced with two kinds of reinforcements respectively was carried out and their mechanical behavior was compared. The

Fig. 2 Reinforcing grids for shotcrete

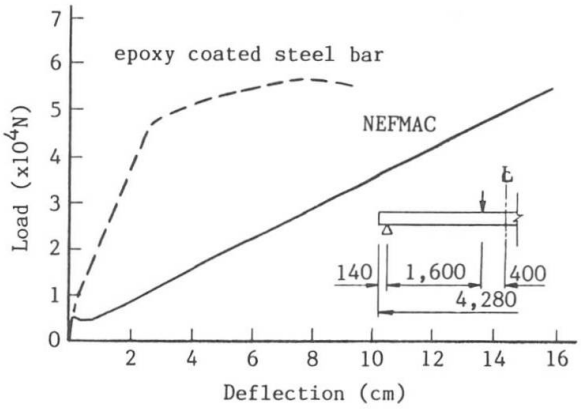

Fig. 3 Load-deflection relationship of specimen

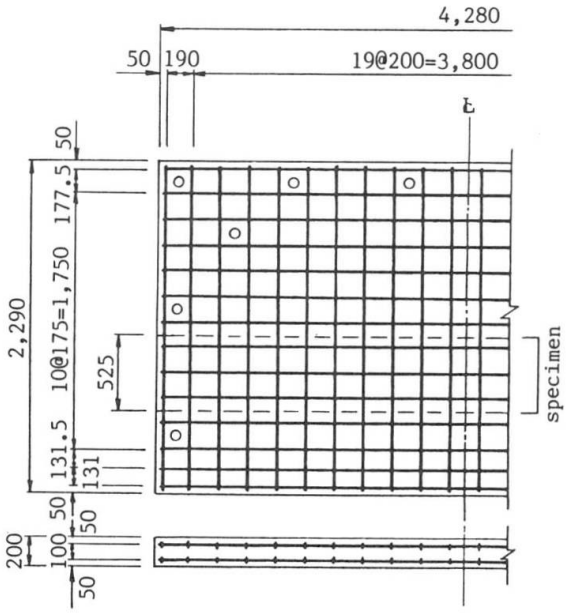

Fig. 4 Reinforcement of fender plate

relationship between the load and the deflection at the midspan is shown in Fig. 3. After the appearance of flexural cracks, the deflection of the beam reinforced with NEFMAC became approximately five times larger than that of one with the epoxy coated steel bars. Thus, it was confirmed that the former beam had a large capacity of absorbing the impact energy. Incidentally, the former beam failed in compression but the latter one failed in tension after yielding of the lower steel bars under the bending moment. Nevertheless, their flexural capacity was almost equal.

Figure 4 shows the arrangement of NEFMAC for the fender plate. After the fender plates had been produced in the precast yard, they were transported to the site by a pontoon and installed in the front of the pier with bolts through rubber bearing (See Fig. 5). At present, their fatigue behavior caused by the wave force has been under investigation.

5. FREE ACCESS FLOOR TILES FOR OFFICE AUTOMATION

According as the development of the office automation for intelligent buildings, free access floor tiles have been widely introduced. Since glass fiber reinforced cement mortar (GRC) floor tiles are beneficial for thermal insulation, comfortable for walking and have a good cost performance, they have begun to replace conventional die cast aluminum floor tiles.

Ordinary GRC floor tiles have enough strength for a static load, but not for a dynamic (especially impact) one. To improve the impact resistivity, the new GRC floor tiles have been developed, which are composed of premix GRC and NEFMAC (See Fig. 6 and Fig. 7).

Figure 8 shows the relationship between the load and the deflection at the center of the new GRC floor tile under the bending test [3]. It was confirmed that the impact resistance and toughness were increased approximately five times higher than that of the ordinary GRC floor tile by

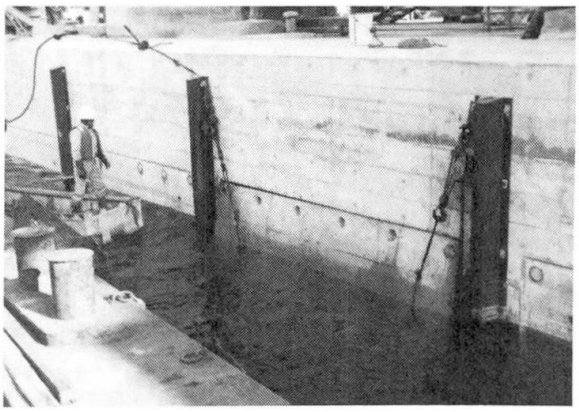

Fig. 5 Installing work of fender plate

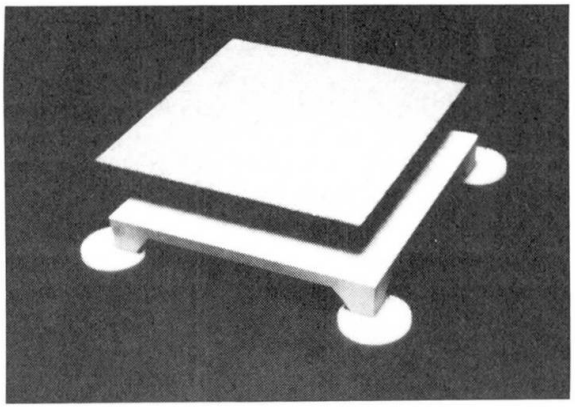

Fig. 6 New GRC free access floor tile

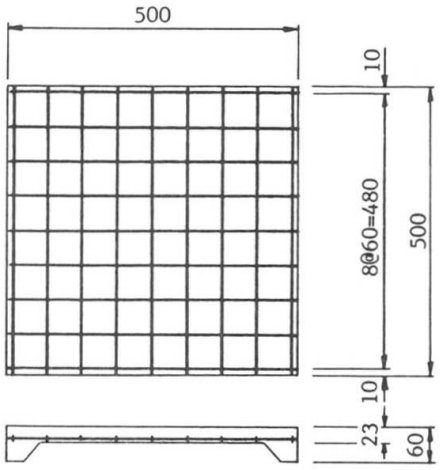

Fig. 7 Reinforcement of new GRC floor tile

reinforcing with NEFMAC. Furthermore, NEFMAC is neither magnetic nor electric conductive, and it does not have a bad influence on the office automation equipment, thus it has been widely applied.

6. PRESTRESSED CONCRETE SLAB OF PEDESTRIAN BRIDGE

The modulus of elasticity of FRP prestressing tendon is generally lower than that of a steel tendon. Thus, FRP tendon has an advantage of a small loss of prestress owing to the elastic shortening of concrete produced by prestressing, creep and shrinkage of concrete. Furthermore, NEFMAC has enough strength at the cross point of grids and provides good anchorage to concrete. Therefore, it can be used as a prestressing tendon for the pre-tensioning system, and the transfer length is extremely short [4].

For the practical application of NEFMAC to prestressed concrete members, we have constructed a full-scale pedestrian bridge in our factory as a trial, which is composed of the prestressed concrete slab with NEFMAC.

As shown in Fig. 9, NEFMAC was used as tendons at the lower position and as reinforcements at the upper one in the prestressed concrete slab. Figure 10 shows a new prestressing system with NEFMAC. First, concrete was placed at the both ends of NEFMAC which was longer than the slab and

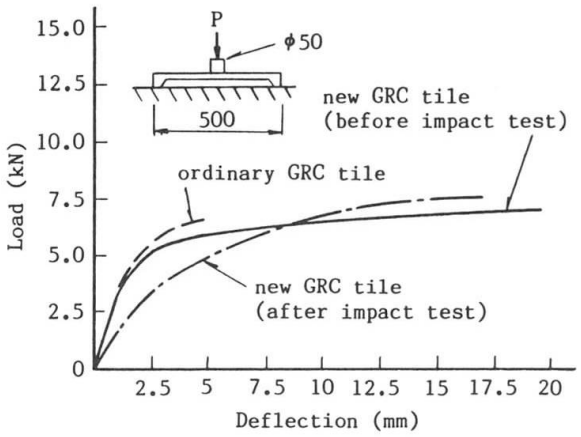

Fig. 8 Load-deflection relationship of GRC floor tile

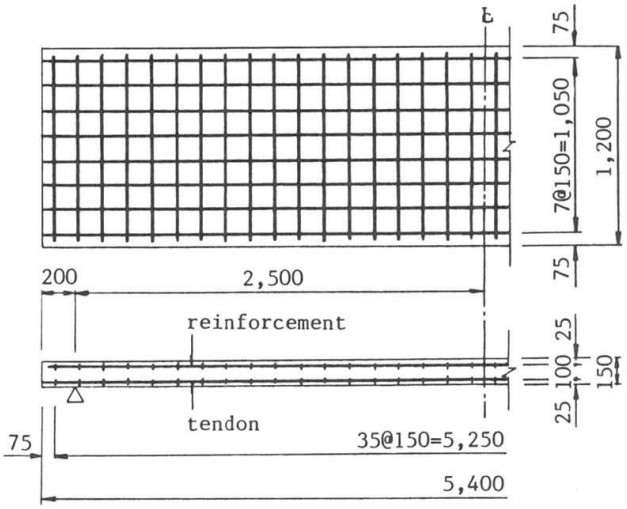

Fig. 9 Tendon and reinforcement of prestressed concrete slab

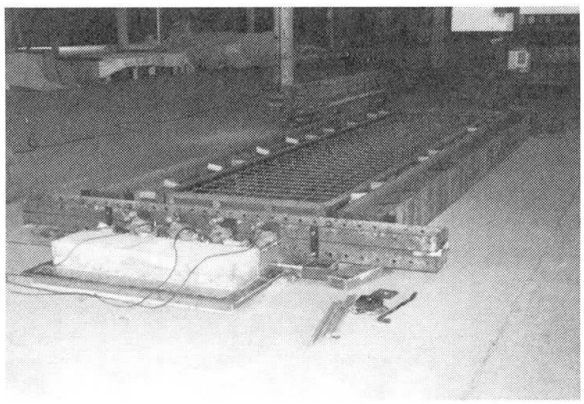

Fig. 10 New prestressing system with NEFMAC

Fig. 11 Prestressed concrete pedestrian bridge

contained another four distribution reinforcements. After the concrete blocks had sufficient strength, a stretching force was applied to NEFMAC by pushing them apart with four mechanical jacks through load cells. The initial tensile force of each tendon was approximately 40 percent of its ultimate tensile capacity (= 106 kN).

After the prestressed concrete slab had been set on the concrete abutments reinforced with NEFMAC, the pedestrian bridge was completed by installing guardrails and slopes (See Fig. 11). Many people walk on it everyday. The success of the construction of this pedestrian bridge gave a great hope to the future application of NEFMAC to prestressed concrete structures.

7. CONCLUDING REMARKS

In this paper, the latest application cases of NEFMAC to various kinds of concrete structures. Currently, NEFMAC is mainly composed of glass fibers because of its reasonable cost performance. In the near future, the cost of high modulus carbon fibers will become low, NEFMAC is expected to be more widely applied.

ACKNOWLEDGMENT

The authors would like to express their deep gratitude to Professor Hajime OKAMURA, the University of Tokyo for his kind guidance and advice on the development and application of NEFMAC to various kinds of concrete structures.

REFERENCES

1. FUJISAKI T., SEKIJIMA K., MATSUZAKI Y. and OKAMURA H., New Material for Reinforced Concrete in place of Reinforcing Steel Bar, IABSE Symposium in Paris-Versailles, September 1987.
2. IKEDA K., SEKIJIMA K. and OKAMURA H., New Materials for Tunnel Supports, IABSE 13th Congress in Helsinki, June 1988
3. SAKURAI M. and KATOH N., New GRC Free Access Floor Tiles of High Impact Resistance for Office Automation, Reports of Research Laboratory, Asahi Glass Co., Ltd., Vol.38, No.1, 1988
4. SEKIJIMA K., FUTAGAWA M. and OKAMURA H., Study on Prestressed Concrete with FRP Grid Tendon, Transaction of the Japan Concrete Institute, Vol.10, December 1988

Three-dimensional Carbon Fabric Reinforced Concrete

Renforcement du béton par un tissu de carbone tridimensionnel

Bewehrung von Beton mit drei-dimensionalen Geflechten aus Kohlefasern

Reiko AMANO
Res. Engineer
Kajima Inst. of
Tokyo, Japan

Toshio OHNO
Res. Engineer
Kajima Inst. of
Tokyo, Japan

Fumio IMADATE
Senior Res. Engineer
Constr. Technology
Tokyo, Japan

Yoichi NOJIRI
Assist. Dir.
Constr. Technology
Tokyo, Japan

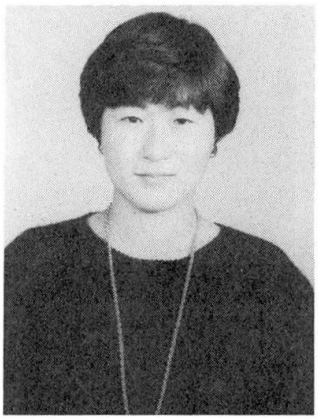
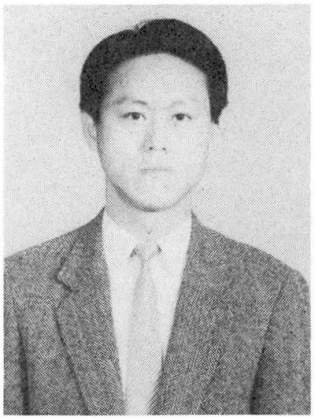
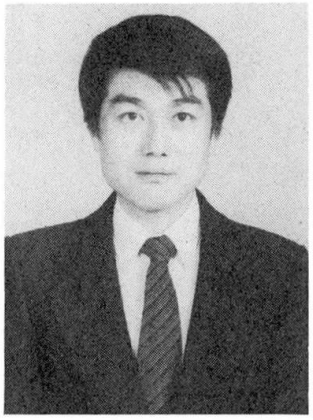


SUMMARY

The possibility of replacing steel reinforcing bars by three-dimensional carbon fabric reinforced plastics is introduced together with experimental results. This new material is a three-dimensional lattice made of rovings of carbon fiber, manufactured by weaving them into three perpendicular directions and impregnated with epoxy resin. The mechanical properties of this reinforced concrete were studied and tests were carried out on the models of side walls of a typical elevated highway structure where an early deterioration due to effects of exhaust from vehicle, deicing salts and so on is serious.

RÉSUMÉ

La possibilité de renforcement du béton par un tissu de carbone tridimensionnel à la place de barres d'armature est présentée avec des résultats expérimentaux. Ce nouveau matériau est fabriqué en tissant des fibres de carbone dans trois directions perpendiculaires, et en l'imprégnant de résine époxy. Les propriétés mécaniques du béton renforcé ont été étudiées et des essais ont été effectués sur des échantillons de voiles latéraux d'un pont-route typique et élevé, présentant une sérieuse détérioration prématurée due aux gaz d'échappement d'automobiles, aux sels de dégel etc.

ZUSAMMENFASSUNG

Dieser Beitrag behandelt die Möglichkeiten, einer Bewehrung mit drei-dimensionalen Geflechten auf Kohlefasern und gibt Versuchsresultate bekannt. Dieses neue Material ist ein drei-dimensionales Fachwerk aus Bündeln von Kohlefasern, die in drei senkrechten Richtungen verwoben und mit Epoxy Harz durchdrungen werden. Die mechanischen Eigenschaften des damit bewehrten Betons wurden untersucht. Versuche wurden an Modellen von Stützmauern typischer Hochstrassen durchgeführt, wo infolge der Einflüsse der Fahrzeugabgase, des Tausalzes usw. eine relativ starke Zersetzung stattfindet.

1.INTRODUCTION

Recently, an early deterioration of steel reinforced concrete structures due to chloride attack, etc., has been becoming a serious problem in Japan. Countermeasures are urgently required, in particular, in coastal zones where structures are being damaged by the heavy corrosion of steel bars.
Under these circumstances, Fiber Reinforced Plastics (FRP) rods manufactured by impregnating various fibers with resin are attracting attention due to their potential for a concrete reinforcing material free from corrosion.
Tests were performed on the models of side walls of typical elevated highway structures, which were reinforced with 3D-CF for the purpose of investigating the mechanical properties of 3D-CF reinforced concrete.

2.THREE-DIMENSIONAL FABRIC(3D-F)

The 3D-F [1][2][3] is a three-dimensional lattice made of rovings of fibers, manufactured by weaving into three perpendicular directions and impregnated with epoxy resin. This allows a flexible choice in fiber material of the rovings (PAN-base carbon fiber was used in the tests, the properties of which are shown in Fig.1), the number of filaments per roving, and the spacing between the rovings. A mechanical bond strength between the 3D-F and concrete is high because of the latticed pattern of the materials. Efficient production is also possible since three-dimensional weaving, impregnation of resin, and hardening can all be carried out by an automatic weaving machine. Fig.2 shows a sample of the 3D-CF.

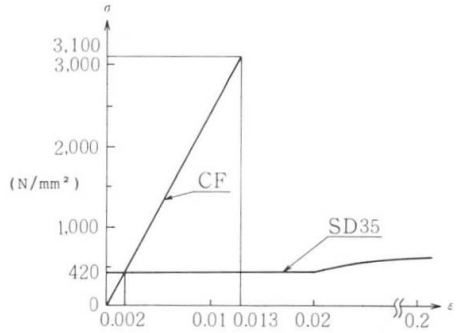

Fig.1 Stress-strain diagram of CF and steel

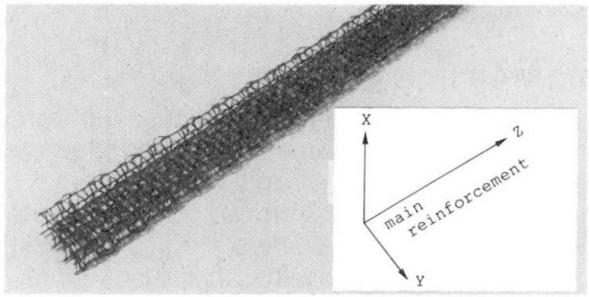

Fig.2 Sample of 3D-CF

3.EXPERIMENTAL RESEARCH

3.1 Flexural Properties

Fig.3 profiles the specimens and the arrangement of reinforcements, with parameters representing the number of filaments per roving in the X, Y and Z directions (the Z direction is the direction of main reinforcement) and the spacing between rovings in the X and the Y directions. The test specimens were subjected to two-point loadings.
All 3D-CF reinforced concrete (3D-CFRC) specimens failed in breaking of axial reinforcements. The test results are shown in Fig.4. The flexural strength

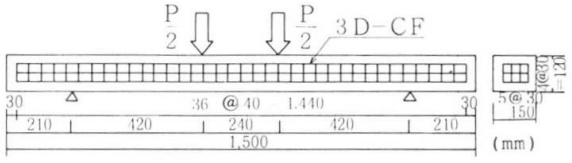

parameters of specimens K:×10³

specimen	number of filaments			spacing (mm)		
	X	Y	Z	X	Y	Z
F-1	48 K	48 K	96 K	40	40	30
F-2				90	90	
F-3	24 K	24 K	48 K	40	40	
F-4				60	60	
F-5				90	90	
F-6				360	360	
F-7	24 K	24 K	24 K	40	40	
F-8	12 K	12 K		40	40	
F-9				90	90	

Fig.3 Specimens for the flexural tests

which is calculated by conventional theory of steel reinforced concrete (the RC theory, [4][5]) is shown by solid line. The observed values are equal to or a little greater than the calculated values. In Fig.5, the observed and the calculated moments are shown in relation to the curvature. The calculated moments are shown for three cases, (1) where the total section is assumed to be effective; (2) where the rigidity is calculated taking an effect of the rigidity of tensile zone into consideration; and (3) where the rigidity of tensile zone is neglected. The observed values show agreement with the values of case (2). From these results, in the 3D-CFRC beams it was confirmed that the flexural strength and moment-curvature relationship can be estimated by the RC theory taking all the rovings of Z direction into account.

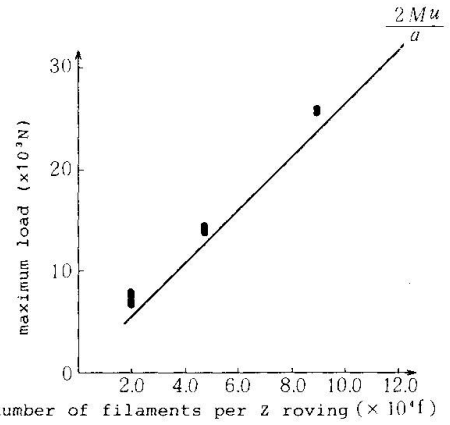

Fig.4 Maximum load vs. the number of filaments per roving in the Z direction relationship

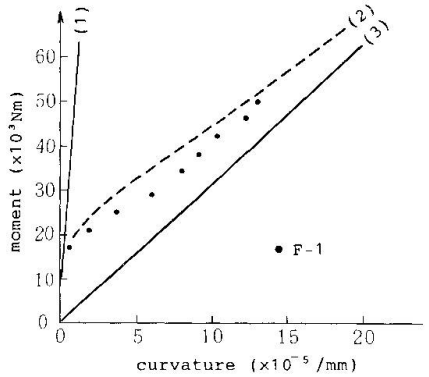

Fig.5 Moment vs. curvature relationship

3.2 Shear Properties

As illustrated in Fig.6, specimens with 3D-CF arranged in the concrete were tested by two-point loadings. Parameters in the tests were the number of filaments per roving and the spacing between rovings in the X and the Y directions.

In all specimens, axial reinforcements broke after diagonal cracking. The test results are shown in Fig.7. In this figure, flexural strength calculated by the RC theory and the shear strength calculated regarding all the Z rovings as the main reinforcement and the X rovings as the shear reinforcement are also shown by solid and broken lines, respectively.

It became clear that the shear strength of the 3D-CFRC beams is greater than the calculated value.

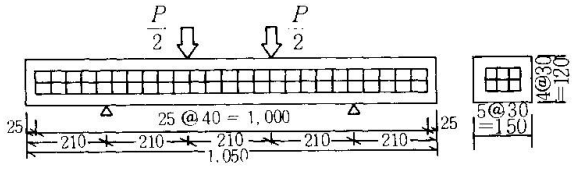

parameters of specimens K:×10³

specimen	number of filaments			spacing (mm)		
	X	Y	Z	X	Y	Z
S-1	48 K	48 K	120 K	40	40	30
S-2				90	90	
S-3	24 K	24 K		40	40	
S-4	12 K	12 K		40	40	
S-5				90	90	

Fig.6 Specimens for the shear tests

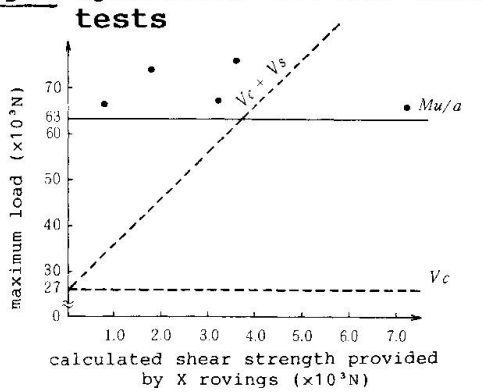

Fig.7 Maximum load vs. calculated shear strength provided by X rovings relationship

3.3 Anchorage Performance

The anchorage performance between 3D-CF and concrete were investigated by using the beams changing the depth of the

cross section which models the corner portion of an L-shaped member as shown in Fig.8. In the tests, the number of layers at the anchorage, the development length and the number of filaments per roving and the spacing between rovings in the X and the Y directions were taken into account as the parameters.
In all specimens, axial reinforcements were slipped out at the anchorage. Fig.9 illustrates the relationship between the development length and the ratio of the bond strength to the square root compressive strength of concrete ($f_{bo}/\sqrt{f_c'}$). The roving diameter is calculated by assuming the section to be circular, and in this calculation periphery of upper rovings is neglected. Fig.9 shows that a longer development length corresponds to a smaller bond stress. And as shown in Fig.9, the bond strength of a two-layer reinforcement is larger than that of a single-layer reinforcement.
It was clear that when 3D-CF is used for the L-shaped member described below, the development length of the 3D-CF can be calculated by assuming a single-layer reinforcement at anchorage.

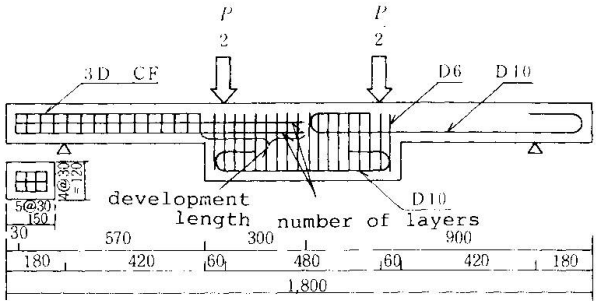

parameters of specimens K:x10³

specimen	number of filaments X	number of filaments Y	number of filaments Z	spacing (mm) X	spacing (mm) Y	spacing (mm) Z
A-1	48 K	48 K	96 K	40	40	30
A-2						
A-3						
A-4						
A-5				90	90	
A-6						
A-7						
A-8						
A-9	24 K	24 K		40	40	
A-10				90	90	
A-11	12 K	12 K		40	40	
A-12						
A-13						
A-14				90	90	
A-15						
A-16						

Fig.8 Specimens for the bond tests

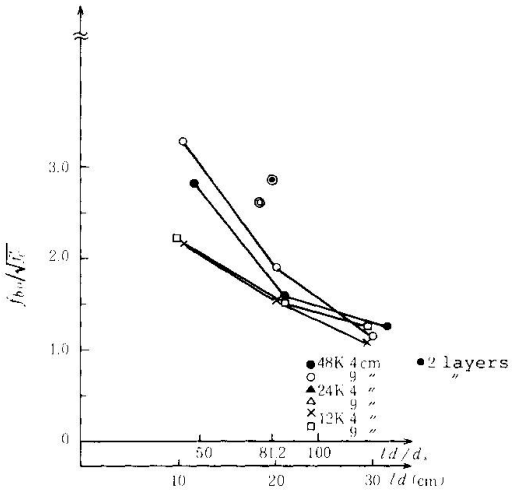

Fig.9 Anchorage strength vs. development length relationship

3.4 Tests on L-shaped Models

3.4.1 Design Condition of The Side Wall Model

The configuration adopted for the models is an L-shaped member arising 60 cm from the slab surface, which are three fifths models of the side wall of an actual highway structure.
The design loads are collision load and the wind load (w = 3000 N/m^2, 1500 N/m^2). The design bending moment (Md) is 14 X10^{3}Nm/m. The collision load is applied horizontally at a height of 42 cm from the slab surface.

3.4.2 Steel Reinforced Concrete (RC) Model

The RC model is designed by the above design condition and provided for the test as a reference specimen to be compared with 3D-CFRC models.
The flexural and shear resistances of the RC model are:

Resisting moment Mu = 32 x10^{3}Nm/m
Moment by shear strength Vu·a = 75 x10^{3}Nm/m

3.4.2 3D-CFRC Models

3D-CFRC models are designed by using the results of the frexural and shear tests. The Z rovings are arranged to retain the larger level of resisting moment as that of the RC model. And rovings in the X and the Y directions are arranged so as to provide larger shear strength than the flexural strength.
The flexural and shear resistances calcurated by the RC theory are:

Resisting moment Mu' = 40 x10^3Nm/m
Moment by shear strength Vu'·a = 142 x10^3Nm/m

Fig.10 profiles the models and the reinforcement arrangements. Three 3D-CFRC models, each consisting of vertical and horizontal 3D-CF units in combination, were tested. In the models, the embeded length of the vertical 3D-CF unit was varied. The embeded lengths were determined by referring the results of the bond tests:
- L-1 ; 10 cm
- L-2 ; 20 cm
- L-3 ; 37 cm

For the model L-1 and L-2, the lapped portion of the vertical and horizontal units was partially bound with CF half-cured ribbon to fix each unit.

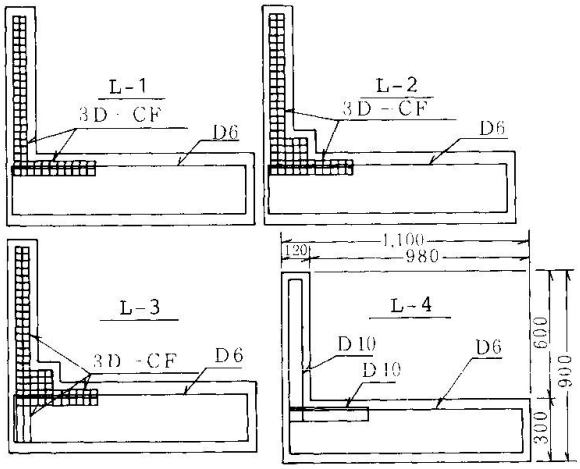

parameters of specimens K:x10³

specimen	number of filaments X	number of filaments Y	number of filaments Z	spacing (mm) X	spacing (mm) Y	spacing (mm) Z
L-1	48 K	48 K	96 K	40	40	30
L-2						
L-3						
L-4		D 10	D 10		120	75

Fig.10 Test specimens

3.4.3 Test Results

Loads were applied at a point of 42 cm from the slab surface shown in Fig.11.
Fig.12 shows the relationship between moment and the deflection obtained from the tests.
As shown in Fig.12, the maximum moment of the model L-2 is equal to the calculated resisting moment, but those of the model L-1 and L-3 are 70% of the resisting moment. Because, in the model L-2 which had the embeded length long enough for the anchorage and bound firmly in the lapped portion, vertical 3D-CFRC axial reinforcements (the Z rovings) were broken. And the model L-1 showed a bond failure due to the short embeded length and the model L-3 showed a bond failure though it had the enough development length determined from the results of the bond tests.
Comparing the deformation characteristics of them with the RC model, in the model L-1 a ductile

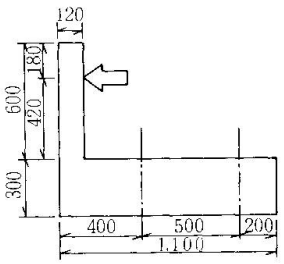

Fig.11 Loading setup

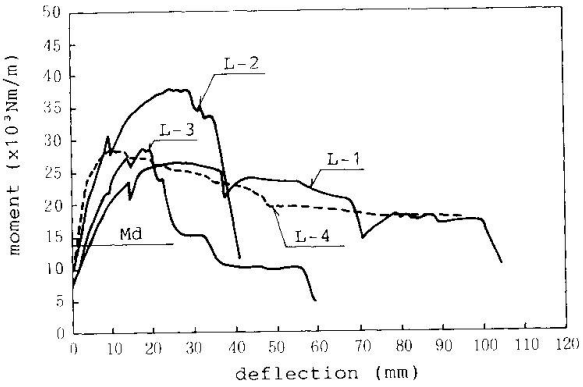

Fig.12 Moment vs. deflection relationship

failure occurred and the amount of deformation is comparable with the RC specimen in which the progressive failure occurred due to breaking of binding ribbons one by one.
From these tests, the ultimate strength of the structure is determined by the arrangement of reinforcing material such as enough embeded length of vertical reinforcement as well as binding of vertical and horizontal units firmly. And 3D-CF can be used as reinforcement of L-shaped members when it is designed and the reinforcing unit is arranged properly.

5.CONCLUSIONS

The new anti-corrosive, lightweight material -- Three-Dimensional Carbon Fabric -- was introduced and various test results were presented. 3D-CF, developed to replace an ordinary reinforcing steel bar, a three-dimensional lattice made of rovings of CF, manufactured by weaving into three perpendicular directions and impregnated with epoxy resin, is believed to be one of promising materials to be used for the structures exposed to severe environmental condition.

REFERENCES

1.H.Nakagawa,S.Akihama,T.Suenaga, Mechanical properties of various types of fibre reinforced concretes, International Concrete on Recent Developments of Fiber Reinforced Cements and Concretes, September 1989.

2.H.Nakagawa,T.Suenaga,S.Akihama, Mechanical properties of three-dimensional fabric reinforced concretes and their application to buildings, First Japan International SAMPE Symposium, November 1989. fibre reinforced concretes, International Concrete on Recent Developments of Fiber Reinforced Cements and Concretes, September 1989.

3.R.Amano,F.Imadate,T.Ohno, Study on three-dimensional carbon fabric reinforced concrete, Annual Report of Kajima Institute of Construction Technology, V01.37, October 1989.

4.Japan Society of Civil Engineers, Standard Specifications for Concrete, 1986.

5.Y.Murayama,K.Suda,K.Furuichi, Moment-curvature relationships of reinforced concrete members subjected to combined bi-axial bending moment and axial force, Annual Report of Kajima Institute of Construction Technology, V01.37, October 1989.

Design of Sandwich Panels against Thermal Loads

Dimensionnement de panneaux sandwich sous charges thermiques

Bemessung von Sandwichtragwerken auf Temperaturbeanspruchungen

Paavo HASSINEN
Senior Scientist
Techn. Res. Centre
Espoo, Finland

Paavo Hassinen received his Civil Engineering degree from the Helsinki University of Technology in 1976. He currently works on the research of steel structures and bridges.

Antti HELENIUS
Research Scientist
Techn. Res. Centre
Espoo, Finland

Antti Helenius received his Civil Engineering degree from the Helsinki University of Technology in 1980. Since 1982 he has been involved in the research of lightweight steel structures.

SUMMARY

Lightweight structural sandwich panels possess a high stiffness and strength and good insulating properties. In the panels the thin outer face is exposed to rapid changes of the outside temperature, which cause deflections and stresses in the panel. These thermal stresses are much influenced by the flexibility of the panel, which consists of bending and shear deformations of the face and core layers. In addition, the shear creep of the core and the deformations of connections are of great consequence in reducing the termal stresses especially in thick and short multispan panels. In this paper the design of panels against thermal stresses is discussed with the aid of examples.

RÉSUMÉ

Les panneaux sandwich des structures légères présentent une rigidité et une résistance élevées ainsi qu'un bon pouvoir d'isolation thermique. La couche extérieure mince des panneaux est exposée aux variations rapides de la température externe, provoquant des déformations et des contraintes dans les éléments sandwich. Ces sollicitations thermiques sont fonction de la rigidité du panneau, impliquant des déformations à la flexion et au cisaillement des couches constitutives de l'élément sandwich. En outre, le fluage au cisaillement de la couche centrale et les déformations dans les joints jouent un rôle important dans la réduction des contraintes thermiques, tout particulièrement dans les panneaux sandwich épais et courts à portées multiples. Le dimensionnement des panneaux soumis à des sollicitations thermiques est illustré par des calculs effectués sur certains exemples pratiques.

ZUSAMMENFASSUNG

Leichte Sandwichtragwerke haben eine hohe Steifigkeit und Tragfähigkeit und gute Wärmedämmeeigenschaften. Die äussere Deckschicht des Elementes ist der schnellen äusseren Temperaturschwankung ausgesetzt. Dies verursacht im Tragwerk Durchbiegungen und Spannungen, deren Höhe von der Biege- und Schubsteifigkeit des Tragwerkes abhängig ist. Schubkriechen und Deformationen in den Fugen spielen eine wichtige Rolle in der Verminderung der Temperaturspannungen, insbesondere bei dicken und kurzen mehrfeldrigen Sandwichelementen. Das Bemessen von Sandwichtragwerken auf die Temperaturbeanspruchungen wird anhand numerischer Beispiele diskutiert.

1. INTRODUCTION

Strutural sandwich panels composed of a foam or a mineral wool core and of thin metal faces are widely used in wall and roof structures in cold storages and industrial buildings. The temperature difference between the faces of the panel in a cold storage can in summer time reach the value $\Delta T = T_{outside} - T_{inside} = +80-(-20) = 100\ ^{o}C$ and in an industrial building in the arctic climate in winter time $\Delta T = T_{outside} - T_{inside} = -60-(+20) = -80\ ^{o}C$.

Insulation material between the face layers escapes the temperatures in faces to become even. Thus, the temperature differences cause large curvatures and large deflections and stresses to a panel. Temperature differences between the different structural layers in multilayer panels produce also high local shear stresses to the joints of the layers. In the most cases the shear stress level in the core caused by thermal curvatures is low and the most critical components in the panels are the face layers. Alone or together with the other loads the thermal stresses can easily lead the thin compressed face layer to the buckling failure.

2. THERMAL LOADS IN SANDWICH PANELS

Evaluation of thermal stresses of an elastic sandwich panel is usually based on the well known fourth order differential equations for sandwich beams with thick or profiled faces and second order differential equations for beams with thin flat or slightly profiled faces /1, 2/. The problem can be formulated also using finite elements

$$\{F\} = [K]\ \{d\} \qquad (1)$$

In the numerical analysis it is also possible to take into account the flexibilities of the other structures having joints with the panels like the supports and connections. Numerical results of the thermal stresses depend strongly on the bending and shear stiffnesses (table 1). The theory of elasticity yields often too high thermal stresses, because it does not take into account the time dependent deformations in the core or the local flexibilities in the joints of the panel.

Table 1. Support reactions and bending moments on the intermediate support of two and three span thin faced sandwich beams. B means the bending stiffness and S the shear stiffness of the panel. $\vartheta = (\alpha_2 T_2 - \alpha_1 T_1)/e$ and $k = 3B/L^2S$.

Static system	R	M
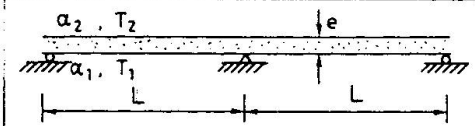	$\frac{3\ \vartheta\ B}{e\ L}\ \frac{1}{1+k}$	$-\frac{3\ \vartheta\ B}{2\ e}\ \frac{1}{1+k}$
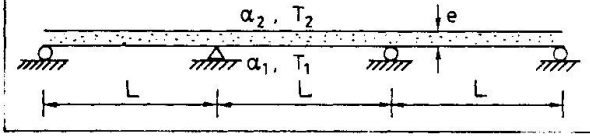	$\frac{6\ \vartheta\ B}{e\ L}\ \frac{1}{5+2k}$	$-\frac{6\ \vartheta\ B}{e}\ \frac{1}{5+2k}$

3. SHEAR CREEP IN CORE LAYER

The behaviour of the structural core materials is usually desribed by elastic material models. Their behaviour actually depends on the stress level, the temperature and the time. The foams particularly are so called thermo-viscoelastic materials. In the engineering calculation models the shear creep is desribed by the time dependent shear modulus /1/

$$G_t = \frac{G_o}{1 + \varphi(t)} \tag{2}$$

The more accurate method to take the shear creeping into account is to use a linear visoelastic material model for the core.

$$G(t) = \frac{\tau(t)}{\gamma_o}, \quad J(t) = \frac{\gamma(t)}{\tau_o} \tag{3}$$

With the relaxation modulus G(t) and the creep function J(t) the shear stress carried by the core can be integrated in time using the equation.

$$\tau = \int_0^t G(t - t') \left(\frac{d\gamma}{dt'}\right) dt' \tag{4}$$

The equation (1) to the viscoelastic sandwich beam can now be written in an iterative form

$$[K]_1 \{d\}_2^{n+1} = \{F\} - ([K]_2^n - [K]_1) \{d\}_2^n \tag{5}$$

where {F} is the loadvector. The subscripts 1 and 2 refer to times t_1 and t_2 and the superscripts to the iteration cycles.

The linear viscoelastic models used in the above equations are still not able to model the structural foams completely, because in the loading and unloading phases some plastic deformations remain in the foams /3/. Some special methods are needed to take them in consideration in the calculations. The shear creep phenomenon of the core means that the stresses caused by a constant temperature difference between the face layers are reduced gradually due to the relaxation of the core layer. The level of the thermal stresses, ie. compressive and tensile stresses in the faces and shear stresses in the core, is dependent on the rate and the duration of the action of the temperature.

4. FLEXIBILITY OF THE SUPPORTS

Tensile stiffnesses of connections with common through going screws are mainly determined by the thickness and the profiles of the outer face and the compressive stiffness of the core layer. For the calculation models the constant tensile stiffness can be evaluated from the linear part of the force-displacement curve

$$k = F/(u_1 - u_2) \tag{6}$$

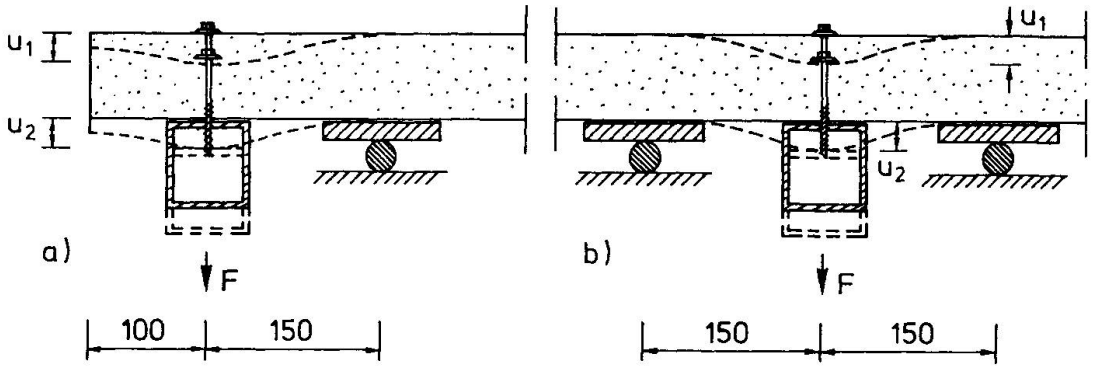

Fig.1. Test arrangements to determinate the tensile stiffness and the strength of a through going screw connection for a sandwich panel with steel faces and a polyurethane core.

Table 2. Tensile stiffness and strength of a screw connection used in sandwich wall panels (see Fig. 1). Diameter of the screw and of the washer were 6.3 mm and 19 mm. Thickness outer steel face was 0.58 mm and the yield and tensile strength of the steel sheet 363 N/mm^2 and 451 N/mm^2. Density of the polyurethane core was 39 kg/m^3 and its compressive modulus of elasticity 2.0 N/mm^2 (e = 75 mm) and 3.7 N/mm^2 (e = 150 mm).

Specimen	e(mm)	F_{exp}(kN)	k(N/mm)	Specimen	e(mm)	F_{exp}(kN)	k(N/mm)
F1	75	4.3	200	F8	150	4.6	280
F2	75	3.5	220	F9	150	4.6	260
mean value		3.9	210	mean value		4.6	270
F3	75	3.8	270	F10	150	4.8	360
F4	75	4.3	260	F11	150	4.6	350
F5	75	4.0	300	F12	150	4.5	380
F6	75	4.6	330	F13	150	4.2	350
F7	75	4.3	310	F14	150	4.7	340
mean value		4.2	290	mean value		4.6	350

5. EXPERIMENTAL RESULTS

A test series in a cold chamber was performed in the Laboratory of Structural Engineering at VTT to study thermal stresses in sandwich panels. The tests were also analyzed with the finite element method. In the tests two span panels with nearly flat faces were subjected to cyclic temperature loading. The test arrangement is given in Fig. 2 and the loading in Fig. 4a. Figures 3 show the displacements on the supports and were used to evaluate the flexibilities of the connections. During the tests the end supports were connected against both upward and downward movements using 'rigid' continuous support beams.

The approximate temperature history in fig. 4a was used in the numerical analysis. In Figures 4b and 4c the experimental results for the central support reaction and the midspan deflection are compared with the corresponding calculated values. Three numerical analyses have been done, purely elastic, elastic with flexible supports and viscoelastic with flexible supports.

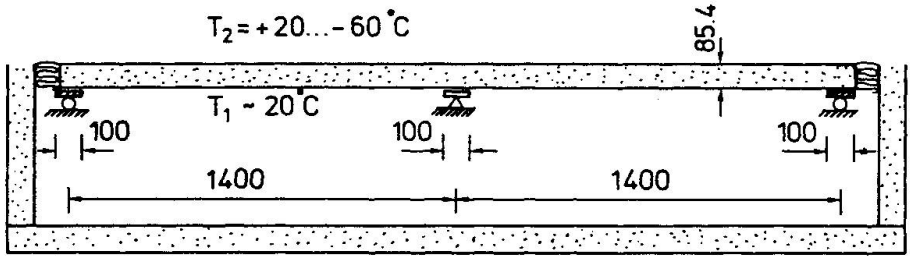

Fig.2. Figurative loading arrangements. Thickness of the steel faces was 0.46 mm, width of the panel 600 mm and the initial shear modulus of the core at T = +20 °C 4.08 N/mm^2.

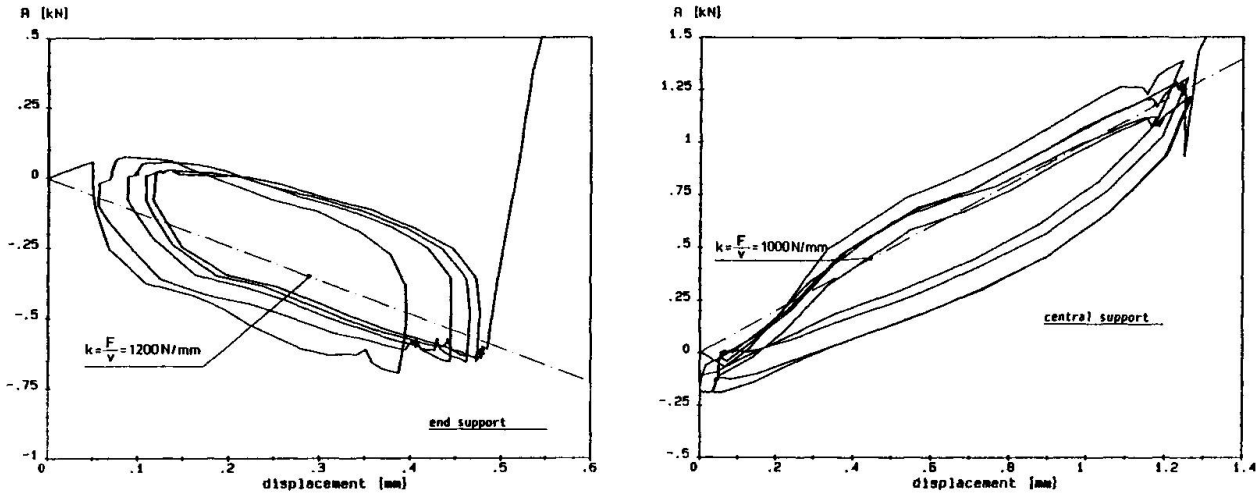

Fig.3. Displacements from(-, upward) and to(+, downward) the support plate on the end and central supports during the temperature cycles.

6. CONCLUSION

In practical design light weight sandwich panels are treated elastic for short term loads and viscoelastic for long term loads. The test results confirm that in short 'daily' temperature cycles the influence of the timedependent behaviour of foams is negligible. On the other hand the results emphasize the importance of the flexibility of the connections and suggest that they should be considered in design. On the other hand the connectors with the support beams restrain rotation of the panel and increase both the stiffness of the structure and thus also thermal stress and this should be studied too.

REFERENCES

1. Stamm, K. & Witte, H., Sandwichkonstruktionen. Springer-Verlag. 1974
2. Chong, K.P., Engen, K.O. & Hartsock, J.A., Thermal stresses and deflections of sandwich panels. J. Struct. Div., Vol. 103, No ST1, Jan. 1977. pp. 35 - 49.
3. Burkhardt, S., Zeitabhängiges Verhalten von Sandwichelementen mit Metalldeckschichten und Stützkernen aus Polyurethan-hartschaumstoffen. Bericht der Universität Karlsruhe. 1988.

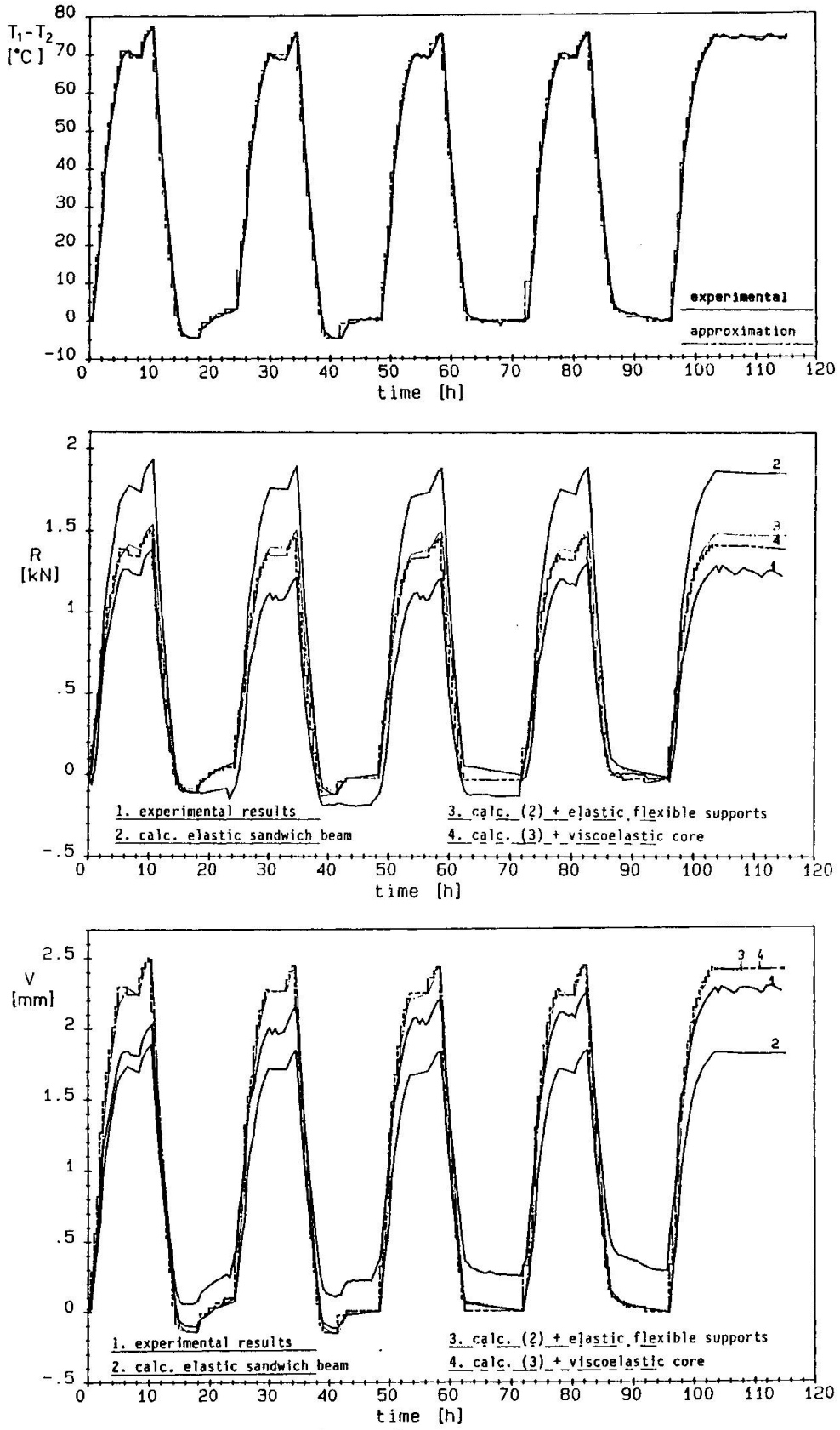

Fig.4. a) Temperature loading history, b) central support reaction and c) deflection in the mid span of the test specimen given in the fig. 2. In the calculations Findley's model was used $J(t) = 0.2452 + 0.03\ t^{0.37}$ (mm^2/N, the time in hours).

Zum Tragverhalten von Betonbauteilen mit gemischten Bewehrungen

Load Bearing Behaviour of Concrete Structural Components with Mixed Reinforcement

Capacité portante d'éléments en béton à armatures mixtes

Martin FAORO
Dr.-Ing.
Strabag Bau-AG
Köln, BR Deutschland

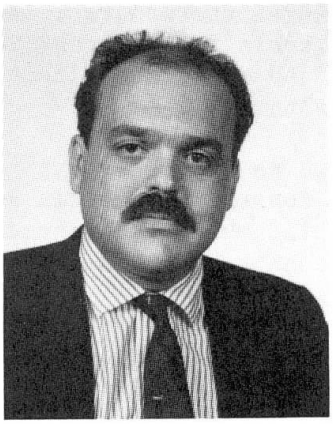

Martin Faoro, geboren 1956, wurde als Bauingenieur an der RWTH Aachen 1981 diplomiert. Nach mehrjähriger Tätigkeit als wissenschaftlicher Mitarbeiter erfolgte seine Promotion 1988 an der Universität Stuttgart. Er beschäftigt sich mit Werkstoff- und Konstruktionsproblemen des Massivbaus. Seit 1989 ist er Mitarbeiter der Strabag Bau-AG, Abteilung Forschung und Entwicklung.

ZUSAMMENFASSUNG

In letzter Zeit werden immer häufiger Betonbauteile mit Bewehrungen aus völlig unterschiedlichen Werkstoffen, beispielsweise mit üblichen Betonstählen und Glasfasererstäben, gemischt bewehrt. Jedoch ist das Tragverhalten dieser Konstruktionen noch nicht ausreichend bekannt. Im folgenden werden anhand eines Rechenmodells die wesentlichen Einflußparameter auf die Spannungsumlagerungen zwischen den unterschiedlichen Bewehrungselementen diskutiert. Für die Praxis resultiert hieraus, daß zur Vermeidung einer Überbeanspruchung der dehn- bzw. verbundsteiferen Bewehrung deren Menge ausreichend zu dimensionieren ist.

SUMMARY

With increasing frequency, structural components have recently been furnished with mixed reinforcement comprising completely differing materials, for example conventional reinforcing steels and glass fiber bars. However too little is known of the bearing behaviour of these structures. The main parameters of influence on the stress redistributions between the various reinforcing elements will be discussed in the following on the basis of a theoretical model. For practical purposes, the results show that in order to avoid overstressing of the reinforcement, which is stiffer in respect to strain and bond, an adequate quantity thereof must be foreseen in the design.

RÉSUMÉ

Dernièrement, l'emploi d'armatures mixtes a augmenté constamment pour les éléments en béton, utilisant des matériaux tout à fait différents, comme par exemple l'acier traditionnel d'armature et les barres de fibres de verre. Cependant, la capacité portante n'est pas encore suffisamment connue pour ces constructions. L'auteur analyse au moyen d'un modèle de calcul les paramètres essentiels d'influence sur la distribution des contraintes entre les divers éléments d'armatures. Pour les applications pratiques, il en résulte qu'un dimensionnement suffisant des armatures est indispensable pour éviter tout dépassement des déformations et des contraintes d'adhérence.

1. EINLEITUNG

Das Zusammenwirken von Bewehrungssträngen extrem unterschiedlicher Verbundeigenschaften und Dehnsteifigkeiten (E-Moduln) und die daraus resultierende gegenseitige Beeinflussung ist für eine materialgerechte Dimensionierung sowie die Dauerhaftigkeit von gemischt bewehrten Bauteilen von entscheidender Bedeutung. Die im Bereich von Rissen in die vorhandenen Bewehrungen einzuleitenden Kräfte und die dadurch verursachten unterschiedlichen Dehnungen in den Rissen können bisher allenfalls grob abgeschätzt werden.

Bei teilweise oder beschränkt vorgespannten Bauteilen wird insbesondere bei Ermüdungsbeanspruchung die Mitwirkung der Spannglieder aus Spannstahl oder Glasfaserverbundstäben in der Regel überschätzt. Daher besteht häufig die Gefahr, die im Querschnitt vorhandene schlaffe Bewehrung zu überfordern, was zu nicht mehr akzeptabelen Rißbreiten und damit zur Einschränkung der Gebrauchsfähigkeit des gesamten Bauwerks führen kann.

Zur Lösung dieser Fragen wurde vom Verfasser ausgehend von den Verhältnissen bei gemischt bewehrten Konstruktionen ein Rechenmodell erarbeitet, welches im Gegensatz zu den bisher üblichen Rechenansätzen Gleichgewicht und Verträglichkeit sowohl im Rißquerschnitt als auch im Einleitungsbereich zwischen den Rissen gleichermaßen berücksichtigt.

Im vorliegenden Beitrag wird die zugrundeliegende Modellvorstellung kurz erläutert, und die wesentlichen Einflußparameter werden kurz diskutiert.

2. ERMITTLUNG DER SPANNUNGEN UND VERSCHIEBUNGEN IN DEN RISSQUERSCHNITTEN GEMISCHT BEWEHRTER BAUTEILE

2.1 Modellierung

Die Abb. 1 zeigt einen gemischt bewehrten Dehnkörper mit Bewehrungselementen, die sich im Hinblick auf ihre Verbundeigenschaften, Elastizitätsmoduln, Durchmesser und Bewehrungsmengen unterscheiden können.

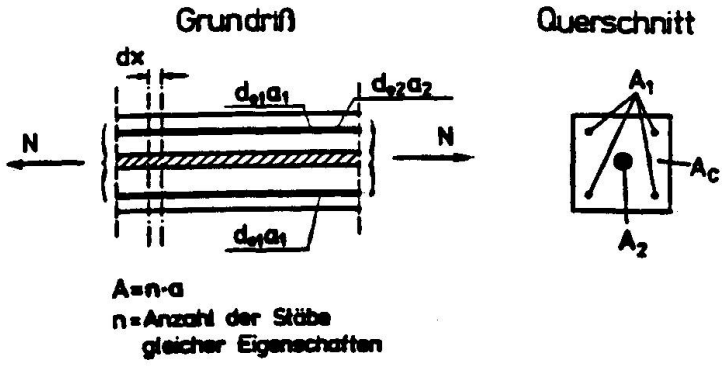

Abb. 1: Gemischt bewehrter Dehnkörper (schematisch)

Eine Betrachtung der Kräfte und Verschiebungen an einem Element der Länge dx führt für die Relativverschiebungen $s_i(x)$ der Bewehrungen gegenüber dem umgebenden Beton zu einem gekoppelten Differentialgleichungssystem 2. Ordnung für $s_i(x)$, welches in [1] detailliert hergeleitet wurde. Da die Relativverschiebungen der Bewehrungen von den jeweiligen nichtlinearen Verbundspannungs-Schlupf-Beziehungen $\tau_i = f(s_i)$ abhängig sind, bietet sich eine Lösung des Differentialgleichungssystem durch schrittweise Integration an.

Man erhält unter Zugrundelegung linearer Spannungs- und Verschiebungsverläufe sowie konstant über das Berechnungsintervall Δx verlaufende Verbundspannungen die folgenden Rechenbeziehungen:

$$\sigma_{1,2}(x+\Delta x) = \sigma_{1,2}(x) + \Delta\sigma_{1,2}(x) \quad (1)$$

$$\Delta\sigma_{1,2}(x) = \tau_{1,2}(x) * u_{1,2}/A_{1,2} * \Delta x \quad (2)$$

$$\sigma_c(x+\Delta x) = \sigma_c(x) + \Delta\sigma_c(x) \quad (3)$$

$$\Delta\sigma_c(x) = \tau_{1,2}(x) * u_{1,2}/A_c * \Delta x \quad (4)$$

Für die Relativverschiebungen ergibt sich hieraus:

$$s_{1,2}(x+\Delta x) = s_{1,2}(x) + \Delta s_{1,2}(x) \quad (5)$$

$$\Delta s_{1,2}(x) = \frac{\Delta x}{2 * E_{1,2}}\left(2\,\sigma_{1,2}(x) + \Delta\sigma_{1,2}(x)\right) - \frac{\Delta x}{2 * E_c}\left(2\,\sigma_c(x) + \Delta\sigma_c(x)\right) \quad (6)$$

Man erkennt, daß die Verteilung der Spannungen, Verbundspannungen und Relativverschiebungen beider Bewehrungen über die Betonspannungen miteinander gekoppelt sind. Die Rechenannahmen (Gln. (1) bis (6)) sind mit den von Eligehausen in [2] angegebenen Rechenbeziehungen identisch. Allerdings sind im vorliegenden Fall keinerlei "Symmetriebedingungen" vorhanden, wie gleiche Stabdurchmesser und E-Moduln sowie gleiche Verbundeigenschaften. Die schrittweise Lösung der Differentialbeziehungen erfordert deshalb ein besonderes Iterationsverfahren, welches in [1] erarbeitet wurde.

2.2 Stoffgesetze

Bei den theoretischen Parameterstudien wurden die Verbundspannungs-Schlupf-Beziehungen $\tau_i = f(s_i)$ für Betonstahl bzw. Spannstahl der Literatur ([3] - [5]) und diejenige für Bewehrungselemente aus kunstharzgebundenen Glasfaserstäben eigenen Untersuchungsergebnissen ([1]) entnommen. Das Spannungs-Dehnungs-Verhalten der Stahlbewehrungen wurde mit einem bilinearen $\sigma - \varepsilon$ - Gesetz (E_1 = 210.000 N/mm²) beschrieben. Das Spannungs-Dehnungs-Verhalten der verwendeten Glasfaserverbundstäbe wurde mit einer linear elastischen σ-ε-Linie (E_2 = 52.000 N/mm²) beschrieben. Die Werkstoffgesetze sind schematisch in Abb. 2 wiedergegeben.

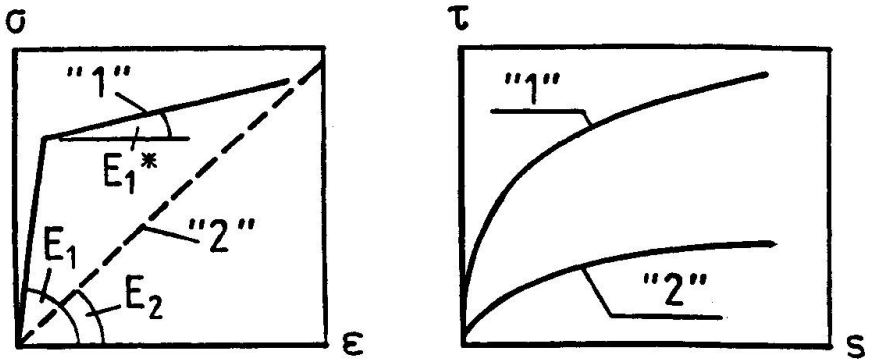

Abb. 2: Verwendete Werkstoffgesetze (schematisch)

Eine Überprüfung der Brauchbarkeit des Rechenmodells anhand der Ergebnisse von Zugversuchen an zentrisch beanspruchten Dehnkörpern, die mit konventionellen Betonstählen und sogenannten Hochleistungsverbund(HLV)-Elementen (Glasfaserstäbe) bewehrt waren, konnte mit sehr zufriedenstellendem Resultat vorgenommen werden ([1]).

3. ERGEBNISSE DER PARAMETERSTUDIEN

3.1 Relevante Einflußparameter

Die Höhe der Bewehrungsspannungen im Rißquerschnitt ist von einer Reihe unterschiedlicher Parameter abhängig. Bei den umfangreichen Parameterstudien in [1] wurden als wichtige Einflußgröße erkannt:

- Verbundqualität der Bewehrungen
- Im Verbund liegende Staboberflächen (Durchmesser)
- Elastizitätsmoduln der Bewehrungen
- Langzeitige und/oder nicht ruhende Beanspruchungen
- Bewehrungsmenge der jeweiligen Bewehrungen und Gesamtbewehrungsgrad
- Höhe der Beanspruchung

3.2 Gemischte Bewehrungen aus Betonstählen und Glasfaserstäben (HLV-Elemente)

Für das Studium des Verhaltens von Bauteilen, die mit konventionellen Betonstählen und Glasfaserstäben gemischt bewehrt sind, müssen die unterschiedlichen E-Moduln und die verschiedenen Verbundqualitäten Berücksichtigung finden. Für das Verhältnis der E-Moduln gilt:

$$E_{Stahl} / E_{HLV} = E_1/E_2 \approx 4 \qquad (7)$$

Vergleicht man die Verbundqualitäten dieser Bewehrungen, so läßt sich nach den Ergebnissen in [1] ein Verhältinswert angegeben von etwa:

$$\tau_{Stahl}(s) / \tau_{HLV}(s) = \tau_1(s) / \tau_2(s) \approx 4 \qquad (8)$$

Aus Gründen der Übersichtlichkeit wurden im hier diskutierten Rechenbeispiel gleiche Stabdurchmesser angenommen ($d_{Stahl} = d_{HLV}$; $d_{Stahl}/d_{HLV} = 1$).

Damit ergibt sich für den Zustand der Einzelrißbildung eine in der Stahlbewehrung ca. 4fach höhere Spannung als in der Glasfaserbewehrung: $\sigma_{r1}^{I}/\sigma_{r2}^{I} \approx 4$.

In der Abbildung 3 sind die Rechenergebnisse für die zuvor genannten Verhältnisse für den Zustand der abgeschlossenen Rißbildung unter Variation des mittleren Riβabstandes a_{rm} exemplarisch dargestellt. Aufgetragen ist die auf die mittlere Bewehrungsspannung σ^{II} im Zustand II bezogene Rißspannung σ_{r1} in Abhängigkeit der Beanspruchungshöhen σ^{II}. Ferner wurde als Scherparameter der Bewehrungsanteil der Glasfaserbewehrung "2" variiert:

$$\lambda = \mu_2/\mu = \frac{A_2}{(A_1 + A_2)} \qquad (9)$$

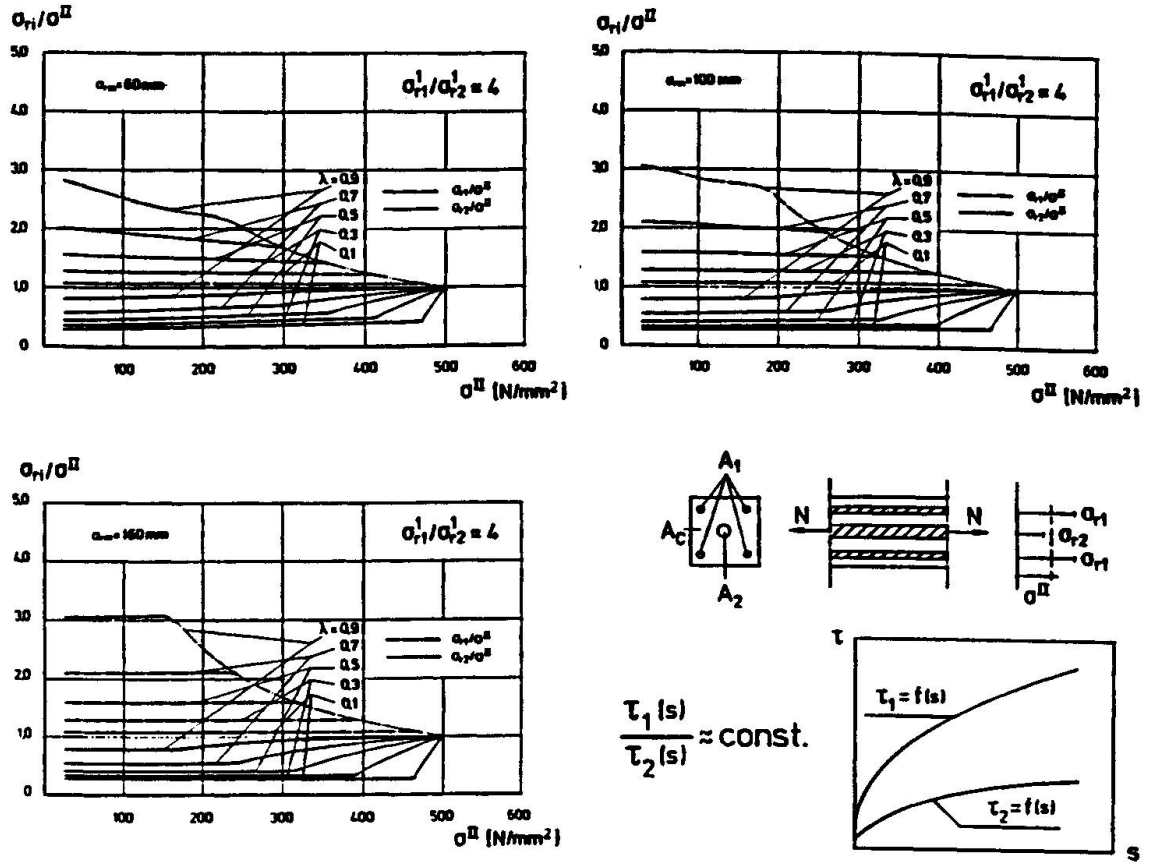

Abb. 3: Bezogene Spannungen im Riß σ_{r1} in Abhängigkeit der Beanspruchungshöhe σ^{II} und des Bewehrungsverhältnisses λ für verschiedene Rißabstände a_{rm}.

Aus der Darstellung ist zu entnehmen, daß die Unterschiede der Rißspannungen mit zunehmendem Rißabstand anwachsen. Bei großen Rißabständen sind demnach generell ungünstigere Verhältnisse zu erwarten. Unter Laststeigerung nehmen die Spannungsunterschiede bis zum Fließen der verbundsteiferen Stahlbewehrung (BSt 500/550) nur geringfügig ab. Die Höhe der bezogenen Rißspannungen ist daher nur wenig vom jeweiligen Lastniveau abhängig. Bei großen Rißabständen a_{rm} sind die bezogenen Spannungen im Riß im elastischen Dehnungsbereich der Bewehrungen praktisch unabhängig von der Belastungshöhe, und es stellen sich etwa die Verhältnisse wie bei der Einzelrißbildung ein.

Erwartungsgemäß wachsen die Spannungsunterschiede zwischen beiden Bewehrungen mit zunehmendem Bewehrungsanteil λ an. Bei einem geringen Anteil von Bewehrungsstäben mit guter Verbundqualität liegen demnach ungünstige Verhältnisse vor, und die verbundsteifere Bewehrung beginnt bereits bei vergleichsweise geringer äußerer Belastung zu fließen. Eine weitere Laststeigerung führt dann zu einem erheblichen Spannungszuwachs in der verbundweicheren Glasfaserbewehrung.

4. FOLGERUNGEN FÜR DIE PRAXIS

Im Hinblick auf das Tragverhalten verbundstabbewehrter Bauteile ist festzustellen, daß die auf die Glasfaserstäbe im Rißquerschnitt entfallenden Lastanteile wegen deren niedrigen Elastizitätsmoduls und wegen der im Vergleich zu üblichen Betonstählen schlechten Verbundqualitäten unbedenklich gering sind. Jedoch ist im Falle gemischt mit Betonstählen und Glasfaserstäben bewehrter Konstruktionen

stets zu überprüfen, ob die Betonstähle aufgrund der geringen Mitwirkung der Glasfaserbewehrung bei Rißbildung nicht unzulässig hohen Beanspruchungen ausgesetzt sind.

Bei langzeitiger und/oder nicht ruhender Beanspruchung der Bauteile können nach [1] bei Bewehrungen, die sich sowohl im Hinblick auf die Verbundcharakteristiken als auch im Verbundkriechverhalten stark voneinander unterscheiden, zusätzlich beträchtliche Spannungsumlagerungen infolge von Dauerlasten oder Ermüdungsbeanspruchungen von der verbundweicheren Glasfaserstabbewehrung zur verbundsteiferen Stahlbewehrung stattfinden.

5. LITERATUR

[1] FAORO, M.: Zum Tragverhalten kunstharzgebundener Glasfaserstäben im Bereich von Endverankerungen und Rissen in Beton. -Stuttgart: Fakultät 2, Universität Stuttgart, Dissertation 1988. IWB-Mitteilungen 1988/1

[2] ELIGEHAUSEN, R.: Übergreifungsstöße zugbeanspruchter Rippenstäbe mit geraden Stabenden. Heft 301, Deutscher Ausschuß für Stahlbeton. -Berlin: Verlag Wilhelm Ernst & Sohn 1979

[3] ELIGEHAUSEN, R.; POPOV, E. P.; BERTERO, V. V.: Local Bond Stress-Slip Relationships of deformed Bars under generalized Excitations. Earthquake Engineering Research Center, College of Engineering, University of California. -Berkeley: University of California 1983. Report No. UCB/EERC-83/23

[4] MARTIN, H.: Zusammenhang zwischen Oberflächenbeschaffenheit, Verbund und Sprengwirkung von Bewehrungsstählen unter Kurzzeitbelastung. Heft 228, Deutscher Ausschuß für Stahlbeton. -Berlin: Verlag Wilhelm Ernst & Sohn 1973

[5] TROST, H.; CORDES, H.; THORMÄHLEN, U.; HAGEN, H.: Teilweise Vorspannung - Verbundfestigkeit von Spanngliedern und ihre Bedeutung für Rißbildung und Rißbreitenbeschränkung. Heft 310, Deutscher Ausschuß für Stahlbeton. -Berlin: Verlag Wilhelm Ernst & Sohn 1980

[6] WOLFF, R.; MIESSELER, H.- J.: HLV-Spannglieder in der Praxis, Erfahrungen mit Glasfaserverbundstäben. In: beton. Heft 2/89, Seite 47-51

Pultruded Glass Fibre Reinforced Plastic Profiles

Profils pultrudés en composites fibres de verres

Glasfaserbewehrte Plastikprofile

Godfried DERVAUX
Civil Engineer
Ingenieursbureau Dervaux
Gent, Belgium

Luc TOUSSEYN
Civil Engineer
Ingenieursbureau Dervaux
Gent, Belgium

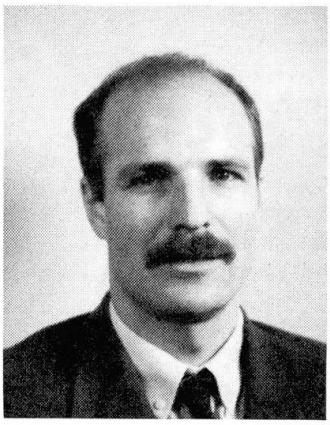

SUMMARY

In an electrolysis hall, the atmosphere is heavily loaded with sulphuric acid vapours. For that reason, the roof supporting structure consists of pultruded glass fibre reinforced plastic profiles. A three-dimensional framework, of which the profiles are glued together, is constructed. Composites have advantages over conventional materials, such as their high chemical resistance, their high specific stiffness and their high specific strength.

RÉSUMÉ

Dans un atelier où l'on pratique l'électrolyse, l'atmosphère est fort chargée par des vapeurs sulfuriques. Dès lors, la charpente est réalisée au moyen de profilés en matière plastique pultrudés et renforcés de fibres de verre. Les profilés sont collés les uns contre les autres dans un treillis spatial. Par rapport aux matériaux conventionnels, les composites offrent l'avantage d'une bonne résistance chimique, d'une grande rigidité spécifique et d'une parfaite solidité spécifique.

ZUSAMMENFASSUNG

Die Tragstruktur des Daches einer Elektrolysenhalle, deren Atmosphäre stark mit Schwefelsäuredämpfen angereichert ist, wird aus glasfaserverstärkten Kunststoffprofilen hergestellt. Ein räumliches Fachwerk, dessen Profile aneinandergeklebt sind, wurde entworfen. Verbundstoffe haben Vorteile gegenüber herkömmlichen Werkstoffen dank ihres guten chemischen Widerstandes, ihrer hohen spezifischen Steifigkeit und ihrer hohen spezifischen Festigkeit.

1. INTRODUCTION

To renovate the roof supporting structure of the electrolysis hall wind tunnel of an important zinc-works, the authorized departments opted for a supporting structure made of pultruded glass fibre reinforced plastic profiles.

The atmosphere in these electrolysis halls is heavily loaded with sulphuric acid vapours. That is why the existing reinforced concrete structure resulted inappropriate. The formation of etringite caused the reinforced concrete structure to crumble quite rapidly, so that a new structure was required.

In order to withstand this highly corrosive atmosphere, we have designed a GRP profile braced frame structure.

2. MATERIALS

2.1. Reinforcement

Glass fibres are used in a variety of forms as reinforcement in plastics. The forms of reinforcement and their positions are defined by the method of production of the final product, the properties required and the cost.
Compared to steel, glass fibres have a low stiffness modulus and a high tensile strength (see Table 1).

material	specific gravity	ultimate tensile strength (MPa)	ultimate compressive strength (MPa)	modulus of elasticity (GPa)	Poisson's ratio
polyester resin matrix	1.1-1.4	45-65	90-130	2.5-4.0	0.3-0.4
E-glass reinforcement	2.58	3450	-	72	0.2
structural steel	7.8	400-550	-	210	0.3
struct. aluminium alloy	2.8	200-450	-	70	0.3
concrete	2.4	3	40	15-35	0.1-0.3

Table 1 Comparison of the mechanical properties of various materials

After formation of E-glass into rovings or textile fabrics and after processing these into composites, the ultimate tensile strength of the E-glass is considerably reduced. The magnitude of the reduction, which varies from fibre to fibre, depends on the voids content, the nature and degree of handling, the amount of fibre misalignment,... For the determination of the working stress, see 3.2.

In order to minimize the size of the profiles and the deflections of the structure, the frame, the roof truss and the joints are made into braced structures. Hence, the profiles are not subjected to flexural strength, but only to tensile or compressive strength. Therefore special attention has been paid to buckling and the realization of the joints.

2.2. Matrix

In order to withstand the chemical corrosion of the sulphuric acid atmosphere, all GRP profiles have a vinylester matrix.

2.3. Production technique

The profiles are fabricated by means of pultrusion. The pultrusion process is one of the techniques designed for the production of a continuous product. The process consists of impregnating continuous glass strands and glass cloth in a resin bath before drawing them through a die to obtain the desired shape of the section. Due to the continuity of the reinforcement the final products possess an exceptionally high strength in the direction of the reinforcement.

2.4. Profiles

To realize the braced structures, two different profiles are used, i.e. a boxbeam 80/43/3 and a ⌊⌋-profile 90/30/3/5. The properties of the profiles will depend on the properties and the proportions of fibres and matrix (rule of mixture) :

$$C = C\ (E_f, \nu_f, G_f, V_f, E_m, \nu_m, G_m, Vm)$$

where the subscripts f and m refer to the fibres and matrix, respectively, E is Young's modulus, ν is Poisson's ratio, G is modulus of rigidity and V is proportion by volume in the composite. The properties of the profiles (in the longitudinal direction) are :

- Profile 80/43/3 : $E = 24$ GPa, $\nu = 0{,}3$, $G = 5$ GPa
- Profile 90/30/3/5 : $E = 28$ GPa, $\nu = 0{,}3$, $G = 5$ GPa

3. STRUCTURE

3.1. Description of the structure

The final structure has a total length of 43.40 m, a height of 5.15 m and a span of 5.65 m (see fig. 1 and fig. 2).

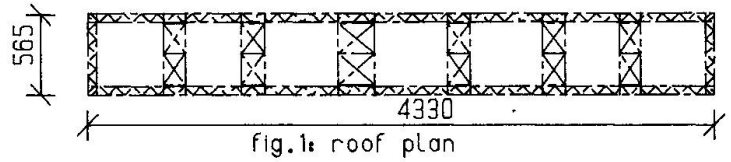

fig.1: roof plan

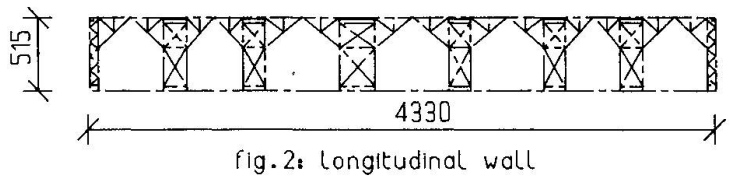

fig.2: longitudinal wall

In fact, a three dimensional trussed system is formed by two adjacent frames joined together, both in the vertical plane of the wall and the horizontal plane of the roof (see fig. 3 and fig. 4).

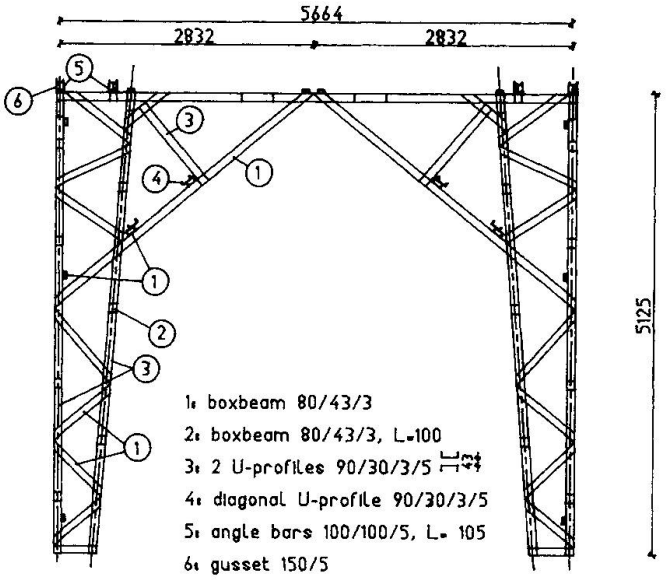

fig. 3: cross-section

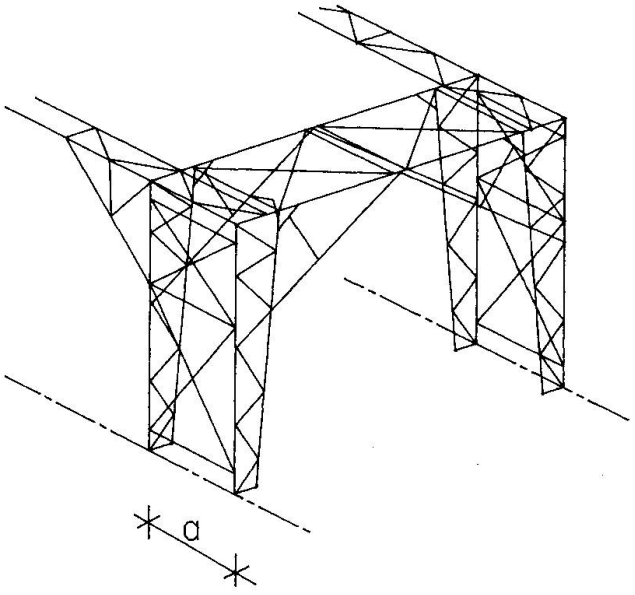

fig. 4: perspective truss

The two frames are placed at a distance "a", varying between 0.60 and 2.46 m. The frame units are placed at 6.50 m from each other. The frames are joined together in the roof plane by means of a roof truss, also braced. The frames are joined at the bottom to the existing structure by means of stainless steel elements.

3.2. Calculation of the frames

The loads working on the frames include the self-weight, the fixed loads of wall and roof covering, the snow loads and wind loads. All affecting loads were increased with a "load factor" of 1.5. With respect to GRP profiles, the average strain at rupture is assumed to be 1.5 % (short-term properties).

When a unidirectional glass fibre reinforced composite is subjected to compression in the direction of the reinforcement, the failure load appears to be controlled by buckling of the fibres. From the theoretical point of view, the ultimate compressive strength X_c is given by

$$X_c = \frac{G_m}{1 - V_f}$$

for values of $V_f > 0.2$
where G_m is the modulus of rigidity of the matrix and V_f is the proportion of the fibres by volume in the composite.
The experimental values of X_c tend to be much lower than those predicted by the analysis described in theoretical works. Failure occurs at a strain of approximately 1.2 %.

This failure strain value for tensile and compression leads to a varying ultimate stress according to the properties (E moduli) of the profiles concerned. In order to determine the working stress, a safety coefficient = 4 on this ultimate stress is taken into account. This safety coefficient covers the long-term failure behaviour.

Results from literature suggest that over a period of 50 years a unidirectionally continuously reinforced composite containing a reasonably high percentage of fibres may lose approximately 40 % of its short term stiffness. After a period of 30 years, the strength of glass-reinforced composites will be reduced to about 50 % of the short term strength. However, composites containing a high percentage of UD (= unidirectional) continuous reinforcement and loaded in the direction of the fibres may show rather more favourable characteristics.

3.3. Assembly of the structure

For GRP, adhesive joints are normally used because bolted joints can shear out under load.

The profiles are joined together by means of epoxy adhesive and stainless steel rivets. These rivets are mainly used to obtain a certain pressure during glueing; this results in a perfect adhesive joint.

Several kinds of joints are applied (see fig. 5). In order to resist great tensile forces, the area of adhesion can be considerably increased as in fig. 5b en c.

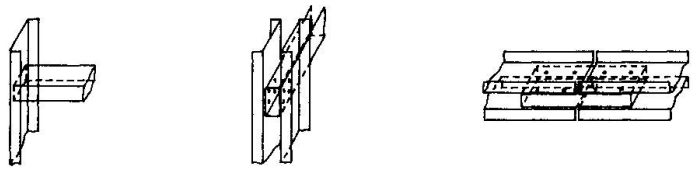

a b c

fig. 5: joints

The length of the joints is calculated assuming that the adhesive has a shear strength τ_{au}. Thus, for sheets of thickness t, and a joint length of L_j, the single lap joint can transmit a stress σ_{ju} where

$$\sigma_{ju} = L_j \cdot \tau_{au} / t$$

Most of the joints are factory made. So, we can immediately reckon upon its strength and we have a better quality control of the joints. A few of them are site made.

4. CONCLUSION

This realization opens new perspectives for the application of GRP structures in chemical industry; especially, in structures with considerable spans at little loads.

These profiles have some major advantages, thanks to their high chemical resistance, their high specific stiffness (EI/δ) and their high specific strength (σ_{fr}/δ), with a very low specific gravity δ.

BIBLIOGRAPHY

1. M. HOLMES and D.J. JUST, GRP in Structural Engineering, Applied Science Publishers Ltd, 1983.

2. S. LAROZE and J.-J. BARRAU, Mécanique des Structures, Tome 4, Calcul des structures en matériaux composites, Eyrolles Masson, 1987.

Application of Carbon Fiber Reinforced Cables to Concrete Structures

Application des câbles renforcés par fibres de carbone aux structures en béton

Verwendung von kohlenstoffaserverstärkten Drahtseilen in Betonbauwerken

H. MUTSUYOSHI
Assoc. Prof.
Saitama University
Saitama, Japan

Hiroshi Mutsuyoshi, born in 1953, received his Dr. Eng. degree from the Univ. of Tokyo in 1984. His research interests are development of new materials and seismic problems of reinforced concrete structures.

A. MACHIDA
Professor
Saitama University
Saitama, Japan

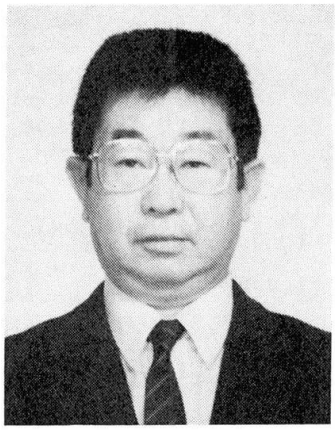

Atsuhiko Machida, born in 1940, received his Dr. Eng. degree from the Univ. of Tokyo in 1976. His research concerns composite structures, seismic design of concrete structures and construction materials.

N. SHIRATORI
Manager
Tokyo Rope Co., Ltd.
Tokyo, Japan

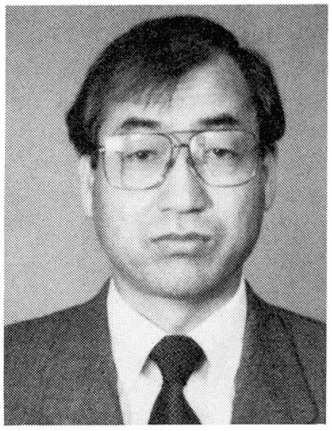

Nobuyoshi Shiratori, born in 1943, received his M. Eng. degree from Tohhoku Univ. in 1969. He has been engaged in development of new materials in Tokyo Rope MFG. Co., Ltd.

SUMMARY

This paper describes the fundamental mechanical properties and the design method for concrete members using carbon fiber reinforced cables as the main reinforcement in place of steel tendons and reinforcing bars.

RÉSUMÉ

Dans cet article sont décrites les caractéristiques mécaniques fondamentales et les techniques de conception et de calcul des éléments en béton dans lesquels les câbles renforcés par fibres de carbone sont utilisés en tant que matériaux principaux de renforcement à la place des câbles de précontrainte ou des aciers pour béton armé.

ZUSAMMENFASSUNG

In der vorliegenden Abhandlung werden die grundsätzlichen dynamischen Eigenschaften und Konstruktionsmethoden von Betonbauteilen mit kohlenstoffaserverstärkten Drahtseilen untersucht, die als Spannglieder oder anstelle von Stahlbewehrungen eingesetzt werden.

1.INTRODUCTION

Recently, deterioration of durability of concrete structures due to corrosion of steel has become a serious social problem. Furthermore, steel may not be used as reinforcements for the structures used for linear motor trains, which are being planned in Japan and run by strong magnetic power, because steel can be easily magnetized. Only traditional steel and concrete may not satisfy sufficiently the requirements for future structures. New materials which are stronger, lighter and have better characteristics against corrosion than conventional steel are strongly required. Carbon fiber composite cable, called CFCC in this paper, developed recently is one of new structural materials which can satisfy the above requirements. This paper describes the applicability of CFCC to actual concrete structures as main reinforcements in place of steel tendons and reinforcing bars.

2.CHARACTERISTICS OF CFCC

Fiber reinforced composite material, such as glass fiber reinforced plastics(GFRP), aramid fiber reinforced plastics(AFRP) and carbon fiber reinforced plastics(CFRP), have been developed recently as structural reinforcements. Table 1 shows their general fundamental characteristics. Comparing each characteristics of them, it is clear that CFRP is the most appropriate material among them as reinforcements for concrete structures. Carbon fiber composite cable(CFCC), shown in Fig.1, made by twisting high strength continuous carbon fibers impregnated with resin has some excellent properties such as 1)high tensile strength and high bond strength in concrete, 2)light weight, 3)non-corrosion, 4)non-magnetization, 5)very small relaxation loss comparing with steel tendons and 6)flexibility like cables. Figure 2 shows a typical stress-strain relation of CFCC and a steel tendon under uniaxial tensile load, and Table 2 indicates the mechanical properties of them. Note that CFCC finally fails in a brittle manner without showing a yield point and a yield plateau like steel as shown in Fig.2.

Characteristic	Steel	CFRP	AFRP	GFRP
Tensile Strength	○	○	○	△
Elongation	○	△	△	△
Elastic Modulus	○	△	×	×
Relaxation and Creep	○	○	×	△
Fatigue Strength	○	○	○	○
Alkali Proof	○	○	△	×
Corrosion Resistance	×	○	○	○
Specific Gravity	×	○	○	○
Magnetization	×	○	○	○

○ ; Excellent, △ ; Poor, × ; Bad

Table 1 General characteristics of FRP

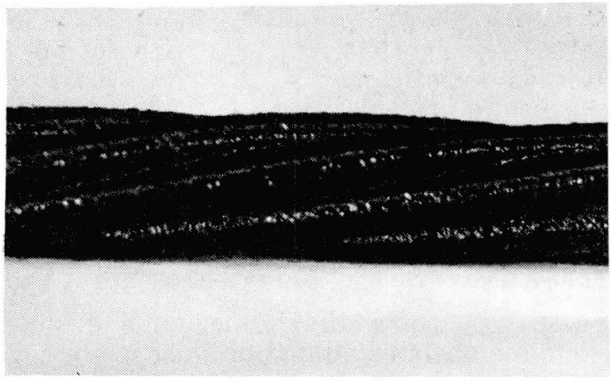

Fig.1 Carbon fiber composite cable

3.APPLICATION OF CFCC TO PC MEMBERS

In order to use the high strength of CFCC effectively, the applicability of CFCC to PC members was investigated. Figure 3 shows the details of the test beams. All beams were cured in wet condition for one month after placing of concrete, and then prestress was

Mechanical Properties	Steel Tendon	CFCC
Tensile Strength (MPa)	1460	1803
Elongation (%)	>3.0	1.5
Young's Modulus (GPa)	201	123
Bond Strength (MPa)	——	4.2

Table 2 Mechanical properties

introduced. An anchorage device consists of nuts and steel tubes. The loosened strands, the length of which is 20 cm from each end of CFCC, are fixed with resin in the steel tube. This anchorage device was used also for uniaxial tensile tests and bond tests. No damage was observed even at the failure of CFCC in the tensile tests. The magnitude of the design prestress was 40 to 60% of the tensile strength. The prestress was introduced by controlling an oil jack with a load cell installed on an anchorage plate. To compare the behaviour of PC members using CFCC with that using steel tendons, the test beams using ordinary steel tendons were made in the same manner as those using CFCC. Table 3 indicates the experimental variables. All beams were tested up to the failure under monotonic loading. The average loss of the introduced prestress just before the tests was about 5% in all beams.

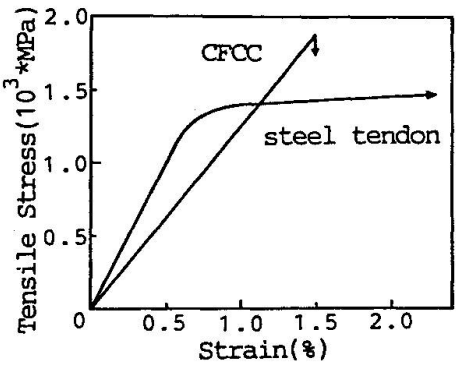

Fig.2 Stress-strain curve

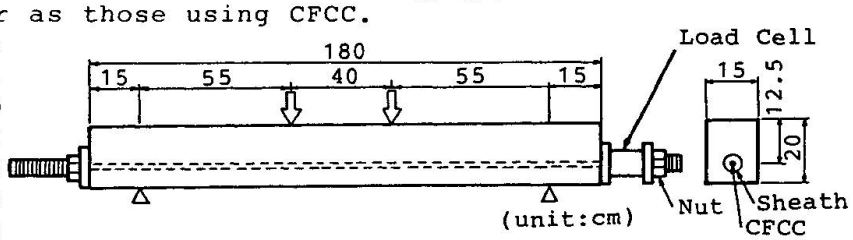

Fig.3 Details of test beams

Figure 4 shows the load-deflection curves of Beams A1, A2, B1, B2, C3 and D3. Comparing Beam B1(steel tendon) with Beam B2(CFCC), both beams showed almost the same stiffness and behaviour before the initial cracking. The difference of the maximum strength between both beams may depend on the magnitude of the introduced prestress and the amount of the CFCC and the steel tendons. After the maximum strengths in both beams, the loads decreased gradually. Beam B1 reached the ultimate state with the failure of concrete after yielding of the steel tendon while Beam B2 failed finally due to crushing of the concrete in the compression zone. In Beams C3 and D3, they showed ductile behaviour until the failures.

Beam No.	Material (Number X Diameter)	Bond Type	Introduced Prestressing Stress (MPa)(*)	Concrete Strength (MPa)
A1	CFCC (ϕ10.5)	A	694 (0.42)	53.7
A2	CFCC (ϕ10.5)	C	695 (0.43)	53.7
B1	steel tendon (ϕ13)	A	1012 (0.74)	51.3
B2	CFCC (2Xϕ12.5)	A	2X878 (0.44)	51.3
C1	steel tendon (ϕ13)	A	536 (0.39)	53.7
C2	steel tendon (ϕ13)	A	573 (0.41)	51.3
C3	CFCC (ϕ12.5)	A	879 (0.44)	53.7
D1	CFCC (ϕ12.5)	B	1329 (0.67)	45.4
D2	CFCC (ϕ12.5)	A	1224 (0.61)	45.4
D3	CFCC (ϕ12.5)	B	954 (0.48)	45.4

A;Perfect bond. B;Vinyl tape was wrapped around CFCC to reduce bond strength. C;Unbond method.
*;(Introduced Prestress/Tensile Strength)

Table 3 Experimental variables

The CFCC of Beam C3 finally broke due to its high bond strength and brittleness, and the load decreased suddenly after breaking of CFCC. The beam seemed to be failing showing some warning until the collapse even if CFCC finally broke. However, such a failure mode should be avoided as far as possible in actual structures. On the other hand, Beam D3, the bond strength of which was reduced by wrapping a vinyl-tape around CFCC, showed ductile behaviour up to the failure without breaking of CFCC. As a matter of fact, Beam A2, which is an unbonded system, showed a ductile load-deflection behaviour though its maximum strength was smaller than that of Beam A1, which is a bonded system and failed due to breaking of CFCC. It is clarified that CFCC can be used as suitable tendons for

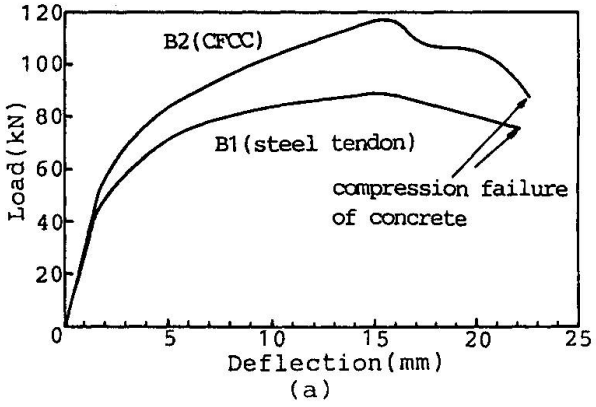

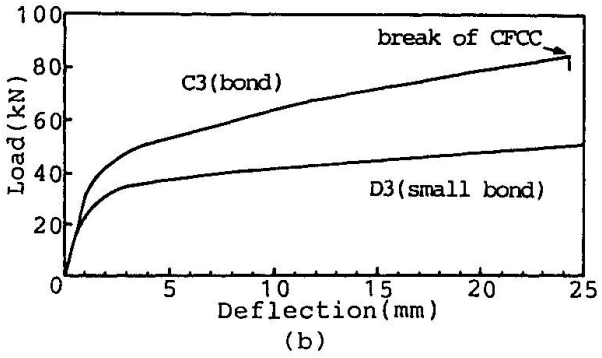

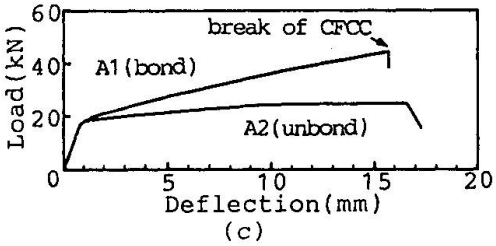

Fig.4 Load-deflection curves

PC members in place of ordinary steel tendons if the magnitude of introduced prestress and the bond strength are appropriately designed.

4.APPLICATION OF CFCC TO R/C MEMBERS

This chapter describes the applicability of CFCC to concrete members as non-prestressed main reinforcements in place of reinforcing steel bars. Flexural behaviour of concrete members using CFCC was mainly studied. The dimensions of the test specimens used for the tests were the same as those of the previous ones. The specimens were designed changing the amount of CFCC and compressive strength of concrete in order that three final failure modes may occur, namely, 1)breaking of CFCC, 2)crushing of concrete in the compression zone and 3)the balanced failure. The properties of the test specimens are shown in Table 4. Load was applied monotonically to each specimen up to the failure.

Beam No.	CFCC	Concrete Strength (MPa)	Cracking Load (KN)		Ultimate Load (KN)		Failure Mode
			Cal.	Exp.	Cal.	Exp.	
F 1	2Xϕ7.5	29.3	10.9	8.8	60.5	60.5	●
F 2	2Xϕ12.5	33.8	12.3	10.0	94.0	91.8	○
F 3	4Xϕ12.5	32.2	12.0	11.8	114.8	122.2	○
F 4	2Xϕ7.5	65.7	19.4	13.2	63.3	61.4	●
F 5	4Xϕ12.5	64.3	19.6	19.3	181.9	166.3	○
S 6	2XD16	60.4	19.4	14.4	70.3	74.2	*

S6 ; Usual deformed bars were used.
○ ; Concrete in compression zone failed finally.
● ; CFCC was finally broken.
* ; Flexural tensile failure.

Table 4 Experimental variables and test results

Figure 5 shows the load-deflection curves of Specimens F4(CFCC), F5(CFCC) and S6(ordinary reinforcing bar). The initial cracks were produced at relatively small loading stages in all specimens, and after initial cracking, the loads of F4 and F5 increased linearly. Since the stiffness of F4 and F5 after initial cracking, which depend on the

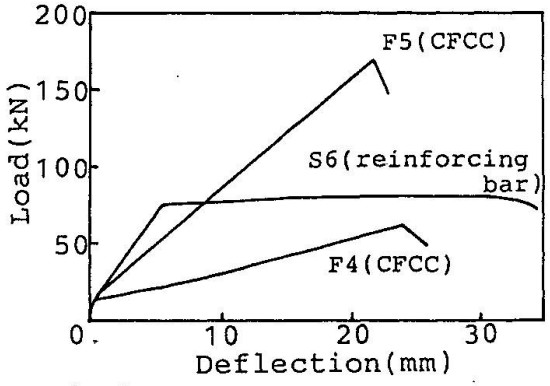

Fig.5 Load-deflection curves

amount of CFCC, became smaller than that of S6 due to the low Young's modulus of CFCC, the deflections of F4 and F5 at the maximum strength were clearly larger than that of S6. The ultimate failure mode was due to either breaking of CFCC or crushing of concrete as expected in the design of the specimens, so that the loads of F4 and F5 at the ultimate state decreased suddenly without showing any warning of approaching the beam failure. Figure 6 shows the moment-curvature relations obtained from the tests and analysis. The curvature was obtained from two displacement transducers installed at the compression and tension sides of the beam. The theoretical moment-curvature relation was obtained from the ordinary flexural theory assuming the stress-strain curve of CFCC and concrete. The calculated values agreed well with the experimental ones. The loads at the initial cracking and the ultimate state obtained from the tests and analysis are shown in Table 5. These results indicate that the usual flexural theory used for reinforced concrete also can be applied for concrete members reinforced with CFCC.

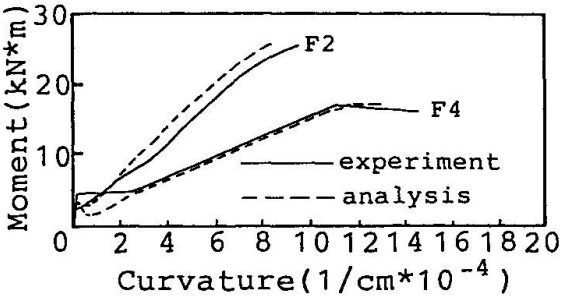

Fig.6 Moment-curvature relation

5. PROPOSAL OF DESIGN CONCEPT FOR CONCRETE MEMBERS USING CFCC

Though CFCC has some excellent properties, it has also some mechanical defects such as a low Young's modulus and a small elongation at failure comparing with steel. However, as described above, it was clarified that CFCC can be used for concrete members if design factors are properly selected. Applying CFCC to actual concrete structures as main reinforcements in place of reinforcing bars or steel tendons, the main problem is how the structure should be designed reasonably as well as safely. When concrete structures are designed, it is well known that the limit state design method, based on an ultimate state, a serviceability state and a fatigue state of a structure, is the most reasonable one. This chapter describes one example of flexural design concepts for concrete members using CFCC based on the ultimate limit state. The ultimate flexural failure mode of the concrete members using CFCC is classified into 1)breaking of CFCC and 2)crushing of concrete. It was proved that if CFCC breaks finally, the whole member will fail suddenly. On the other hand, in the case of a compression failure of concrete, the load also may decrease suddenly. However, the concrete in a compression zone can be strengthened by arranging CFCC as compression reinforcements and confining the concrete with ties to prevent the member from failing suddenly. Furthermore, controlling the bond condition of CFCC by wrapping with a tape is also a appropriate method to avoid the sudden failure. Consequently, the following assumptions were made for the flexural design concept:

1)the concrete in the compression zone fails before breaking of CFCC at the ultimate state,
2)the high strength of CFCC is used effectively at a serviceability state as well as an ultimate state without breaking.

Figure 7 shows the relation between $Mu/(b*d^2*fc')$ and $As*fsd/(b*d*fc')$ changing the ratio of introduced prestress to the specified tensile strength of CFCC from 0 to 0.8, where Mu=ultimate resisting moment, b, d=width and effective depth of a cross section respectively, fc'=compressive strength of concrete, As=area of CFCC and fsd=specified tensile strength of CFCC. In addition to the above relation, Fig. 7 also shows the relation between $As*fsd/(b*d*fc')$ described above and the ratio of the stress of CFCC at Mu to the specified tensile strength of CFCC under the same variables as the previous ones. The specified

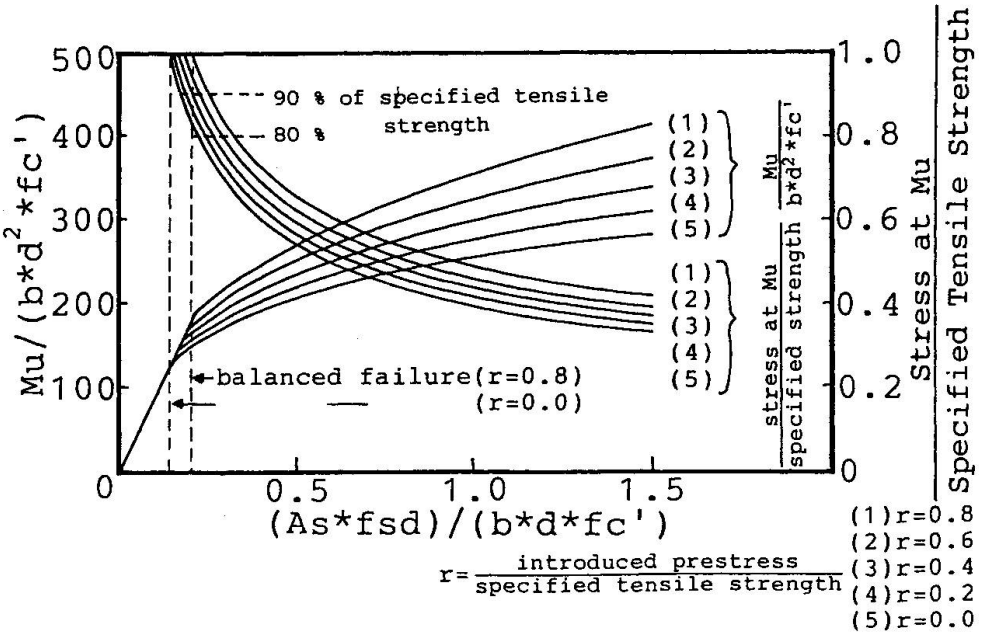

Fig.7 Flexural ultimate state of rectangular beam reinforced with CFCC

tensile strength of CFCC was defined as follows; $fsd=\overline{fs}-3*\sigma$, where $\overline{fs}$=average tensile strength of CFCC and σ=standard deviation obtained from a number of tensile test results.

Based on the first assumption, the value of As*fsd/(b*d*fc') must be in the right part of the balanced failure line drawn with broken lines in Fig.7 because a compression failure of concrete must occur before breaking of CFCC at the ultimate state. Furthermore, supposing that the available stress limit of CFCC at Mu is between 80 and 90 % of the specified tensile strength of CFCC according to the second assumption, the range of (As*fsd/b*d*fc') can be determined depending on the magnitude of the introduced prestress. The concrete member reinforced with CFCC can be designed efficiently as well as safely in accordance with this method. The proposed design concept is only one example based on the ultimate limit state. Moreover, the other design concepts on serviceability and fatigue should be also investigated in the future.

6. CONCLUSIONS

Carbon fiber composite cable(CFCC), which has some excellent properties such as high tensile strength, light weight, non-corrosion, non-magnetization, and flexibility like cables, can be used for concrete structures as main reinforcements in place of ordinary steel tendons and bars. In order to use CFCC efficiently for concrete members, the flexural design concept was proposed newly based on the ultimate limit state.

REFERENCES

1. Report of Shinmiya bridge containing new material. Dept. of Civil Engineering in Ishikawa Pref. in Japan, October 1988
2. Standard Specification for Design and Construction of Concrete Structures, Part 1(design), Japan Society of Civil Engineers, 1986

Degree of Safety in Mixed Structural Systems

Degré de sécurité dans les systèmes à structures mixtes

Sicherheitsgrad im Mischbauwerksystem

Boris ANDROIC
Senior Lecturer
University of Zagreb
Zagreb, Yugoslavia

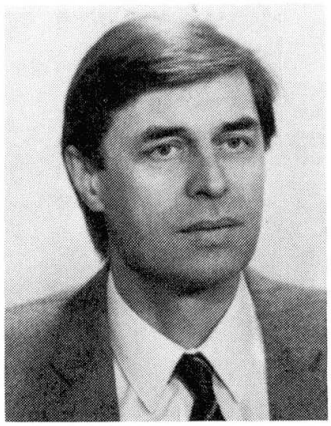

Boris Androic, born 1944, received Ph.D. from Zagreb University. Since 1986 Senior Lecturer at Civil Engineering Faculty, Zagreb Univ.

Vuk MILCIC
Professor
University of Zagreb
Zagreb, Yugoslavia

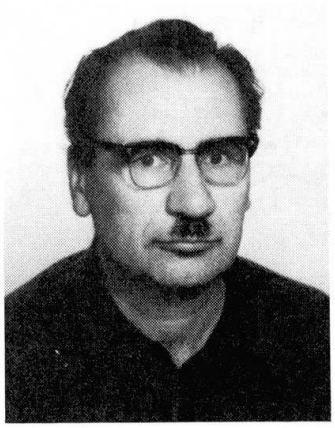

Vuk Milcic, born 1921, At present he is Professor at Civil Engineering Faculty, Department of Steel Structures, Zagreb University.

N. MUJKANOVIC
Res. Assistant
University of Zagreb
Zagreb, Yugoslavia

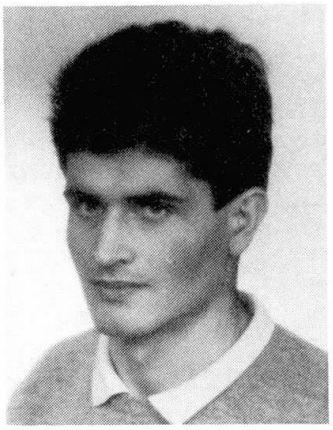

Nijaz Mujkanovic, born 1961. Since 1987 has been working at Civil Engineering Institute. At present he is Assistant Lecturer in Steel Structures, Zagreb University.

SUMMARY

A probabilistic analysis of mixed structural elements can be used to equalize the degree of safety of several layers in various limit states. The method has been illustrated by means of a practical example for the manufacturer of these elements.

RÉSUMÉ

L'analyse probabilistique des éléments de structures mixtes peut être utilisée pour égaliser le degré de sécurité de plusieurs couches dans les divers états limites. La méthode est présentée à l'aide d'un exemple pratique par les fabricants de ces éléments.

ZUSAMMENFASSUNG

Mit der probabilistischen Analyse von Verbundkonstruktionselementen ist es möglich, die Sicherheitsgrade verschiedener Schichten in den Grenzzuständen auszugleichen. Die Methode wird an einem praktischen Beispiel dargestellt.

1. INTRODUCTION

The calculation of internal forces in elements composed of several layers of different materials is based on the theory elaborated in [1]. The appearance of new materials has greatly increased the choice of mixed layered elements used in civil engineering.

In this, the materials in the various layers have very different mechanical properties and modes of bearing capacity loss. This points to the fact that safety verification based on present methods cannot include the problems of equalizing the safety of individual layers.

Since the standards are inadequate, it is not possible to prescribe the bearing capacity of equalized safety degree according to the chosen safety indices . As a result, the composite elements are not safe enough or economical.

The problem of practical application is analyses for the manufacturer and safety equalization of different layers in composite elements, bringing the damage or failure risk in individual layers to the levels prescribed by the society and required by the regulations.

2. LIMIT STATES EQUATIONS

The differential equation of the deflection line caused by flexural and shear deformations in a multi-layered element loaded with a transversal action is presented in [1]. The solution consists of the homogeneous part w_h and the particular part w_p:

$$w_h = C_1 + C_2 \cdot x + C_3 \cdot e\exp\left[(x-l)\sqrt{\frac{B \cdot A}{B_s \cdot B_d}}\right] + C_4 \cdot e\exp\left[-x\sqrt{\frac{B \cdot A}{B_s \cdot B_d}}\right] + M_L\left(\frac{x^3}{6 \cdot B \cdot l} - \frac{x^2}{2}\right) - M_R \frac{x^3}{6 \cdot B \cdot l} \quad (1)$$

$$w_p = \frac{q}{2 \cdot B}\left[\frac{x^4}{12} - \frac{x^3 l}{6} + \frac{x^2 B_s}{A}\left(\frac{B_d}{B} - 1\right)\right] - \frac{x^2 \cdot B_s \cdot \vartheta}{2 \cdot B} \quad (2)$$

The symbols are taken from [1]. Equations (1) and (2) contain an indefinite vector $k^T\{C_1, C_2, C_3, C_4, M_L, M_R\}$ for which the equations with six known border conditions have to be determined. If the element consisting of n continuous fields is observed, where the field is a part of an element with an uninterrupted function for continuous transversal loading, $6 \cdot n$ border conditions or rather continuity conditions for internal characteristic points have to be defined. This yields a system consisting of $6 \cdot n$ linear equations accompanied by vector k with $6 \cdot n$ unknown constants. The system in the matrix form is:

$$\{w\} = [z] \cdot \{k\} + \{s\} \quad (3)$$

where: $\{w\}$ - displacement vector , $[z]$ - coefficients matrix,
$\{k\}$ - unknown coefficients vector , $\{s\}$ - load vector.

Further analyses are made if the statical system of the element is a field with two supports. The cross-section of the element consists of three mixed layers. The element is used for the facade, and its resistance to wind was tested.

From the safety aspect, i.e. the probability of bearing capacity failure, there is a margin between the safety and non-safety zone in an n-dimensional vector space, and this margin is expressed with a limit state equation:

$$Z = G(X,K) = 0 \tag{4}$$

where: Z - safety margin, G - bearing capacity value function, X - basic variables vector, K - deterministic parameters vector.

In an element mixed of three layers, four limit state equation can be written:

1. Ultimate limit state of the compressive face:

$$Z_1 = X_6 \sqrt[3]{K_3 X_4 X_5} - \frac{X_8 K_1^2}{8 X_1 X_2} = 0 \tag{5}$$

2. Ultimate limit state of the tensile face:

$$Z_2 = X_3 - \frac{X_8 K_1^2}{8 X_1 X_2} = 0 \tag{6}$$

3. Ultimate limit state of the core:

$$Z_3 = X_7 - \frac{X_8 K_1}{2 X_2 K_2} = 0 \tag{7}$$

4. Serviceability limit state of the element:

$$Z_4 = \frac{K_1}{K_6} - \frac{5 X_8 K_1^4}{192 K_3 X_1 X_2^2} - \frac{X_8 K_1^2}{8 X_5 X_2 K_2} - \frac{K_4 K_5 K_1^2}{8 X_2} = 0 \tag{8}$$

The symbols and meanings of the basic variables and of the deterministic parameters are shown in Table 1.

3. TEST SPECIMENS AND STATISTICAL DATA

Statistical data of the mechanical properties of the layers and of geometrical characteristics of the element are obtained by tests and measurements on random samples from the manufacture, and the result can be considered to represent the real situation in the manufacture. The results are shown by histograms in Fig.1.
Statistical values of the basic variables and deterministic parameter values are comprehensively presented in Table 1.

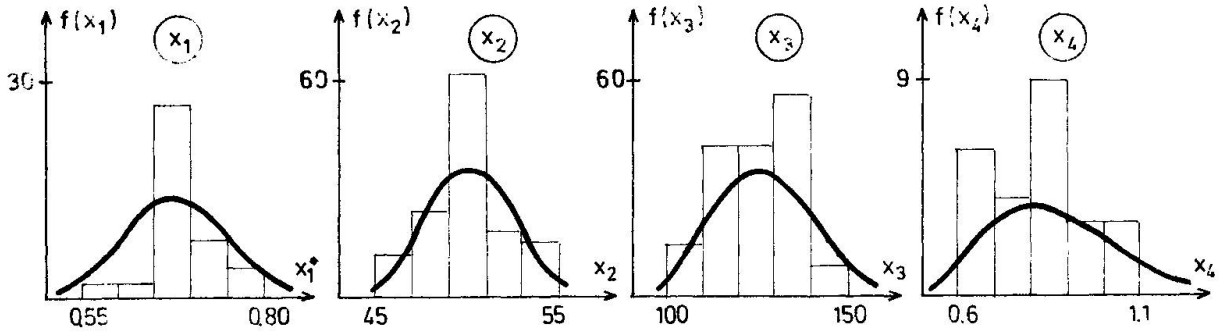

Fig.1a Histograms of basic variables X_1, X_2, X_3, X_4

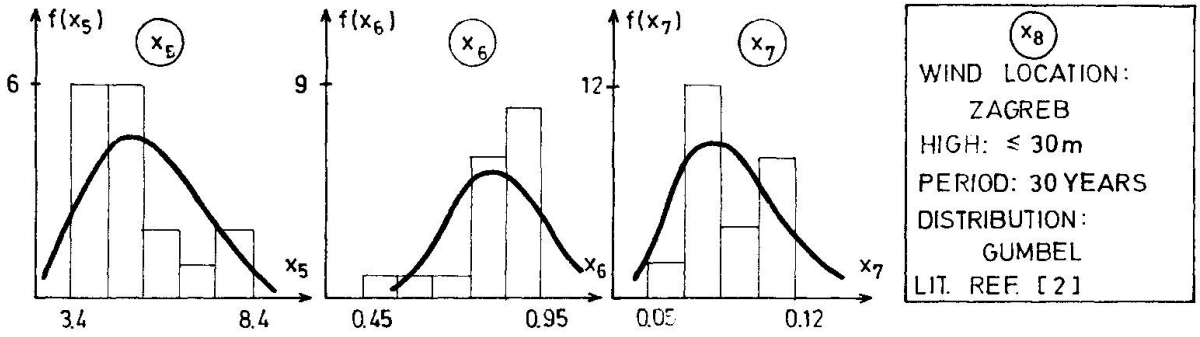

Fig.1b Histograms of basic variables X_5, X_6, X_7, X_8

BASIC VARIABLES $[\vec{X}]$				
VARIABLES	MEAN VALUES	C.O.V.	DISTRIBUTION	
X_1	720 mm^2	0.07	NORMAL	METAL FACE AREA ($X_1 = X_1^* \cdot K_2^*$)
X_2	51 mm	0.03	NORMAL	CENTROID DISTANCE THE FACES
X_3	126 N/mm^2	0.08	NORMAL	YIELD STRENGTH
X_4	8.1 N/mm^2	0.20	LOGNORMAL	ELASTICITY MODULUS OF THE CORE
X_5	5.0 N/mm^2	0.24	LOGNORMAL	SHEAR MODULUS OF THE CORE
X_6	0.812	0.15	LOGNORMAL	FACE BUCKLING COEFFICIENT
X_7	0.085 N/mm^2	0.24	LOGNORMAL	CORE SHEAR STRENGTH
X_8	850 N/m^2	0.28	GUMBEL	UNIFORMLY DISTRIBUTED LOAD
DETERMINISTIC PARAMETERS $[\vec{K}]$				
$K_1 = l$ SPAN OF ELEMENT				$K_2 = b$ WIDTH OF ELEMENT
$K_3 = 70\,000\ N/mm^2$ FACE MODULUS OF ELASTICITY				$K_4 = \alpha_T$ TEMP. COEFFICIENT OF FACES
$K_5 = \Delta T$ TEMP. DIFFERENCE OF FACES				$K_6 = k$ DEFLECTION LIMIT

Table 1 Data for limit states equations

The value of k^* presents the element face length.

4. EQUALIZATION OF SAFETY DEGREE

If statistical values of the basic variables and deterministic parameters from Table 1 are inserted in the limit states equations, safety indices for ultimate limit states and serviceability limit state for various displacement limits are obtained, as shown in Fig.4 and Fig.5.
If the required design value, i.e. safety index for the ultimate limit state $\beta_f = 4.2$ and for the serviceability limit state $\beta_f = 2.0$, the safety equalization is achieved by looking for adequate spans and displacement limits satisfing the required criteria, according to Fig. 2 and 3:
a/ for the ultimate limit state :

$$\beta_1, \beta_2, \beta_3 \Rightarrow \beta_{min} \geq \beta_f = 4.2 \qquad (9)$$

b/ for the serviceability limit state :

$$\beta_4 \geq \beta_f = 2.0 \quad ; \quad \beta_4 = f(K_6) \qquad (10)$$

For example, the chosen span $l = 2.0$ m, $\beta_{min} = \beta_3 = 4.33 > \beta_f = 4.2$ and

the permissible displacement limit 1/150, yield $\beta_4 = 3.61 > \beta_f = 2.0$. Besides safety equalization to the safety index design values, the remaining two β_i in expression (9) can be equalized to the minimum one. This can be done by selecting the materials of lower qualities, by decreasing the cross-section of the layers, etc. Sensibility coefficients α_i show immediately which changes of the basic variables will yield effective results.

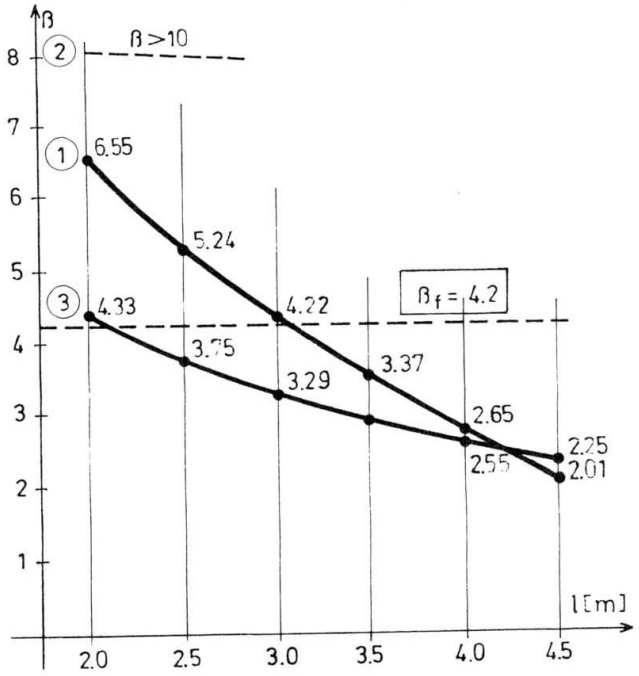

Fig.2 Safety index for ultimate limit states

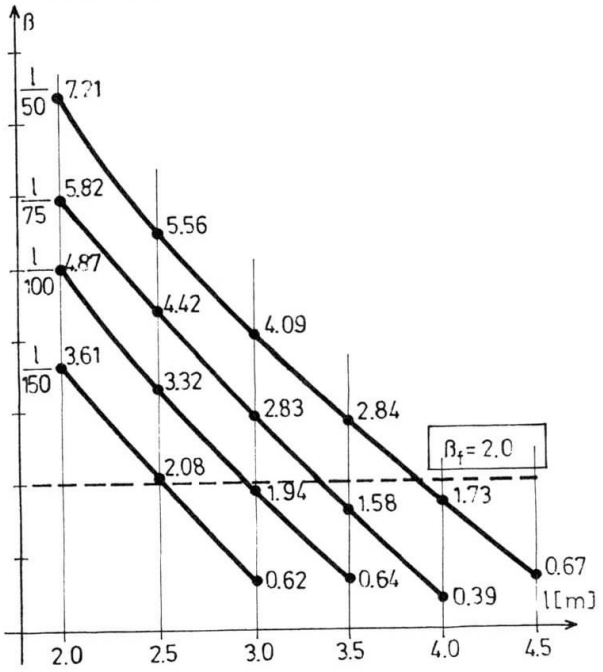

Fig.3 Safety index for serviceability limit state

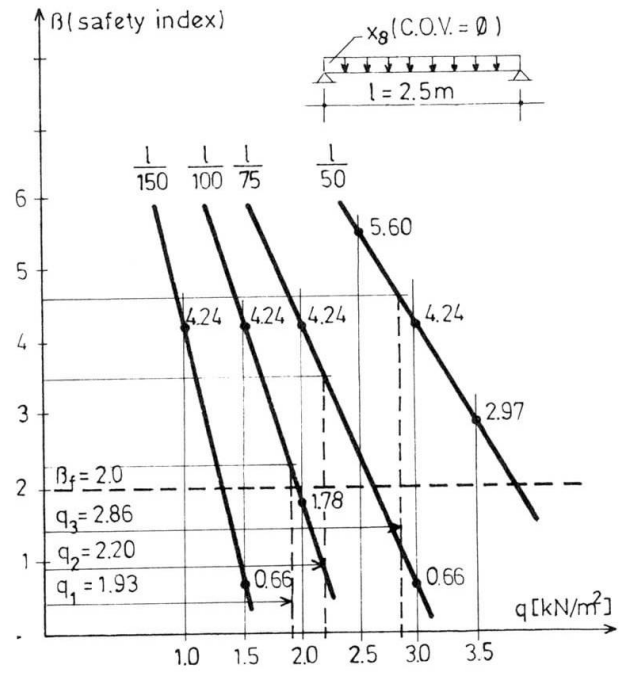

Fig.4 Serviceability limit state for displacement limit

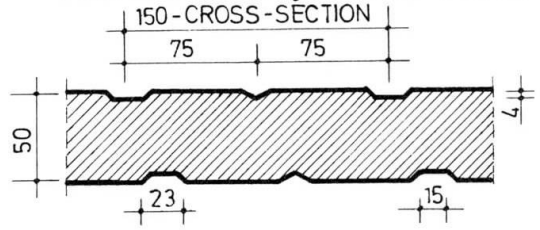

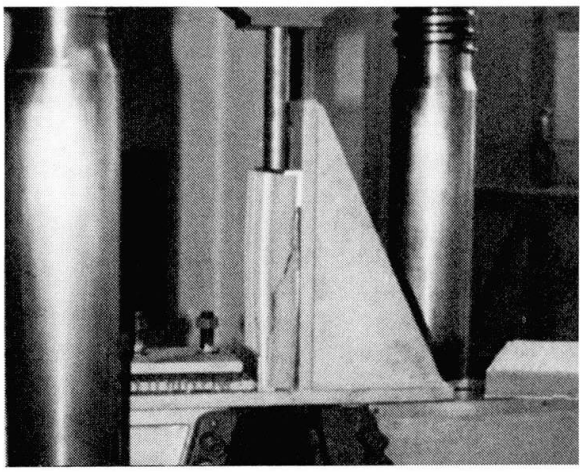

Fig.5 Laboratory testing for shear

Tests on three elements with a span of 2.5 m have shown that, at failure, their loads were q_1, q_2 and q_3. They satisfied the displacement limits 1/110, 1/90 and 1/70 in relation to $\beta_f = 2.0$ (Fig. 4). Fig. 5 shows laboratory testing of shear characteristic of the specimen.

5. DISCUSSION

The results obtained by laboratory testing and by numerical analyses can be discussed regarding the following statements:

The safety indices for tensile face β_2 obtained from the limit state equation (6) are very high as expected.

Safety equalization of individual faces is done in two steps. The first step is with regard to the design values β_f and the second is by decreasing the required basic variable values.
Note: when equalizing the safety degree for all the three layers to the same safety index for the ultimate limit state, we should keep in mind that the probabilities of bearing capacity failure in all the layers should be added, and the common safety index could thus be below the required one. In this case, however, this is only theoretically significant because in only three composite materials the probability of failure does not essentially change.

If the bearing capacity is to be increased to a 4 m span considering the required β_f design value, a core with greater shear strength should be provided, and a span above 3 m should have greater face buckling values (Fig. 2).

An issue still open is adopting the design values β_f. Decision should also be made whether a definite safety index should be required for each of the four limit states, or the ultimate limit state and serviceability limit state should be distinguished as usual.

We consider that the control of composite elements during manufacture to ensure the guaranteed safety can be done by controlling small specimens with a statistical processing of the basic variables data.

6.CONCLUSIONS

This paper presents a probabilistic approach to the safety of composite elements. Since the safety verification of these elements is not yet definitely codified, it can still be discussed, but the results should serve as guidelines for the manufacturer. Equalization of safety is proposed for individual layers as well as for design values, based on probabilistic approach where the probability of failure is expressed with the safety index.

REFERENCES

1. STAMM K., WITTE H., Sandwichkonstruktionen. Springer Verlag, Wien 1974. 337 p.
2. MILCIC V., PAUSE Z., TRUPCEVIC D., A probabilistic approach to defining a wind load, Gradevinar, Vol. 37, No.3.,1985, pp 101-107.

Composite Shells for Television Tower Prague

Voile mince mixte pour la tour de télévision à Prague

Verbundschalen für den Fernsehturm Prag

Miroslav ČERNÝ
Senior Res. Fellow
Build. Res. Inst.
Prague, Czechoslovakia

Miroslav Černý, born 1946, received his civil engineering degree at the Czech Technical University in 1969. For 20 years he has been working on problems of computational mechanics and composite structures. He leads CMEA research for composite structures.

SUMMARY

This paper deals with the design of composite shells for the Television Tower Prague. Shells have been created from contact moulded polyester Glass Fibre Reinforced laminate. Response to wind loading has been analyzed by the finite element method.

RÉSUMÉ

Cet article donne un aperçu du projet des voiles minces pour la tour de télévision à Prague. Ces voiles minces ont été fabriqués par moulage de stratifiés de polymère. Leur réaction sous charge due au vent a été calculée par la méthode des éléments finis.

ZUSAMMENFASSUNG

In diesem Beitrag wird ein Überblick über das Projekt des Fernsehturms in Prag gegeben. Die Schalen wurden aus Polymerkompositen hergestellt. Die Beanspruchung aus der Windbelastung wurde mit der Methode der Finite Elemente berechnet.

1. INTRODUCTION

TV Tower Prague is nowadays under construction in Prague 3, Mahler Gardens. The structure of TV Tower is 216 m high and consist of three steel cylinders of 4.8 and 6.4 m with internal liner from concrete /fig.1/.

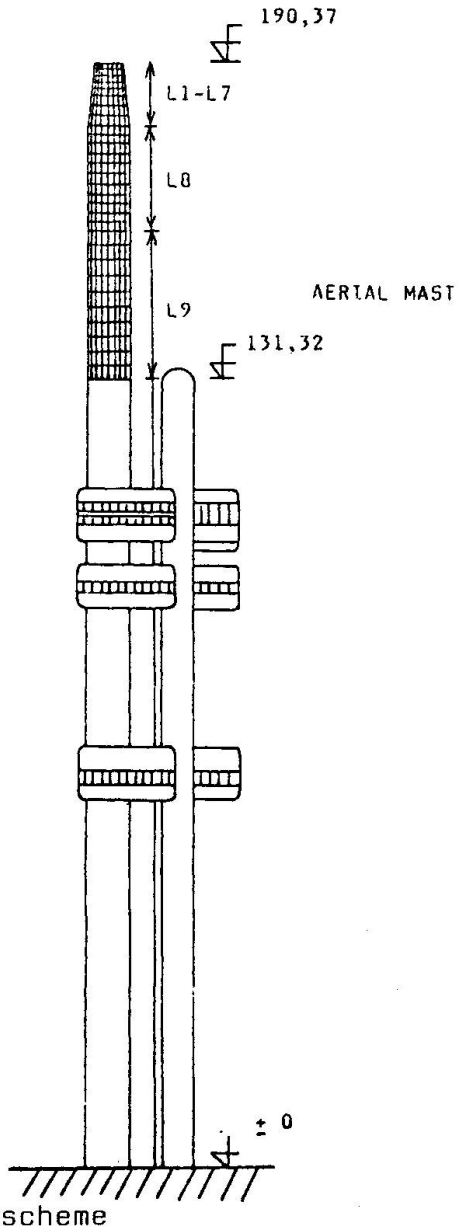

Fig. 1 TV Tower Prague - scheme

The highest part of TV Tower, aerial mast, which is about 60 m long, will be covered by composite shells of special form /Fig.2/. Shape of the shells is determined by the demands on transmission of electro-magnetic waves and by stiffness needs.
GRP covers then consist of 9 shell types of different shape and support. Shells are joined to steel cylinder of aerial mast by filament-wound beams and created by contact moulded method from polyester resin Viapal H 452 EMT, with gel-coat resin Viapal 920B/9010.

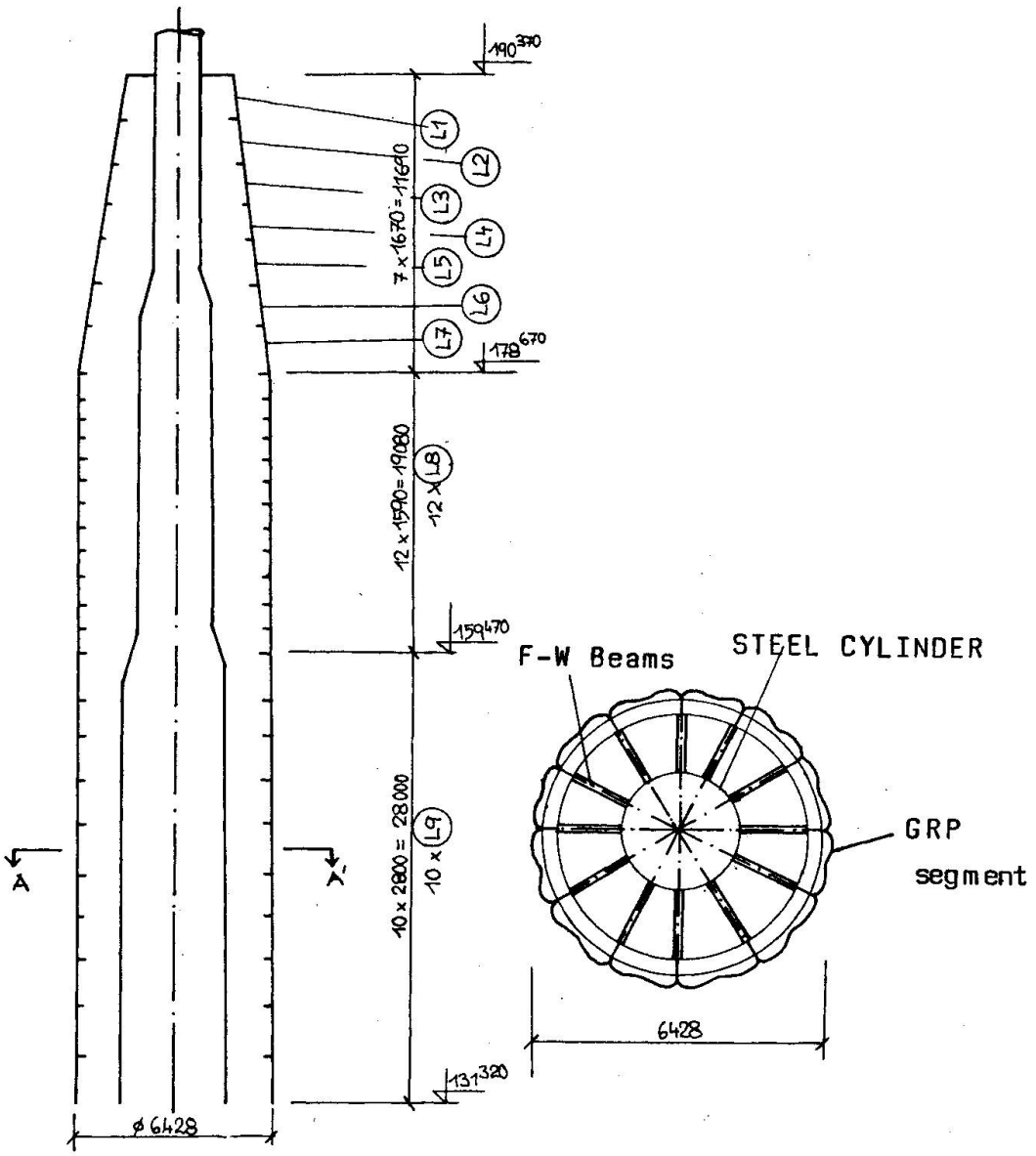

Fig. 2 Aerial mast.

2. ANALYSIS OF COMPOSITE SHELLS FOR TV TOWER BY THE FINITE ELEMENT METHOD

Regarding the complex form of shells the analysis has been done numerically by the finite element method.
The loads considered were static and dynamic part of wind pressure, dead load and thermal load.Shape of shell has been approximated by flat shell triangular elements, which has been recently developped /1/. Bending part of stiffness matrix is obtained from Mindlin bending theory of plates introducing Kirchhoff hypothesis along the element boundary, membrane part includes drilling freedoms what enables good accurary of resulting internal forces.
The displacements, rotations and internal forces, bending moments for shells L1 - L9 have been calculated. Some results of static response of structure on wind pressure are presented below (wind velocity up to 200 $km.h^{-1}$). The shell L9, one of shells constructed over cylinder is simply supported along line sides. Mesh of elements and some results are shown in Fig. 3 and 4.

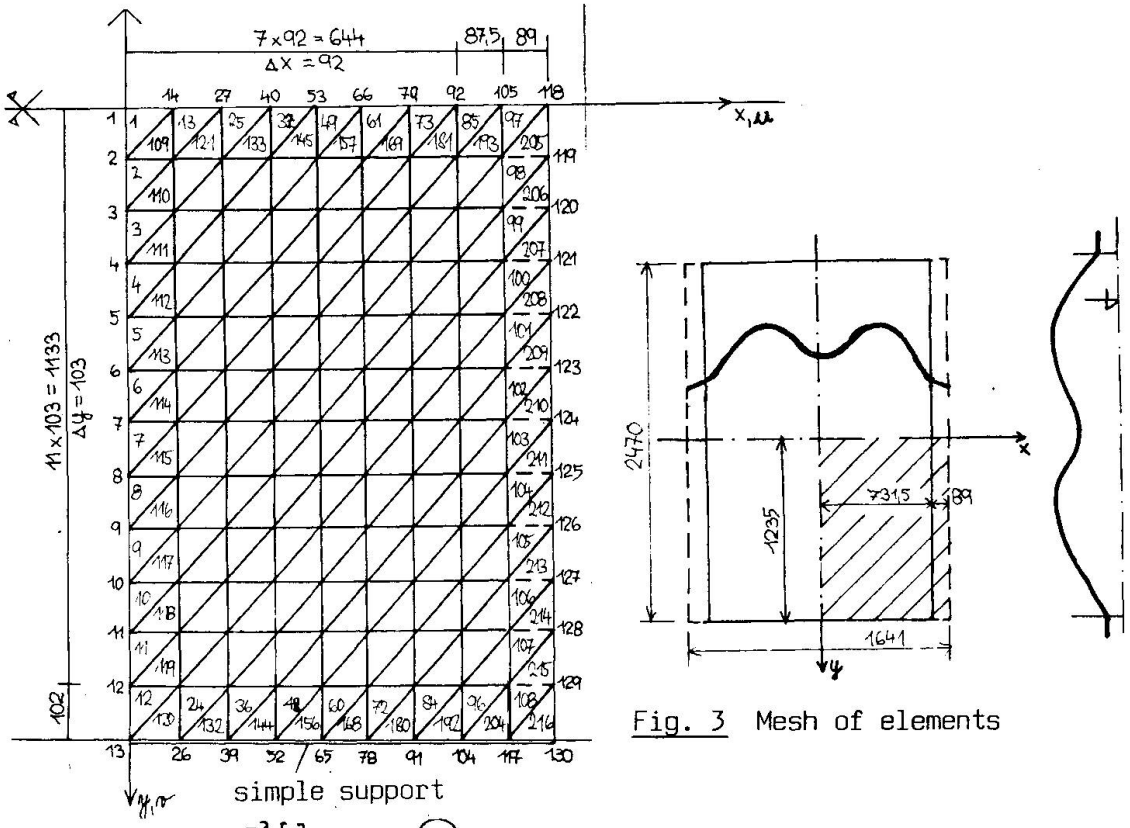

Fig. 3 Mesh of elements

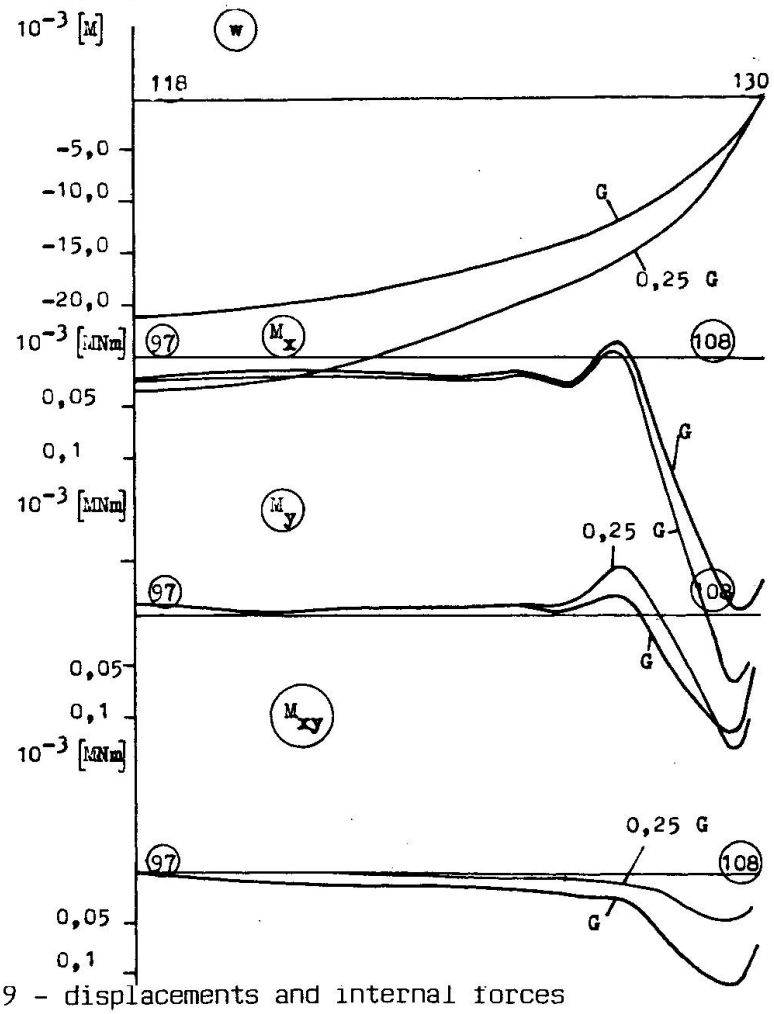

Fig. 4 Shell L9 - displacements and internal forces

3. DESIGN OF SHELL SEGMENTS ON LIMIT STATES

Shells are designed on ultimate limit state corresponding to rupture caused by exceeding the ultimate strength [3].

Results of stresses

Element N°	N_x [MN]	M_y [MNm]	$\lvert\sigma^1\rvert$ [MPa]	$\lvert\sigma^2\rvert$ [MPa]	$\lvert\sigma\rvert$ [MPa]
61	$-0,5200.10^{-1}$	$-0,1117.10^{-3}$	7,76	14,9	22,66
108	$0,3475.10^{-1}$	$0,1832.10^{-3}$	5,19	24,49	29,68

The condition of reliability then can be formulated in terms of stress [4].

$$\sum \sigma_j(t) \leq \gamma_R \cdot \gamma_t \frac{1}{\gamma_{sa}} R^n$$

where γ_i are material coefficients
R^n is characteristic strength

REFERENCES

1. CERNY M., A Numerical Analysis of Composite Shells for TV Prague, conf. Composites 89, Proceedings, Paris, June 1989
2. CERNY M., Recent Static and Dynamic Finite Element Analysis of Arbitrary Thin Shells, Int. Congress IASS, Proceedings, Moscow, Sept. 1985
3. ISO 2394 General Principles on Reliability for Structures, 2nd ed. 1986
4. ST SEV 5060-85 Reliability of Building Structures.Plastic Structures, 1985

Leere Seite
Blank page
Page vide

Composite Shell Columns

Colonnes à coque mixte

Verbund-Hohlstützen

Hassan SHAKIR-KHALIL
Dr. Eng.
Univ. of Manchester
England, UK

Hassan Shakir-Khalil obtained his BSc. and MSc. degrees from the University of Cairo, Egypt, and his PhD. degree from the University of Cambridge, England, UK. He spent two years in the Bridge Department of Krupp, Rheinhausen, FRG and has been in the academic field for most of his life.

SUMMARY

Columns of circular section have been tested to investigate their use as legs of off-shore platforms and similar structures. The section of these composite shell columns is made of outer and inner cylindrical steel shells which are 2 mm and 1 mm thick respectively, and the 12 mm annular cavity between the shells is filled with micro-concrete. Tests and numerical work carried out confirm that columns of such sections are of practical use, and that additional work is required to further investigate their behaviour and utilize their full potential.

RÉSUMÉ

Des colonnes de section circulaire ont été testées pour analyser la possibilité de les utiliser dans les plates-formes en mer ou dans des structures similaires. La section de ces colonnes est composée de deux coques cylindriques en acier disposées concentriquement; l'épaisseur de la coque extérieure est de 2 mm et celle intérieure de 1 mm. La cavité annulaire réservée entre elles est remplie de microbéton. Les essais et les calculs numériques effectués jusqu'ici ont montré que des colonnes ayant de telles sections s'avèrent d'un emploi pratique; toutefois une étude supplémentaire est nécessaire en vue d'analyser leur comportement et de pouvoir utiliser leurs possibilités globales.

ZUSAMMENFASSUNG

Stützen mit Kreisquerschnitt wurden hinsichtlich ihrer Eignung für Bohrinseln und ähnliche Bauwerke geprüft. Sie bestehen aus zwei konzentrischen Stahlrohren, deren Zwischenraum von 12 mm Breite mit Mikrobeton gefüllt ist. Versuche und Berechnungen bestätigen die Eignung derartiger Querschnitte für praktische Anwendungen.

1. Introduction

Steel-concrete-steel composite shells have been developed in the Civil Engineering Department, University of Manchester, England [2, 3]. The section of these composite shells is made of two relatively thin concentric, cylindrical steel shells, and the annular cavity is then filled with a filler material. Resin and grout were first used as the filler material for small scale specimens, and micro-concrete was later used for larger specimens in order to simulate full-scale structures. These shells had originally been developed for use as compression chambers for use in deep-sea structures.

Using this type of composite shell construction, a preliminary series of tests on 4m long columns was conducted with a view to studying the behaviour of such columns and also to establishing their carrying capacity [5, 6]. The composite cylindrical shell of the columns had outer and inner diameters of 200mm and 172mm respectively, and the annular cavity was 12m wide. Both the outer and inner steel shells were 1mm thick, and grout was used as the filler material. The test results of these columns were rather disappointing due to the relatively large shrinkage of the grout, and also as a result of premature failure of the columns due to local buckling of the 1mm thick outer steel shell.

2. Column specimens

The composite shells of the column specimens whose test results are reported here, had outer and inner diameters of 202mm and 172mm, and the outer and inner steel shells were 2mm and 1mm thick respectively, Fig.1. The steel shells of each column were assembled from three outer and three inner steel cylinders. The steel cylinders were rolled from 1220mm long steel plates, and the longitudinal edges of each rolled cylinder were butt welded together.

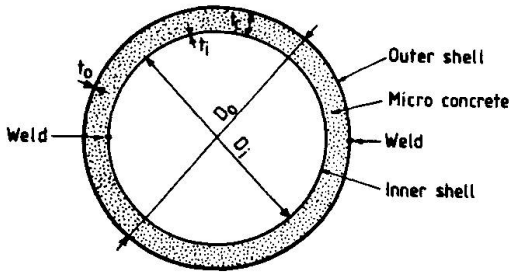

Fig.1 Column cross-section

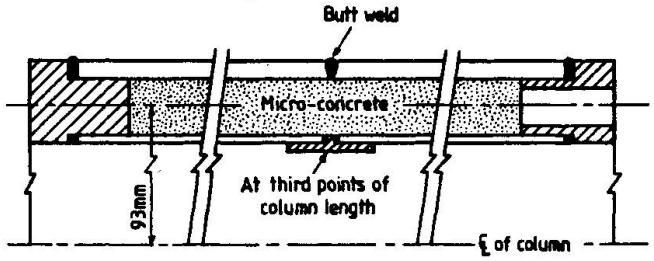

Fig.2 Details of columns

The inner shell was first assembled by fillet welding the 1220mm long and 1mm thick inner steel cylinders to backing steel strips. Four spacers 12mm wide were then welded to the inner shell, and the outer shell was assembled by butt welding the 2mm outer cylinders together. The steel shells of the composite column were finally completed by being welded to two end rings. One of the end rings was solid, and the other was provided with slots to enable the casting of the micro-concrete to be carried out, Fig.2. The completely assembled column was 3680mm long. When the column was ready for the casting of concrete, it was strapped to an I-section column which was bolted at the base to the laboratory strong floor. The 12mm annulus between the outer and inner steel shells was filled with micro-concrete of 3mm maximum aggregate size and the columns were vibrated during the concrete casting process.

In addition to the tests on the columns, tests were carried out on steel tension coupons, 100mm concrete cubes and 150x300mm concrete cylinders to establish the material properties of the steel and micro-concrete used. Tests were also carried out on 200mm high stub columns in order to compare the experimental squash loads with the predictions of the British Standard BS5400 [1]. The section of the stub columns was identical to that of the tested columns, and the experimental failure loads were compared to the BS5400 predictions as given by the following expression in which the material partial safety factors are taken equal to unity:

$$N_u = f_{sd}\, A_s + 0.67\, f_{cu}\, A_s \qquad (1)$$

where the terms are as defined in the notation.

3. Instrumentation

The columns were tested in the horizontal position in a 3,000kN capacity test rig capable of accommodating columns up to 5m long. Fig.3 shows a general view of the test rig together with the data logging equipment used in these tests. The test set up, test procedure and the instumentation have been fully described elsewhere [4]. When bolted to the 50mm thick end loading plates of the rig, the columns had effective buckling lengths of 3990mm and 3860mm in the horizontal and vertical planes respectively. When being tested, the columns were subjected to eccentric end compressive forces. The first four columns were subjected to equal end eccentricities of 10, 25, 75 and 150mm, whereas the last two columns were subjected to unequal end eccentricities of 75 and 25mm for one column, and 150 and 75mm for the other.

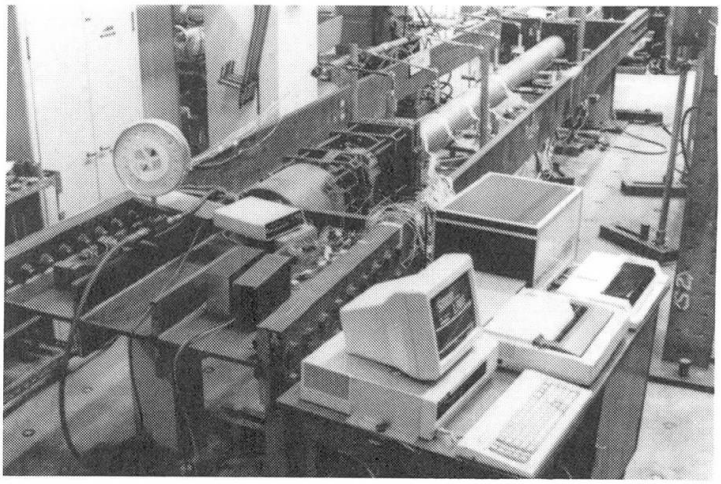

Fig.3 View of 3,000kN test rig

Fig.4 shows locations I – V at which the column sections were instrumented with strain gauges, and also the positions 'T' where vertical and horizontal displacement transducers were located. The first four columns which were symetrically loaded were provided with strain gauges at sections I, II and III only, whereas the last two columns were instrumented at all five sections. Fig.5 gives the details of the strain gauges at the different sections along the column length, and shows that strain gauges were fixed to the inner surface of the inner steel shell at section II of all columns. Sections IV and V were only instrumented at the top and bottom extreme fibres of the outer shell.

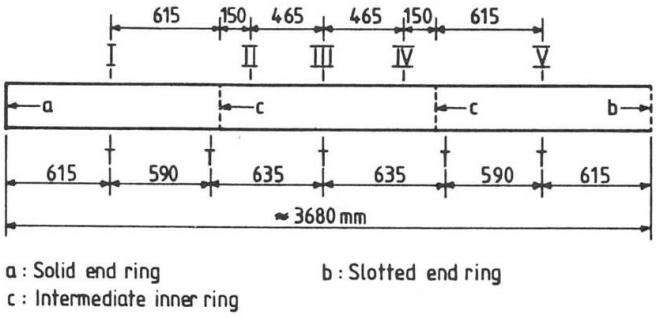

Fig.4 Column details and instrumentation

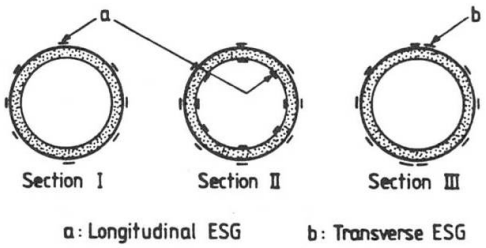

Fig.5 Position of strain gauges

4. Test results

Table 1 gives the material properties as well as the test results of the 200mm high stub tubes. The table shows the actual thicknesses of the steel shells used and also the design strengths f_{sdi} and f_{sdo} of the inner and outer shells. The table shows that the squash loads of the tested stub columns were always in excess of the BS5400 predictions, and that the margin of safety ranged between 2% and 25%.

The properties of the tested columns are given in Table 2, and include the values of the squash load, N_u , and ultimate moment of resistance, M_u , as calculated in accordance with BS5400 when the partial safety factors of the materials are taken equal to unity.

Table 1 Results of tests on short composite tubes

Sp. No.	Height (mm)	t_i (mm)	t_o (mm)	A_{si} (mm^2)	A_{so} (mm^2)	f_{sdi} (N/mm^2)	f_{sdo} (N/mm^2)	f_{cu} (N/mm^2)	N_u (kN) Exp.	N_u (kN) BS	Exp/BS
1	200	1.02	1.93	554	1213	223	219	46.3	758	607	1.25
2	"	"	"	"	"	"	"	45.1	710	601	1.18
3	"	"	"	"	"	"	"	46.2	660	606	1.09
4	"	1.04	1.97	565	1238	234	186	48.2	590	578	1.02
5	"	1.05	1.98	571	1244	218	193	43.0	620	567	1.09
6	"	1.03	"	560	1244	236	178	43.4	640	579	1.11
7	"	1.04	1.97	565	1238	255	178	44.0	610	600	1.02

Table 2 Properties of tested columns

Col. No.	e_1 mm	e_2 mm	t_i mm	t_o mm	A_s mm^2	f_{sd} N/mm^2	f_{cu} N/mm^2	E_s kN/mm^2	(BS5400) N_u(kN)	M_u(kNm)
1	10	10	1.02	1.97	1792	196	44.1	197	555	25.5
2	25	25	"	1.96	1786	216	44.0	195	592	28.0
3	75	75	1.04	1.97	1803	210	48.2	190	578	25.9
4	150	150	1.05	1.98	1815	205	43.0	194	567	26.2
5	75	25	1.03	"	1804	207	43.4	194	579	27.1
6	150	75	1.04	1.97	1803	217	44.0	194	600	28.1

Fig.6 shows the strains in the extreme fibres at the mid-length section of the tested columns. It can be seen that, with the exception of columns 1 and 2, very high strains were recorded both in tension and in compression. These strains were in excess of the yield strains as obtained from the tension coupon specimens. Columns 1 and 2 were subjected to relatively small end eccentricities, and failure occurred before yield was reached in the tension fibres.

The in-plane displacements at mid-span of the columns are shown in Fig.7. With the exception of column 2, the load-diplacement relationships are seen to exhibit large plateau at failure, and the descending branch of the column behaviour was followed whenever possible in the post failure stage.

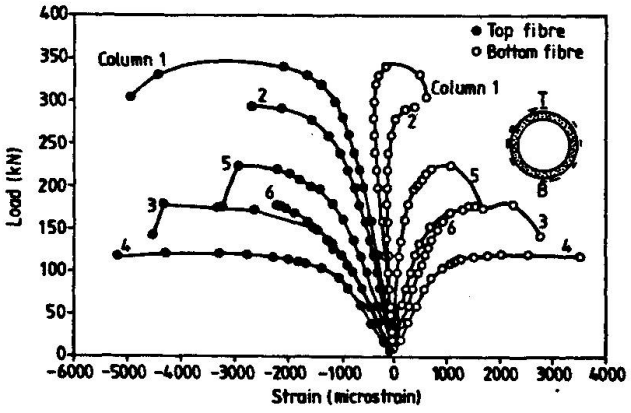

Fig.6 Mid-length strains

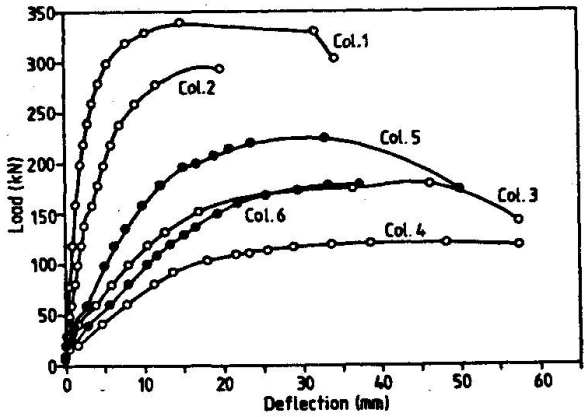

Fig.7 Mid-length displacements

When failure took place, a local buckle was observed to have formed in the outer shell of the columns. The buckle was quite pronounced in the post failure stage, and was accompanied by

the crushing of the micro-concrete and the formation of a series of buckles in the inner shell. This can be seen from Figs.8 and 9 of column 2 after the completion of the test.

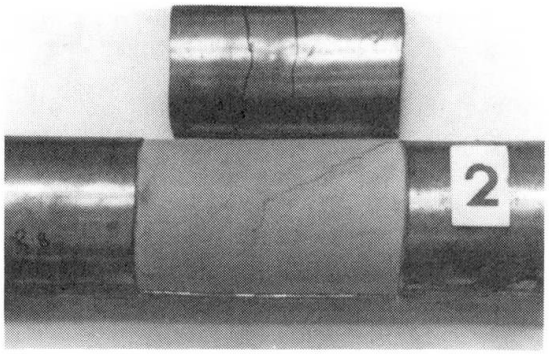

Fig.8 View of outer shell and concrete

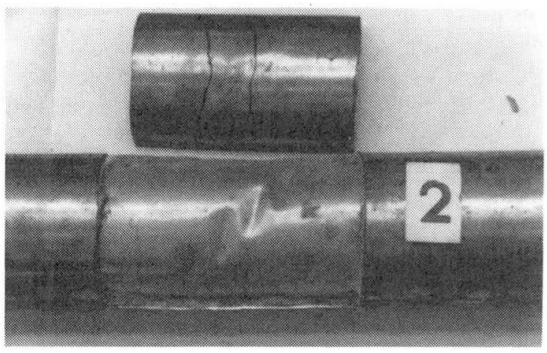

Fig.9 Buckles in inner shell

Table 3 Results of tests on columns

Col. No.	N_e (kN)	N_p (kN)	N_{fe} (kN)	N_e/N_p	N_e/N_{fe}	N_e/N_u
1	340	423	330	0.80	1.03	0.58
2	294	360	303	0.82	0.97	0.49
3	179	207	181	0.86	0.99	0.30
4	119	130	118	0.91	1.01	0.19
5	225	249	N/A	0.90	N/A	0.35
6	161	179	"	1.11	"	0.29

Table 3 gives the results of the column tests. It shows the experimental failure loads, N_e , the predicted failure loads in accordance with BS5400, N_p , and the theoretical failure loads as calculated by the finite element method, N_{fe} [4, 7]. The latter is applicable only to columns 1-4 which were symetrically loaded. The table shows that, for the symetrically loaded columns, the test results are in good agreement with the finite element predictions, but are between 9% and 20% less than the British Standard predictions.

It is noteworthy that when tests were carried on bond slip specimens in which grout was used as the filler material [5, 6], failure always took place between the filler material and the outer steel shell. This was as a result of the relatively large shrinkage of the grout due the high moisture content required to ensure the easy workability into the 12mm annulus. This caused the grout to cling to the inner shell, and perhaps caused partial separation between the filler and the outer shell. In the column tests of that series, this lead to premature failure due to the local buckling of the outer shell in which the half wave lengths of the buckles were about 20mm long [5, 6]. This was overcome in the current series of tests both by using micro-concrete as the filler material, as it does not shrink as much as grout, and also by increasing the thickness of the outer shell from 1mm to 2mm.

Despite the use of micro-concrete and a thicker outer shell, the test results show that the columns failed to reach the failure loads predicted by BS5400. However, as the failure loads of the columns are in good agreement with the finite element predictions, it seems likely that the BS5400 in its current form is not strictly applicable to the type of section investigated here. It should be mentioned that the BS5400 is only applicable to normal density concrete, with no reference to the use of micro-concrete, and that the 2mm thickness of the steel shell violates the minimum wall thickness requirement of BS5400.

5. Conclusions

It should be reiterated here that the columns tested in this series satisfy neither of the BS5400 requirements regarding the type of concrete used nor the minimum wall thickness of the steel section. With the exception of column 6, the experimental failure loads of the columns are seen to be below the predictions of BS5400. However, the results of columns 1-4, which failed to

reach the predictions of BS5400, are seen to be within ±3% of the finite element analysis predictions. This seems to indicate that the BS5400 predictions for this type of composite column are on the unconservative side, and that perhaps a lower column buckling curve should be selected for the design of these columns.

The test results clearly indicate that such composite columns have potential for use in practice. The carrying capacity of such columns would be improved for larger column sections which would allow the use of normal density concrete in the relatively wider annular cavity. This would perhaps improve the concrete–steel bond strength as a result of the reduction in the shrinkage of concrete, and thus enhance the local bucling resistance of the outer steel shell. The structural steel sections used would also be relatively free from the built–in residual stresses due to welding which must have had an adverse effect on the tested columns. Failure of the columns was always accompanied by buckling of the outer shell in the vicinity of the weld at the third points of the column length where the steel cylinders were welded together to form the outer shell. This weld caused circumferential compressive stresses in the heat affected zone, which in turn resulted perhaps in premature buckling of the outer steel shell.

The test results reported here confirm that full scale experimental work is required before the application of BS5400 to the design of columns of unusual dimensions and cross–sections. They also illustrate the practical potential of such columns. However, more tests are required to fully investigate the behaviour of this type of column, and predict its safe carrying capacity.

NOTATION

A_c , A_s Areas of concrete and steel respectively.
A_{si} ,A_{s0} Areas of the inner and outer steel shells.
D_i , D_o Inner and outer diameters of composite shell.
E_c , E_s Elastic moduli of concrete and steel respectively.
e Eccentricity at which the end compressive load is applied.
$\bar{e}$ Eccentricity ratio, given by e/D_0
f_{cd} ,f_{sd} Design strengths of concrete and steel respectively, taken as the respective characteristic strength divided by the material partial safety factor γ_m .
f_{cu} Characteristic 28 day cube strength of concrete.
f_{sdi}, f_{sdo} Design strengths of the steel of the inner and outer shells.
M_u Ultimate moment of resistance of composite section.
N_e Experimental failure load of column.
N_{fe} Failure load as predicted by finite element analysis
N_p Predicted failure load of column in accordance with BS5400.
N_u Squash load of column.
t_c, t_i, t_0 Thicknesses of concrete, inner and outer steel shells, respectively.
γ_{mc}, γ_{ms} Material partial safety factors of concrete and steel respectively, taken equal to unity when comparing predicted with experimental failure loads.

REFERENCES

1. British Standards Institution: "Steel, concrete and composite bridges, Part 5: Code of practice for design of composite bridges". BS5400, 1979.
2. Montague, P. (1975): "A simple composite construction for cylindrical shells subjected to external pressure". Journal of Mechanical Engineering Science, vol. 17, No. 2, Feb. 1975, pp. 105–113.
3. Montague, P. (1978): "The experimental behaviour of double–skinned composite, circular, cylindrical shells under external pressure". Journal of Mechanical Engineering Science, vol. 20, No. 1(b), Feb. 1978, pp. 21–34.
4. Shakir–Khalil, H. and Boufennara, K.: "Columns of concrete–filled concentric steel shells". Accepted for publication, Structural Engineering Review.
5. Shakir–Khalil, H. and Illouli, S. (1987): "Composite columns of concentric steel tubes". Proceedings, "Non–conventional structures", Conference, London, Dec. 1987, vol. 1, pp. 73–82.
6. Shakir–Khalil, H. and Illouli, S. (1988): "Columns of composite cylindrical shells". Structural Engineering Review, vol. 1, 1988, pp. 113–118.
7. Shakir–Khalil, H. and Zeghiche, J. (19898): "Experimental behaviour of concrete–filled rolled rectangular hollow section columns". The Structural Engineer, vol. 67, No. 19, Oct. 89, pp. 346–353.

Rehabilitation of Sewers with an Alternative Material

Rénovation des égouts avec un matériau de rechange

Erneuerung von Abwasserkanälen mit Alternativbaustoffen

G. SINGH
Lecturer
Univ. of Leeds

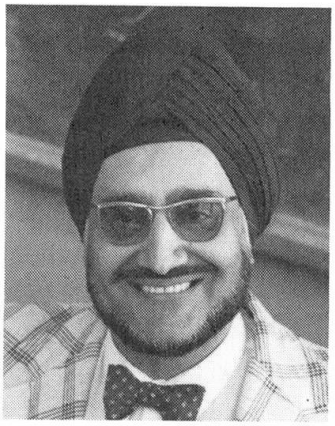

A. B. VENN
General Manager
Ferro-Monk Systems

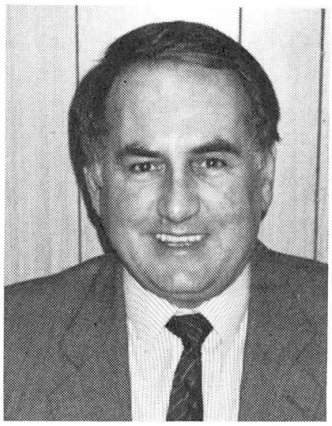

SUMMARY

The magnitude of the task of rehabilitation calls for critical assessment of the existing materials and for development of efficient alternatives. Such a development, using ferrocement, has led to the production of specifications and design procedures for a "mixed" structure. This is now accepted as an "established system" and has been found to be cost-effective and adaptable for use in sewers with variations in alignment and cross-section.

RÉSUMÉ

L'importance de la tâche de rénovation demande une évaluation critique des matériaux existants et le développement d'autres solutions efficaces. Le développement de la technique, utilisant le ferrociment, a conduit à l'élaboration de directives et de procédés de calculs prônant une structure mixte. Cette dernière est actuellement considérée comme un système établi, jugé rentable financièrement, et dont l'emploi est adaptable aux égouts après transformations de l'alignement et de la section.

ZUSAMMENFASSUNG

Die Wichtigkeit der Erneuerung erfordert sowohl eine kritische Beurteilung der vorhandenen Baustoffe als auch die Entwicklung von neuen effizienten Lösungen. Eine derartige Entwicklung unter Verwendung von Ferrozement hat zu Spezifikationen und Bemessungsregeln für ein Mischsystem geführt. Das System hat sich etabliert und führt zu anpassungsfähigen kostengünstigen Lösungen für Abwasserkanäle mit variablem Querschnitt.

1. INTRODUCTION

Needs for maintenance and rehabilitation of infrastructures are drawing a rapidly increasing proportion of finances available to the civil engineering industry. As far as the countries with old sewerage systems are concerned, most of the expenditure on sewers is incurred in improving their structural performance and the capacity of the existing networks. When structural improvement is sought through relining it is important that the impairment to the sewer capacity is minimal. The magnitude of the task of rehabilitation is indicated by, for example, Schrock [1] who estimated that, in 1984, in the USA alone there were about half a million sewer collapses and stoppages and that 75% of the sewers were performing at a 50% capacity or less. A great majority of sewers are brick or stone walled and the estimates of the funds required to keep them operational are vast. It is, therefore, necessary to assess all the old and new alternative materials and methods of rehabilitation carefully so that optimal choices can be made. Up to 1984 the methods for man-entry sewers were restricted to the use of preformed glass reinforced cement/plastic, high density polyethylene and Gunite, the last sometimes carried out in-situ for sewer size of 1500 mm or larger. The authors experienced a number of construction and design problems with the existing methods which have adverse effects on the performance and the cost [2]. For example, existing access shafts had to be renewed, substantial reductions in capacity had to be tolerated, extensive internal and external (e.g. traffic) disruptions had to be tolerated, and Gunite produced rebound problems which had to be paid for. To overcome these it was decided to seek an alternative material and method/process that would be suitable for precast and in situ work. Ferrocement was identified as the most suitable material and the wet spraying method was chosen as the appropriate process for construction. A "mixed structure" resulted from bonding the rehabilitation layer to the old masonry wall. The system developed has proved to be particularly adaptable for use in sewers with variations in alignment and cross-section.

2. FERROCEMENT

Credit for inventing (in 1847) reinforced concrete is often given to Lambot. His description of the then "new" material would today be recognised as "ferrocement". This distinct identity was given to it by Nervi a hundred years later so as to emphasise its distinct characteristics as compared to what is now called reinforced concrete. Figures 1 and 2 compare this material with Gunite and reinforced concrete respectively. It is obvious that ferrocement possesses ductility and toughness combined with excellent control on crack widths. This highly versatile material can be formed into thin sections in which fine wire meshes (or nets or expanded metal) act as reinforcement in Portland cement and sand mortar. Mortar cover of 3 to 7 mm thickness has been found to be adequate even in corrosive environments over many decades. The superior characteristics of ferrocement arise from the high passivity of the cement-rich mortar of very low permeability and from the high cover-thickness to wire-diameter ratio, as well as from the fact that the preferentially oriented meshes, made from closely spaced fine wires, provide an excellent crack control mechanism. The catalogues of examples of successful applications of the composite are very impressive [3].

3. BACKGROUND TO RESEARCH AND DEVELOPMENT

Various detailed studies [e.g. 4] pointed to the necessity of phenomenological investigations in the laboratory and the field. These formed part of the work undertaken by the authors, on the one hand, and the Water Research Engineering

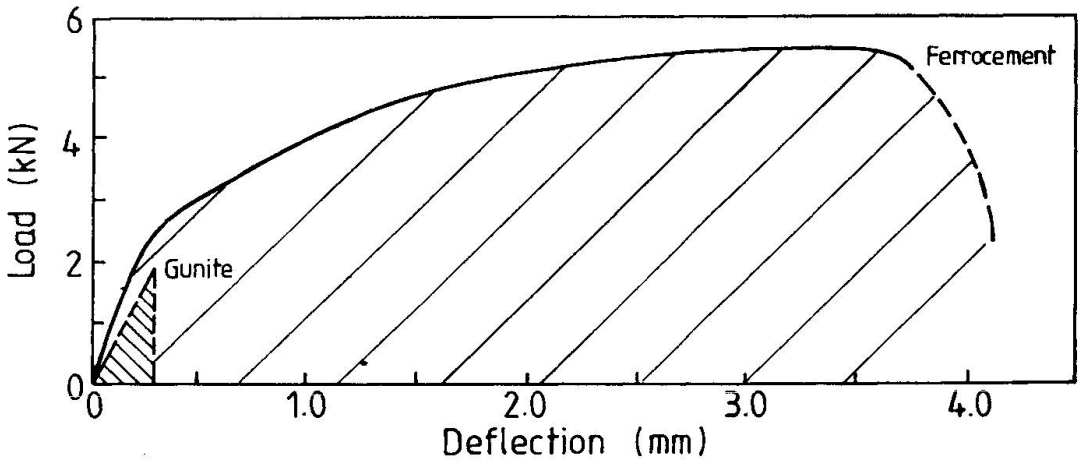

Figure 1 Load-deflection behaviour of ferrocement compared with that of Gunite

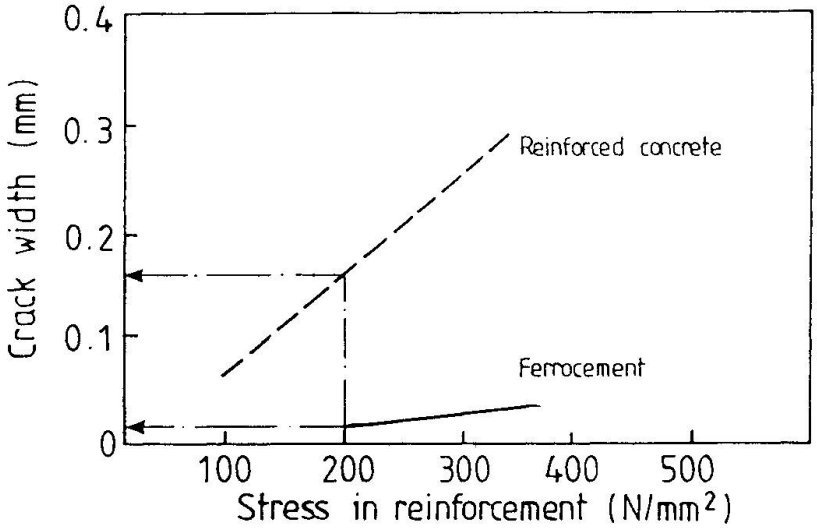

Figure 2 Flexural crack - steel stress behaviour of ferrocement compared with that of reinforced concrete

Centre (WRc UK) on the other. The latter carried out trials with the Department of the Environment to research and assess the various developing renovation systems.

In view of the importance of the durability requirements special attention was paid to the long term monotonic and fatigue strength and abrasive resistance. So as to enhance the nature and reliability of the test results, it was decided to compare the new system with Gunite (shotcrete) which is already an established and accepted method for sewer renovation [5]. The long term tests involved subjecting the specimens to accelerated corrosive environment and to concurrent sustained preload which was equivalent to 200 N/mm^2 stress in the outer layer of the meshes. All the results demonstrated that ferrocement is

superior to Gunite. For example, the abrasion resistance of ferrocement was found to be about six times and the long term flexural strength was not only greater than that of Gunite but it showed no sign of deterioration despite the fact that the ferrocement specimens had cracks under the sustained load and that the cover was only 5 mm thick.

A number of on-site trials were conducted to assess the various practical aspects of "constructability" and effectiveness of in situ coatings and precast linings. These trials proved to be very successful. The high density of the material and its bond to the existing structures were confirmed by core testing. This programme was completed in 1987 by which time about 2200 lin m of sewers, ranging in size from 900 x 600 mm to 1900 x 1200 mm, were rehabilitated. These trials were required by the WRc for formal acceptance of the Ferro-Monk System as an "established system". Subsequently, more than twenty five contracts have been successfully completed by Monk, including one in Brussels.

Cost savings have been experienced by clients and where tenders have included realistic annulus grout figures or have simply asked for a fixed price all-in rate, savings of up to 30% have been experienced in direct comparison with all other structural man-entry rehabilitation systems. This saving and about 33% saving in cross-sectional areas have fully justified the development of the sprayed system.

The above noted work has led to the drawing up of specifications and design procedures, in conjunction with the WRc.

4. DESIGN OF THE MIXED SEWER STRUCTURE

4.1 Design Criteria

The two primary criteria for the design of a ferrocement rehabilitation layer are:

1. The stress in the reinforcement should not be allowed to exceed 200 N/mm^2.

2. The surface track width should not be more than 0.04 mm.

As will be seen later, in this mixed structure the rehabilitation layer is assumed to be in tension. The whole of the tension is assumed to be taken by the reinforcement. Calculation of the steel stress is therefore a simple task. The second criterion addresses the problem of the effects of corrosive environment. Results of a number of studies show that the crack width should be limited to about 0.05 mm. Unfortunately, the crack widths cannot be predicted with an acceptable degree of reliability [4, 6]. For example, the predicted value of maximum crack width can range from 0.01 to .03 mm (for a particular case) depending on the prediction model used. Because of the inadequacies of all the published modes, physical testing of this composite material is imperative. The authors' view supports that taken by the WRc, which seeks assessment of this material through "TypeTesting".

Fortunately, because of the excellent crack arresting mechanism inherent in ferrocement the criterion of steel stress is violated at a load which is considerably lower than that required to produce a maximum crack width of 0.05 mm. Therefore, the design has to be based on the steel stress criterion which is reliably catered for.

4.2 Design Procedures for Coatings and Linings

The WRc [5] recommends that the design should consider structural integrity, material deterioration and hydraulic capacity. The structural design procedure (for Type 1) is described below, briefly:

Type 1 rehabilitation [7] utilises structural capacity of the existing sewer and requires full bond at the interface with the existing masonry. The design procedure calls for two checks.

When precast linings are used the annulus space has to be filled with grout which provides the bond between the new and the old components. During grouting, deformation and buckling are the two risks that have to be avoided. The WRc manual facilitates (through charts) determination of the maximum allowable external pressure. The procedure is simple in which the input information is the geometry and the short term loading strength of the material. This check is referred to as a short term check.

The second check is referred to as long term. The purpose of the ferrocement layer is to provide a tensile capacity particularly at the crown of the sewer which is assumed to experience maximum bending moment. Figure 3 depicts the mixed action of the existing sewer wall and the coating/lining at the crown. Figure 4 gives the design procedure. The design parameters are:

a. Long term vertical pressure from soil and surcharge, P N/mm^2
b. Crown bending moment coefficient, C (dependent on soil conditions)
c. Mean width of existing sewer, d mm
d. Existing wall thickness, t_2 mm
e. Grout thickness (for lining), t_1 mm: 25 mm minimum
f. Rear cover (for coating), t_1 mm: 10 mm minimum
g. Trial thickness, t mm
h. Working tensile strength of mesh, s N/mm^2: based on tests
i. Factor of safety, F: minimum 1.25

The calculation of the lever arm t_d is done as follows:

$$\text{Lining: } t_d = 0.67t_2 + t_1 + 0.5t$$

$$\text{Coating: } t_d = 0.67t_2 + t_1 + 0.5(t - t_1)$$

The crown bending moment, M per unit length of the sewer is obtained, simply, from the expression $CPd^2/4$.

5. CONCLUSIONS

The newly developed mixed system incorporating ferrocement overcomes many of the problems associated with the existing method of rehabilitation of man-entry sewers. Material specifications and design procedures have been subjected to on-site and laboratory trials, the success of which has led to the acceptance of the new system as an "established system". It has proved to be not only a cost-effective system but also to be the one which causes minimal amount of capacity impairment. It can be used, at present, in all the environments in which Portland cement compositions are acceptable.

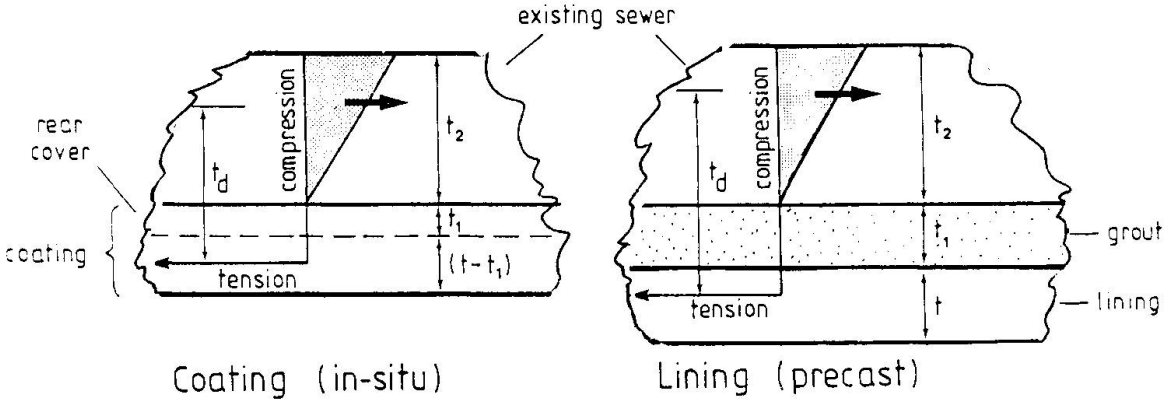

Figure 3 Assumed composite action in flexure (WRc)

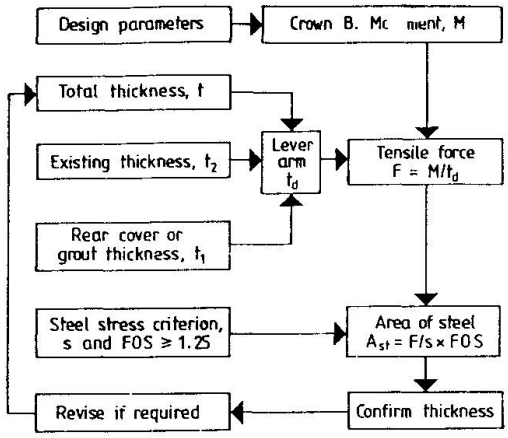

Figure 4 Design procedure

REFERENCES

1. SCHROCK, B.R., Solutions to the Pipeline, Civil Engineering, ASCE, 1985.

2. VENN, A.B. and SINGH, G, The Development of Ferro-Cement for Use in Sewers and Tunnels as a Renovation and Rehabilitation Material, NO-DIG '88, Int. Congress ISTT, Washington, 1988.

3. ACI, State-of-the-Art Report on Ferrocement, Report No. 549R-82, 1982.

4. SINGH, G. and XIONG, G.J., How Reliable and Important is the Prediction of Crack Width in Ferrocement in Direct Torsion? Submitted for publication November 1989.

5. WRc ENGINEERING, Sewerage Rehabilitation Manual, Vol. III, Swindon, UK, 1986.

6. SINGH, G. et al., Alternative Material and Design for Renovating Man-Entry Sewers, NO-DIG 89, Int. Congress ISTT, London, 1989.

7. WRc ENGINEERING, Sewerage Rehabilitation Manual, Vol. III, Addendum No. 2, Swindon, UK, 1988.

Analysis on Shear-Walls Reinforced with Fibres

Analyse des voiles de contreventement renforcés de fibres

Analyse von faserbewehrten Schubwänden

G. CROCI
Ord. Prof.
Univ. of Rome
Rome, Italy

D. D'AYALA
Civil Engineer
Univ. of Rome
Rome, Italy

P. D'ASDIA
Assist. Prof.
Univ. of Rome
Rome, Italy

F. PALOMBINI
Civil Engineer
Univ. of Rome
Rome, Italy

SUMMARY

Aim of this paper is a description of the use of polypropylene fibres in reinforcing masonry shearwalls. The advantages of synthetic fibres allow durability, laying and mechanical behaviour; this last aspect is due not only to the high strength, but also to the possibility that the low elastic modulus allows having a complete distribution of microcracks resulting in a good ductility of the reinforced masonry shear-wall, although the fibre behaviour is fragile.

RÉSUMÉ

Ce rapport décrit l'emploi des fibres en polypropylène afin de renforcer les voiles de contreventement en maçonnerie. L'emploi des fibres synthétiques comporte des avantages en ce qui concerne la durabilité, la pose et le comportement mécanique; ce dernier aspect n'est pas dû seulement à la résistance élevée, mais aussi au fait que le faible module d'élasticité entraîne une répartition complète des microfissures donnant une meilleure ductilité, bien que le comportement des fibres soit fragile.

ZUSAMMENFASSUNG

Dieser Beitrag beschreibt die Anwendung von Polypropylenfasern zur Bewehrung von Schubwänden. Die Anwendung der synthetischen Faser hat die Vorteile der Dauerhaftigkeit, des einfaches Einbaus und des hervorragenden mechanisches Verhaltens. Vom letzten Aspekt hängt nicht nur die Hochfestigkeit sondern auch die Möglichkeit der Verteilung von Mikrorissen ab. Dadurch wird eine gute Dehnfähigkeit der einbetonierten Schubwände erreicht, auch wenn das Faserverhalten spröde ist.

1. INTRODUCTION

Interest in consolidation of ancient masonry building and historical monuments is going to increase the importance of research of new technologies and new materials. Several kinds of tests have been done to define the coupling of the braid with other materials:

- tensile tests on braid samples
- tensile tests on braid and mortar or emako samples
- tests of sandstone masonry reinforced with braids
- tests of tuff masonry reinforced with braids

2. LABORATORY ANALYSIS ON THE BRAID SAMPLES

The material employed for the experiment was made of a polymeric mixture based on propylene, which is specially treated so that the binding between the polymer and the water in cement paste are optimized. The material, initially in the form of a polymeric strand with a single orientation, was then woven into braids by twisting several of the strands. The individual fibre shows a tenfinal stress equal to 500 MPa and an elastic modulus of 14 GPa.

2.1 Tests of tensile-stress, relaxation and confinement on braids

Two sets of tensile tests were carried out, one on two-rope braids and the other one on three-rope braids. In the two cases, the apparent diameter and the equivalent weight diameter was respectively:

-D_2 12 - 12 mm - D_{e2} 8.0 mm
-D_3 22 - 24 mm - D_{e3} 14.3 mm

The samples of the first set were prepared by dipping the braid ropes into a cement paste, that constitutes the cylindric hold for the press, with a diameter of 60 mm and a length of 150 mm. The sample length is .52 m. The tensile tests revealed a σ_m 162.4 Mpa with a mean scattering of values, and a medium elastic modulus E_m of 1275 MPa. Synthetic fibre braids are always subject to release fracture.The second set of tests was carried out on three-rope braids, the ends of which were accurately tied. The overall sample length is .52 m and the length between the ties is .30 m. The σ_m is 197.6 Mpa with E_m = 1373.5 Mpa.

Some cyclic tests were also made on samples similar to the ones employed above, based on 30 cycles between 6.13 and 44.2 MPa and then brought to the collapse. The diagrams show a gradual increase of the modulus during the test, whereas the break-point values are lower than the ones derived from the tensile tests.

The braid behavior under static application of a constant 30% of the ultimate load was then analyzed, under hygrothermic controlled conditions. The viscous extension reached 50% of the initial elastic one, almost within the first 2 hrs.

Several cylindric samples with a length of .30 m and diameter of 40 mm were prepared with braid and mortar and braid and emaku. Such samples simulate, with the exception of the restraint caused on the mortar by masonry, the conditions of braids injected. The results obtained were a substantial increase of the elastic modulus (about 4000 MPa) and an ultimate load increase (σ_m = 290

Fig. 1
Braid tests. 1st set.

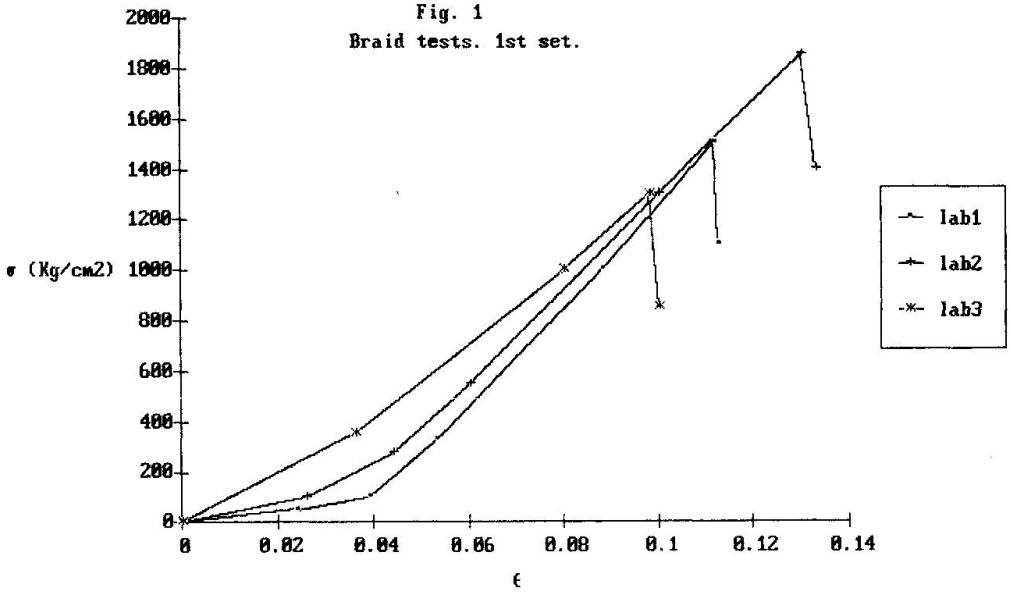

Fig 2.
Braid test. 2nd set.

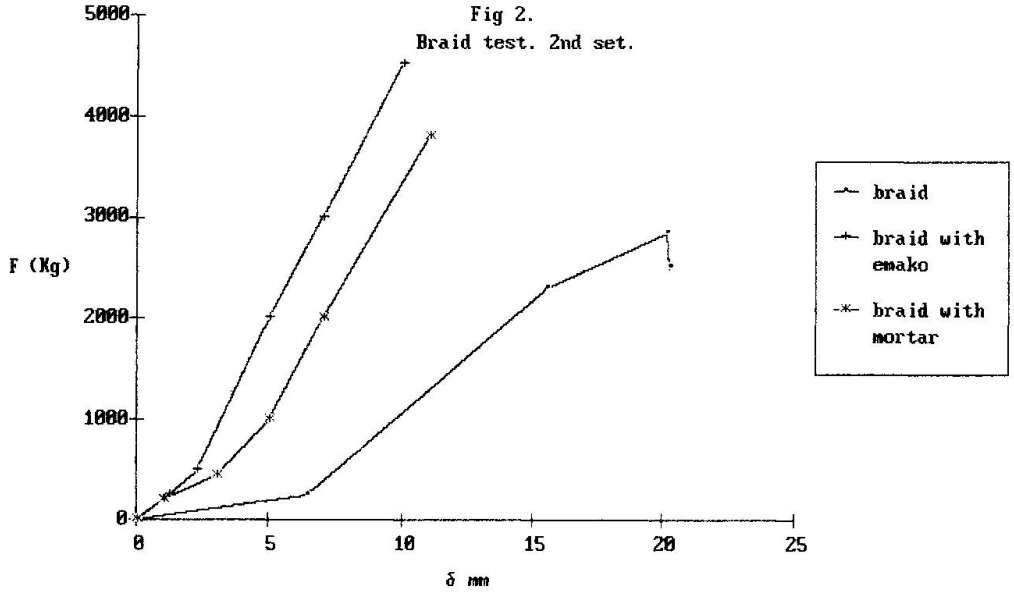

Fig. 3
1st set of cyclic tests

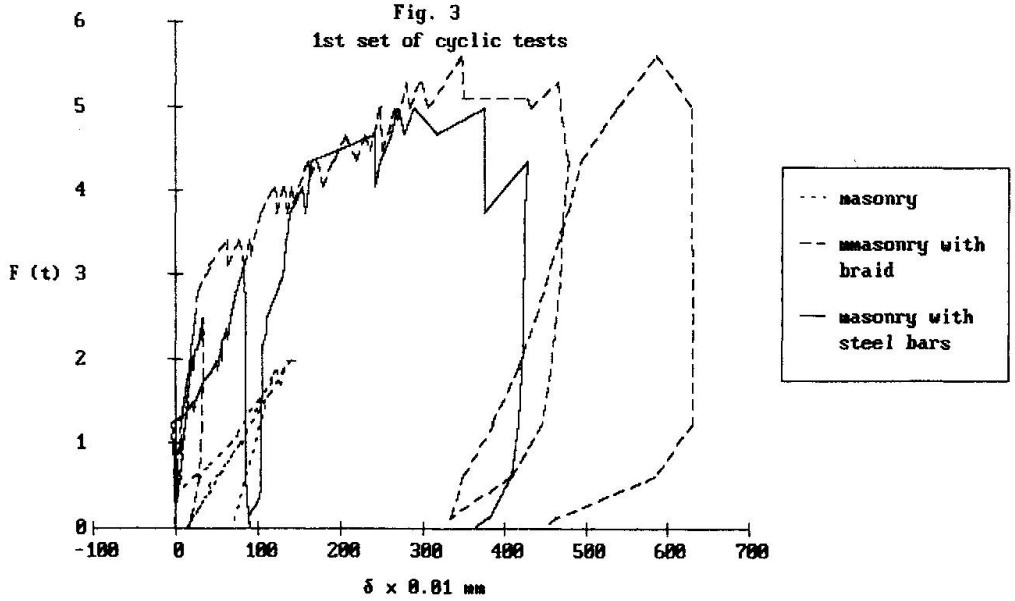

MPa). The samples with emaku show a further improvement in terms of strength, as the bond between the two materials is improved.

3. TESTS ON MASONRY SHEAR-WALLS PREPARED AT YARD

3.1 Test Proceedures

The aim of the tests was to simulate the in situ behavior of the synthetic material as a structural element in stengthening masonry shear-walls which had been damaged by seismic events, in order to prove the competitiveness with respect to the steel elements presently adopted for consolidations. Thus, the first set of samples were prepared in the yard so as to reproduce exactly the characteristics of masonry elements in situ. The samples are .40 x 1.00 x 2.00 m, built with bricks of sandstone and cement mortar and reinforced in several different ways. The seismic action was statically simulated by an horizontal hydraulic jack held in place by an appropriate steel frame; the deformations were measured by means of centesimal comparators. Cycle of loading and unloading without inversion of the force direction were made.

3.2 Results and Comments

The first sample is a non-reinforced masonry element used to determine normal conditions. It has been put trough two loading-unloading cycles; the maximum load reached is about 2 tons.(see fig.3). The second sample (fig. 3) has been reinforced with rectilinear synthetic fibre braids laid along the longer side of the shear wall, wich is under tension. We can obvserve a great increase in the bearing capacity (5 - 6 tons) and high ductility. This ductility, obtained despite the presence of a material with fragile behaviour, is due to the great capacity of the braid to be deformed and its capacity to exploit micro-cracks and anelastic deformations of masonry without losing the mutual exchange of stresses, as happens in the case of steel. The third sample is reinforced with inclined ropes (see fig. 3) so as to provide a better shear-resistance. In this case the ultimate load is 5 tons, slightly inferior to the previous one, but, above all, with much lower ductility. It seems that the shear-wall, subject to this kind of test, has at first a bending behaviour, as it can be observed in the crack frame. At the end of the load history only the inclined masonry rool appears. Effectively it requires substantial rotations of the bearings and hence the ropes along the diagonals support the load only in the final phase of tests, when the masonry shows important disconnections. This was also confirmed by the laboratory set of tests.

4. WORKSHOP TESTS ON MASONRY SHEAR-WALLS

4.1 Modalities of test

A second set of tests have been carried out in a mechanical workshop, so to have a better control on the test itself. This time the masonry shearwalls were built with regular tuff bricks and cement mortar of better quality. The two material were separetly tested and they have shown the following features:

- tuff R_{bk} = 4.00 MPa
- masonry R_{bk} = 2.75 MPa
- mortar R_{bk} = 1.20 MPa.

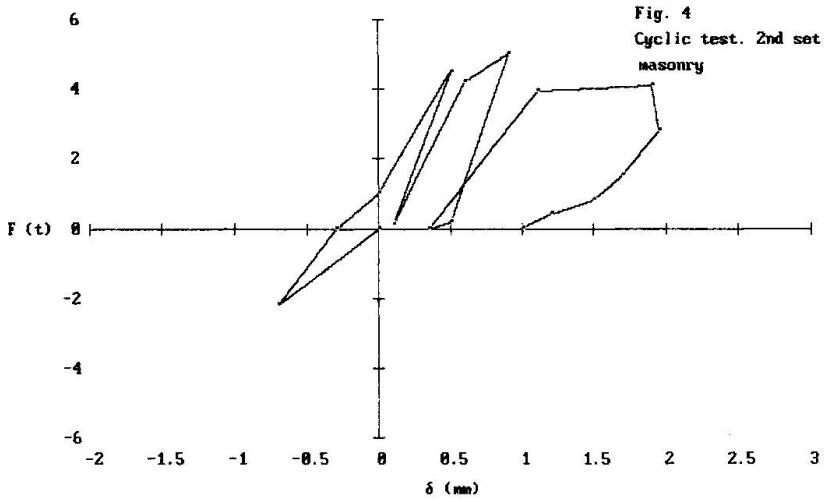

FIG. N° 5 - Cyclic tests 2nd set: masonry with steel bars

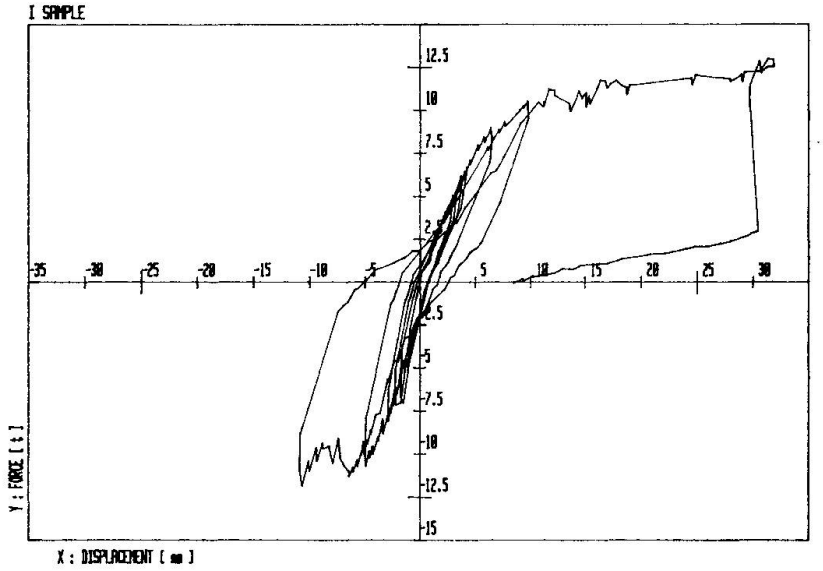

FIG. N° 6 - Cyclic tests 2nd set: masonry with braid

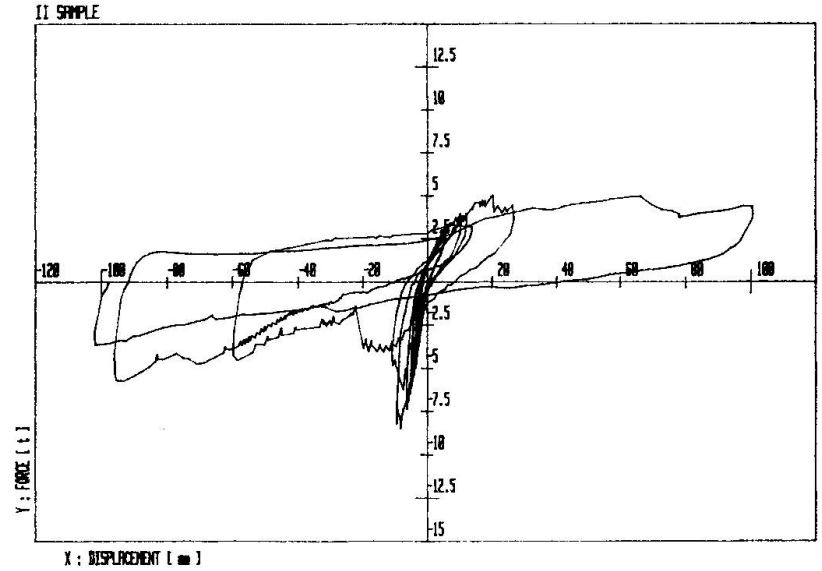

The dimension of the samples are 0.30 x 1.00 x 2.20 m. and they have been tested rotating them of 90½ respect to the building position. Tests equipment was realized with the aim of confer to the shear-wall overall cycles in both directions. The impact of the dead load on the mortar layers, nullified by the test alignments, was restored with a spring system, on the two sides of the shear-wall, so as to provide an orthogonal tension to the layers, which was constant during the tests, equal to the one produced by the dead load. The number of laid braids was equal to the first tests set, and were injected with cement mortar 425. The test, instrumentation, has been placed to measure strain on the principal diagonals of the shear-wall and along the longer sides of the wall. Further on, other inductance transducers have been located to determine the maximum mean camber, and any relative mouvements between the masonry and the ropes. Centesimal collimators are used on the vertical sides of the shearwall to detect horizontal displacements and rotations at the bond devices.

4.2 Results and comments

The tests are in progress and so far three different cases have been analyzed. The first one is a plain shear-wall. It has shown, after three cycles, higher resistance (3.5 tons) than the masonry of the first set, as obviously would be, due to the better characteristics of materials.The second test is the same shear-wall reinforced with steel bars along the two 2.20 m. sides. The bars are two O 16 for side, iniected with cement mortar, so that the total area of steel is equal to thatone of the ropes placed in the third sample. The different resistance of the two material is not important because they don't reach the failure stress.during the test. The elastic strength after six cycles is about 8 ton, without degradation. The hysteretic phenomenon is observed increasing the load until 12 tonn, the level which the shear-wall is able to support with a ductility ratio of about 4.5. The third test realized on a shear-wall with braids showed during the elastic phase a maximum strength of 9 tonn. with a substantial hysteretic behavior, with a max ductility of about 12.50. The maximum displacement at the breaking point is about 100 mm.

5. CONCLUSIONS

These studies, altough, at the moment they don't supply exhaustive answers, they show new perspectives for the use of synthetic fibres in strenghtening existing masonry, and in protecting them from seismic damages, tanks to the high ductility shown by the all different tests.

6.REFERENCES

1. CROCI G., CERONE M., The Onset of Arching Effect in Masonry Walls. Geodynamic Meeting of National Research Council, Report n. 263, Rome 1979.

2. ANDREAUS U., CERADINI G., CERONE. M, D'ASDIA P., Masonry Column under Horizontal Loads: a Comparison between Finite Element Modelling and Experimental Results. Proceedings of 7th International Brick Masonry Conference. Melbourne February 1985.

General Buckling of Fiber Reinforced Composite Plates

Voilement général de plaques composites renforcées de fibres

Beulen von faserverstärkten Verbundplatten

A. N. SHERBOURNE
Prof.
University of Waterloo
Waterloo, ON, Canada

Mahesh D. PANDEY
University of Waterloo
Waterloo, ON, Canada

SUMMARY

The paper presents a general formulation for the buckling of rectangular, orthotropic, laminated composite plates under linearly varying uniaxial compressive force using the method of differential quadrature. The results are reported for various combinations of simple and clamped boundary conditions.

RÉSUMÉ

Cet article présente l'exposé général du voilement des plaques stratifiées composites, de forme rectangulaire et orthotrope, soumises à une force de compression variant linéairement et agissant dans une seule direction, par utilisation de la méthode de la quadrature différentielle. Les résultats sont donnés pour de nombreuses combinaisons des conditions aux limites des plaques, sur appuis simples et encastrés.

ZUSAMMENFASSUNG

Der Beitrag stellt eine allgemeine Formulierung vor für das Beulen von rechteckigen orthotropen geschichteten Verbundsplatten unter linear ändernden Normalkräften. Es wird die Methode der quadratischen Differenzen verwendet. Die Resultate für verschiedenen Kombinationen von einfachen und eingespannte Rändern liegen vor.

1. INTRODUCTION

The effectiveness of fiber reinforced composites in performance improvement of weight-critical aerospace structures is well established. Its use in long span bridges, buildings and offshore structures is only now becoming popular. This emphasises the need for understanding the structural behaviour of various components made of orthotropic composite laminates to thereby develop efficient and reliable design methods. The present study is an effort in this direction.

In composite structures characterized by lightweight, thin walled members, the linear buckling load is one of the most important design consideration. The paper considers the buckling of rectangular, laminated composite plates subjected to uniaxial compression that varies linearly from one loaded edge to the other, a typical problem of local plate instability that might arise in a box beam subjected to nonuniform bending. To satisfy equilibrium under the load gradient, shear force must act along the unloaded edges, a suitable expression for which can easily be written. Libove et al [7] were the first to report the results on the buckling of simply supported isotropic plates under compression gradient using the Rayleigh-Ritz method. At present, the problem is generalized and results are reported for orthotropic laminated composite plates with various combination of simple and clamped boundary conditions.

The analysis of the present problem using classical energy methods is not straightforward since these methods require a priori selection of displacement functions satisfying the boundary conditions; an uneasy task, especially in cases of mixed boundaries. Whitney [8] has reported few cases of orthotropic plate buckling under uniform compression or pure shear with mixed boundaries. A common approach to problems of this class involved the use of beam vibration functions as displacement functions in the Rayleigh- Ritz [1] or extended Galerkin methods [9]. Thus, a priori selection of displacement functions and subsequent application of variational calculus often require a sound knowledge of the principles of mechanics. Computational methods such as finite elements or finite differences are less attractive due to excessive cost, storage requirements and data preparation. This has motivated the search for an effective approximate method for solving plate buckling problems in a direct manner without recourse to variational principles. The paper proposes the use of method of the differential quadrature (DQ) as introduced by Bellman and Casti [2] and further elaborated by Civan and Sliepcevich [4] for solving directly the partial differential equation governing the problem with prescribed boundary conditions. Bert and his coworkers have illustrated various applications of the DQ method in structural mechanics [5].

2. ANALYSIS

The differential equation of equilibrium of a rectangular anisotropic plate of length, a, and width, b, under uniaxial compression, N_x, and shear force , N_{xy},

$$d_{11} w_{,xxxx} + 2 (d_{12} + 2 d_{33}) w_{,xxyy} + d_{22} w_{,yyyy} = N_x w_{,xx} + 2 N_{xy} w_{,xy} \tag{1}$$

combined with the boundary conditions defines the plate buckling problem of present interest. The subscripts preceded by a comma denote differentiation with respect to the corresponding coordinates. Here, d_{ij} , $i,j = 1..3$ are the bending stiffness of the laminated plate [6], w is out of plane deflection and $\beta = a/b$ is the plate aspect ratio. In the case of orthotropic approximations, $d_{13} = d_{23} = 0$. It is assumed that the plate is subjected to linearly varying compressive forces per unit length N_{min} at x = 0 and N_{max} at x = a (Fig. 1) such that compressive stress at any section x can be written as

$$N_x = 2 N_{av} (R_1 X + R_2) \quad where \quad N_{av} = N_{max} \frac{(1+r)}{2} \tag{2}$$

Here, $R_1 = (1-r)/(1+r)$, $R_2 = r/(1+r)$ and $r = N_{min}/N_{max}$. N_{av} is the average compressive stress and r is the ratio of minimum to maximum compressive stresses. The conditions of equilibrium of mid-plane stresses

$$\frac{\partial N_x}{\partial x} + \frac{\partial N_{xy}}{\partial y} = 0 \quad \text{and} \quad \frac{\partial N_y}{\partial y} + \frac{\partial N_{xy}}{\partial x} = 0 \tag{3}$$

provide the following expression for shear stress distribution [7] in the prebuckling state

$$N_{xy} = -\frac{N_{av}}{\beta} R_1 (2Y - 1) \tag{4}$$

X = x/a and Y = y/b are non-dimensional coordinates. The boundary conditions may be defined, for simple supports, as

$$w = 0 \quad at \quad x = 0,a \quad \text{and} \quad y = 0,b$$
$$M_x = d_{11} w_{,xx} + d_{12} w_{,yy} = 0 \quad at \quad x = 0, a \tag{5}$$
$$M_y = d_{12} w_{,xx} + d_{22} w_{,yy} = 0 \quad at \quad y = 0,b$$

and, for clamped supports, as

$$w = 0 \quad at \quad x = 0,a \quad \text{and} \quad y = 0,b$$
$$w_x = 0 \quad at \quad x = 0, a \quad \text{and} \quad w_y = 0 \quad at \quad y = 0, b \tag{6}$$

Mixed boundaries can be defined in a similar way.

3. METHOD OF DIFFERENTIAL QUADRATURE

In this method, partial space derivatives of a function are approximated by means of a polynomial expressed as the weighted linear sum of the function values at a preselected grid of discrete points. For example, the first partial derivative of a function, f(x), at the i th discrete point is approximated by

$$\frac{\partial f(x_i)}{\partial x} \cong \sum_{j=1}^{N} A_{ij} f(x_j) \qquad i = 1, 2..N \tag{7}$$

where, x_i are the set of discrete points in the x-direction and A_{ij} are the associated weighting coefficients which can be derived by assuming the function, f(x), of the following polynomial form :

$$f(x_i) = x_i^{k-1} \qquad k=1, 2..N \tag{8}$$

From eqn. (7) and (8), one can write

$$\sum_{j=1}^{N} A_{ij} f(x_j) = (k-1)\, x_i^{k-2} \qquad i,k = 1, 2..N \tag{9}$$

This represents N sets of N linear, simultaneous algebraic equations which have a unique solution for the weighting coefficients, A_{ij}. The weighting coeff. for higher order partial derivatives can be obtained by an alternative technique of utilizing individual quadratures [4] which, in essence, implies that, for example, the second order derivative can be written as

$$\left(\frac{\partial^2 f}{\partial x^2}\right)_i = \sum_{j=1}^{N} B_{ik} f(x_k) \tag{10}$$

where B_{ik} is obtained by simple matrix multiplication, [B] = [A] × [A]. The weighting coeff. for 3 rd and 4 th order derivatives, C_{ij} and D_{ij}, respectively, can be derived in a similar way, [C] = [A] × [B] and [D] = [B] × [B].

Using the nondimensional coordinates, X,Y and W, the differential equation of equilibrium, eqn.(1), under a known prebuckling stress state is approximated as follows

$$d_{11} \sum_{k=1}^{N} D_{ik} W_{kj} + 2 (d_{12} + 2 d_{33}) \beta^2 \sum_{m=1}^{N} B_{jm} \sum_{k=1}^{N} B_{ik} W_{km} + d_{22} \beta^4 \sum_{k=1}^{N} D_{jk} W_{ik}$$
$$= 2 N_{av} a^2 (R_1 X_i + R_2) \sum_{k=1}^{N} B_{ik} W_{kj} - 2 N_{av} a^2 R_1 (2 Y_j - 1) \sum_{m=1}^{N} A_{jm} \sum_{k=1}^{N} A_{ik} W_{km} \qquad i,j = 3.. (N-2) \tag{11}$$

The boundary conditions for simple supports are defined as

$$W_{1j} = W_{Nj} = W_{i1} = W_{N1} = 0 \qquad i,j = 1..N$$
$$d_{11} \sum_{k=1}^{N} B_{ik} W_{kj} + d_{12} \beta^2 \sum_{k=1}^{N} B_{jk} W_{ik} \quad i = 2,(N-1) \quad \text{and} \quad j,k,m = 2.. (N-1) \tag{12}$$
$$d_{12} \sum_{k=1}^{N} B_{ik} W_{kj} + d_{22} \beta^2 \sum_{k=1}^{N} B_{jk} W_{ik} \quad j = 2,(N-1) \quad \text{and} \quad i,k,m = 2.. (N-1)$$

and for clamped supports

$$W_{1j} = W_{Nj} = W_{i1} = W_{N1} = 0 \quad i,j = 1..N$$
$$\sum_{k=1}^{N} A_{ik} W_{kj} = 0 \quad i = 2,(N\text{-}1) \text{ and } j,k = 2..(N\text{-}1) \tag{13}$$
$$\sum_{k=1}^{N} A_{jk} W_{ik} = 0 \quad j = 2,(N\text{-}1) \text{ and } i,k = 2..(N\text{-}1)$$

The above equations lead to the generalized eigen-value problem which is solved for the minimum buckling load using NAG subroutine F02BJF based on the QZ algorithm. The mixed boundary conditions can easily be accommodated by combining equations (11) and (13). The method can be extended to include rotational boundary restraints as well.

3.1 Computation

A computer program is developed which, for an assumed grid of points in the X and Y directions, computes weighting coefficients for partial derivatives, generates the bending stiffness matrix from specified lamination parameters and finally solves the eigenvalue problem defined by eqn. (11) with appropriate B.C. using the QZ algorithm. Zero edge displacement conditions are obviously applied at X,Y = 0,1 but zero moment or slope conditions, as the case may be, are applied at points very close to the plate boundaries which require grids of nonuniformly spaced points as shown in Figure 1.

4. RESULTS AND DISCUSSION

A numerical method for buckling analysis under general loading and boundary conditions is developed. The results are reported for the plate with four different combinations of simple and clamped boundary conditions (B.C.) under three loading conditions corresponding to r = 1, 0.5, -0.5. The edge conditions are denoted by the letter S for simple and C for clamped along the four edges in the following order, x = 0, x = a, y = 0 and y = b. The accuracy of the method is established by comparing results for isotropic, square plates under uniform, uniaxial compression, i.e., r = 1, with those obtained by the classical methods [3]. The comparison, as shown in Table 1, is found to be satisfactory. The average buckling stress, $K_{av} = N_x a^2 / \sqrt{d_{11}\, d_{22}}$, for square, symmetric angle-ply for the fiber angle θ = 0 to 90 in steps of 15 are presented in Figures 2 - 5 for B.C. SSSS, CCCC, SSCC and SSCS respectively. In general, the average buckling stress in the case of compression gradient is found to be less than that of uniform compression. Of course, the value of maximum stress for buckling under prescribed gradient is much higher than the uniform buckling stress. For simple supports and its combinations, the sharp optima associated with θ = 45 starts diminishing when one of the stress becomes tensile, e.g. for r = -0.5. This might have interesting implications in the design - optimization of laminated plates.

The quadrature method proves to be a simple and efficient tool for handling complex combinations of simple and clamped boundaries. The basic concept of this method is the polynomial fit to the derivative of a function. The accuracy of the approximation increases as the number of grid points or the order of the polynomial increases. Beyond a certain extent numerical ill conditioning can result which introduces gross errors. At present, results are reported using grids of 8 and 9 points which appears to be within acceptable accuracy. The proposed analysis awaits further verification by classical methods which assure the converging eigenvalue problem.

5. REFERENCES

1. ASHTON, J.E. and WADDOUPD, M.E., Analysis of Anisotropic Plates. J. Compo. Mat., 3(1), 1969, pp.148-165.

2. BELLMAN, R.E. and CASTI, J., Differential Quadrature and Long-term Integration. J.Math.Anal.Appl., 34, 1971, pp.235-238.

3. BULSON, P.S., The Stability of Flat Plates. Chatto & Windus, 1970.

4. CIVAN, F. and SLIEPCEVICH, C.M., Differential Quadrature for Multi-dimensional Problems. J.Math.Anal.Appli., 101, 1989, pp.423-443.

5. JANG, S.K., BERT, C.W. and STRIZ, A.G., Application of Differential Quadrature to Static Analysis of Structural Components. Int.J. Numer.Meth. Engrg., 28, 1989, pp.561-577.

6. JONES, R.M., Mechanics of Composite Materials, McGraw Hill Co. NY, 1975.

7. LIBOVE, C., FERDMAN, S. and REUSCH, J.J., Elastic Buckling of a Simply Supported Plate Under a Compressive Stress that Varies Linearly in the Direction of Loading. NACA Tech. Note 1891, 1949.

8. WHITNEY, J.M., Structural Analysis of Laminated Anisotropic Plates. Technomic Publ., 1987.

9. ZANG, Y. and MATTHEWS, F.L., Postbuckling Behavior of Anisotropic Laminated Plates Under Pure Shear and Shear Combined with Compressive Loading. AIAA J., 22(2), 1984, pp.281-286.

Table 1: Uniaxial Plate Buckling : Comparison

B.C.	No. of Points	Buckling Load Coeff. Kav	
		DQM	Classical [3]
SSSS	9	39.484	39.478
CCCC	8	101.510	99.389
SSCC	8	84.326	84.878
SSCS	8	57.060	56.750

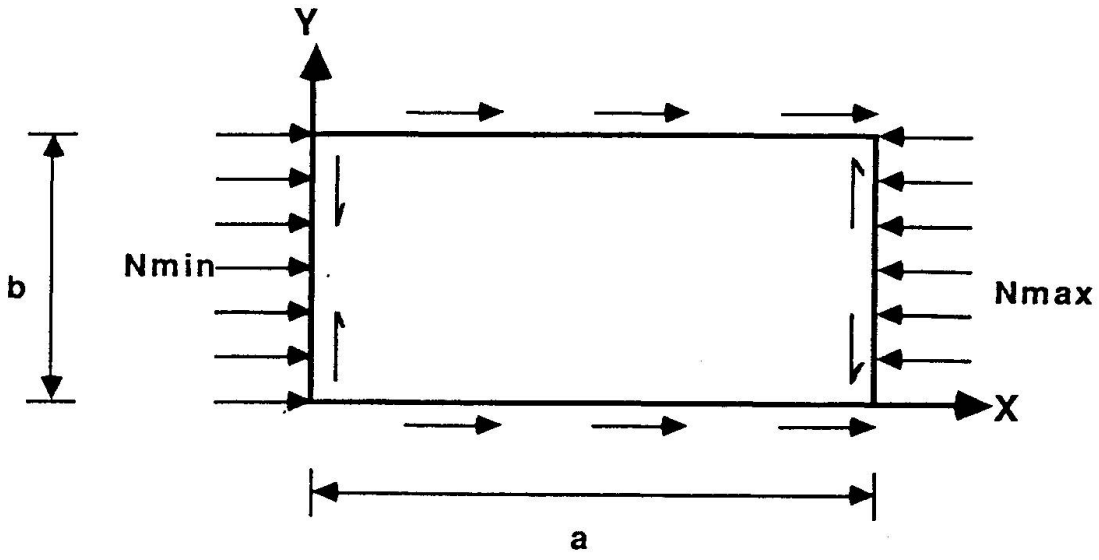

Figure 1 : Plate Buckling under Compression Gradient

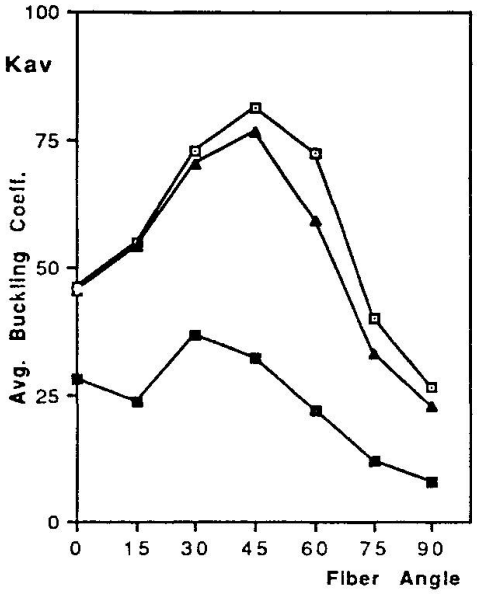

Figure 2 : SSSS Plates

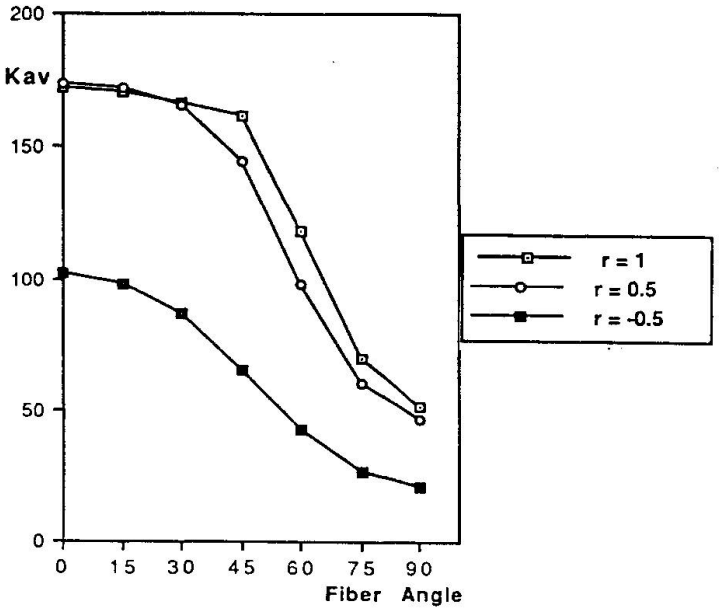

Figure 3 : CCCC Plates

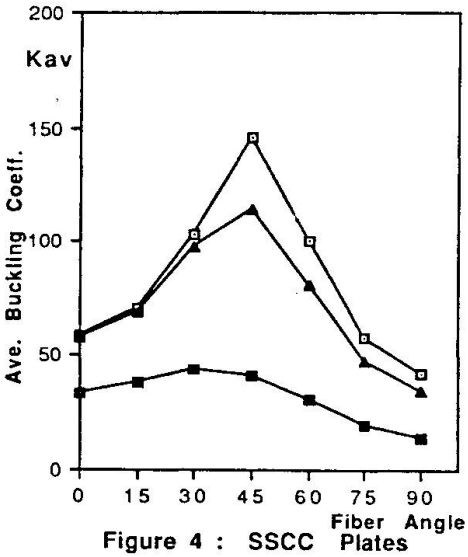

Figure 4 : SSCC Plates

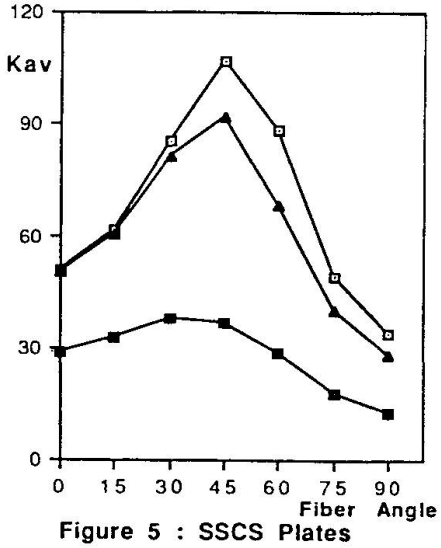

Figure 5 : SSCS Plates

Retaining Walls containing Reinforced Fly Ash

Terre armée aux cendres volantes pour murs de soutènement

Stützmauern aus bewehrter Erde mit Flugasche

Bob SARSBY
Reader
Bolton Inst.
Bolton, Lancs., UK

After Graduation in 1968 lectured at Manchester University for six years whilst working for his doctorate on the deformation of sand. He then worked as a Geotechnical Engineer for 5 years before returning to academic life. Currently responsible for all Geotechnical matters in the Department of Civil Engineering.

SUMMARY
The Author was responsible for monitoring the performance of two retaining walls which contain Fly Ash reinforced with plastic grids. Further research work is being conducted by erecting and testing full-size "model" walls. The most important findings to date are presented in this paper.

RÉSUMÉ
L'auteur avait la responsabilité du contrôle du comportement de deux murs de soutènement composés de cendres volantes renforcées par des grillages en matière plastique. Une étude plus poussée se poursuit par la construction de murs grandeur nature soumis à une série d'essais. Les résultats essentiels obtenus jusqu'à présent figurent dans cet article.

ZUSAMMENFASSUNG
Der Autor hat das Verhalten von Stützmauern aus Flugasche mit einer Plastikbewehrung untersucht. Versuche wurden an Wänden im Massstab 1:1 weitergeführt. Die Resultate werden hier vorgestellt.

1 INTRODUCTION

The Reinforced Soil Technique is a well-established method of construction for retaining walls and bridge abutments. The traditional form of Reinforced Soil utilises good quality free-draining fill in association with Tensile reinforcement (usually metallic). Because of the large volume of fill utilised the cost of this method of construction can be significantly reduced by the use of cheaper fills such as the waste ash obtained from coal-fired electricity generating stations, i.e. Pulverised Fuel Ash (PFA). Most industrialised countries have large stockpiles of this material which is particularly useful because of its low bulk density, effective cohesion and self-hardening properties. Until recently PFA was specifically classified in the United Kingdom as being suitable for use in Department of Transport Reinforced Soil structures [1] because of concern over corrosion of metallic reinforcement when buried in PFA. However with the advent of strong, chemically-inert, non-metallic reinforcing elements, e.g. Tensar, Paraweb, Fibretain, etc., this situation has changed.

In 1983 a trial retaining wall incorporating reinforced PFA was erected and test loaded successfully by West Yorkshire County Council [2] and subsequently the first commercial use was made of this composite construction in retaining walls which formed part of the Dewsbury Ring Road in Yorkshire. The walls, which were erected between 1985 and 1987, are used to support elevated sections of the ring road and because of the novelty of this form of construction sections of the walls were extensively instrumented. As a result of the successful use of this form of Reinforced Soil many retaining walls and abutments incorporating reinforced-PFA have been built in the United Kingdom. Monitoring of the walls at Dewsbury is still being undertaken and further research work into the behaviour of reinforced fly ash is being undertaken in the large scale test facility at Bolton Institute.

2 EXPERIMENTATION

2.1 Field Work

Field work consisted of the instrumentation and monitoring of retaining walls which form part of the Dewsbury Ring Road. The walls have the usual constituent components of Reinforced Soil structures, i.e. facing, bulk fill and reinforcement. The facing is composed of 'I'-section columns with precast concrete planks fitted into the vertical slots formed by the flanges of the columns. At the start of construction temporary props and walings were used to hold the columns upright and the walls were built up by progressively inserting concrete planks and laying and compacting the fly ash in layers behind the facing. A vertical sand drain was interposed between the facing and the PFA and this was gradually raised with the wall. At the appropriate elevations contiguous sheets of grid reinforcement were laid horizontally on top of the compacted PFA and one end of each sheet was passed in between vertically-adjacent concrete planks and anchored to the steel columns. The grid was then tensioned by pulling the free end and further PFA was placed and compacted. The process was repeated until the wall was built to full height. The temporary props were removed when the fill was approximately two-thirds of its final height and after completion of the filling a false masonry face was erected in front of the facing.

As the walls were constructed a large number of monitoring instruments (earth pressure cells, inclinometer tubes, magnetic extensometers, etc.) were installed to measure pressures and deformations both on the boundaries of the reinforced PFA block and inside the block [3]. The scope of the monitoring programme was enhanced by the Transport and Road Research Laboratory (TRRL) who arranged a variation to the design so that two different types of reinforcement, i.e. Paraweb and Fibretain, were utilised in two sections of one retaining wall.

2.2 Laboratory Work

The Laboratory Work is being undertaken in the Large Scale Test Facility at Bolton. This 'laboratory' is dedicated to experimental research into the behaviour of engineering 'structures' and forms of construction using large and full-scale 'models'. The grid-reinforced PFA research work is undertaken using the 'model' retaining wall which is 12m long, and which retains a 3.5m height of fill which extends for 6m back from the wall facing. The facing is identical to that used on the Dewsbury Ring Road and during wall erection the facing is rigidly supported by props and horizontal jacks (in a similar manner to the restraint at Dewsbury. The fill and reinforcement are placed in layers and when the full height of PFA has been placed the props are removed and the jacks are released - the jacks are mounted as a safety frame which is bolted to the ground beams and which is present to prevent extensive movement or catastrophic collapse of the facing. Discrete loads and uniformly-distributed loading is then applied to the surface of the fly ash using large concrete blocks. Instrumentation, of the same type as used at Dewsbury, is used to measure boundary pressures and displacements.

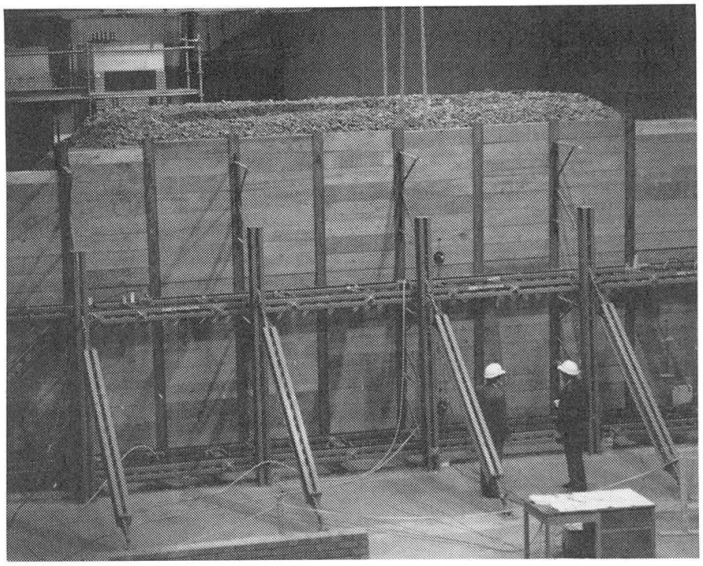

Fig. 1. 'Model' Retaining Wall Apparatus

The first series of tests is concerned with the influence of reinforcement length (relative to wall height) on wall strength and stiffness and the dispersion of applied surface loads within the reinforced mass. Walls containing unreinforced fly ash and PFA with very short reinforcement (0.25 x height) have been tested and further walls with reinforcement lengths in the range 0.5 to 1.0 times the height are currently being built. Future test series will investigate the influence of reinforcement extensibility, foundation soil compressibility and cyclic loading on the behaviour of reinforced fly ash.

3 DATA

Only those trends which have been observed in both the field and laboratory investigations are outlined herein.

3.1 Vertical pressure beneath the reinforced block

The data in figure 2 relates to six different instrumented test sections and three different reinforcement types. There is a random variation of pressure about a value equal to the calculated overburden. However adjacent to the facing there is consistently a reduction in vertical stress - this is believed to be due to friction between the facing and the fill which helps to support the fill in this vicinity. At Dewsbury earth pressure cells were also cast into the concrete strip below the facing so that they were in contact with the underlying ground. The high values of pressure indicated by certain of these cells may result from 'downdrag' on the facing from the fill. Once the filling was completed the pressure cells indicated virtually no change in either the magnitude or the distribution of pressure with time - removal of the props, erection of the false masonry facing, and opening of the road to traffic had no significant effect.

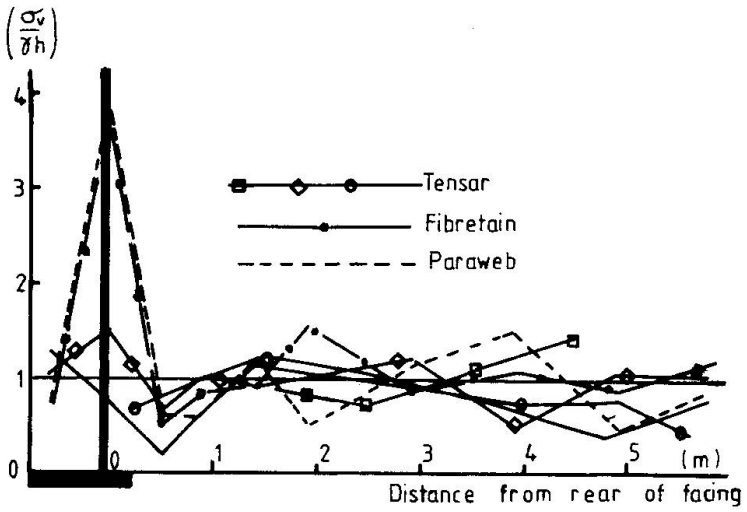

Fig. 2. Vertical pressure on base of PFA

3.2 Lateral pressures on the wall facing

At the end of construction the compaction process determined the pressure acting on the facing for a depth of approximately 3m down from the top of the fill. These compaction-induced stresses masked the influence of the shear strength properties and self-weight of the fill. The maximum pressure on the facing occurred in the vicinity of the upper propping position. However this method of wall erection is beneficial as removal of the props permits virtually complete dissipation of the compaction stresses, despite the presence of tensile reinforcement in the fill, as indicated in figure 3. At the same time there was a slight increase in the pressures acting on the lower half of the facing. The resultant pressure distribution approximates that predicted by earth pressure theory for a cohesive-frictional soil, i.e. zero stress in the upper zone and a linear increase with depth in the lower part - figure 3. To finish the retaining walls at Dewsbury a substantial concrete footing was cast along the

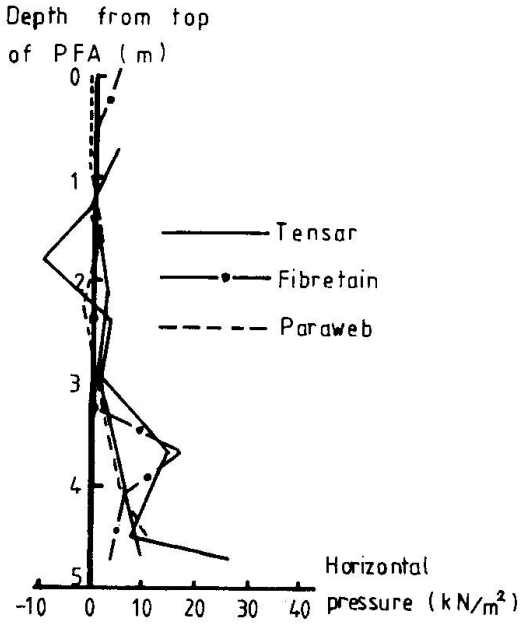

Fig. 3. Lateral pressures on facing

base of the facing and a masonry skin was erected on the footing. The gap (150mm) between the masonry and the facing was then filled with concrete. This had the effect of stiffening and restraining the facing considerably so that the earth pressures increased significantly, as shown in figure 4, and the forces in the soil reinforcement became very small. The rigidity of the final facing was such that it acting as a partial, gravity retaining wall. Nevertheless the upper 'zero-pressure' zone still remained, indicating that in the long-term the cohesion of the PFA was reliable and was not lost due to deformation of the block of fly ash.

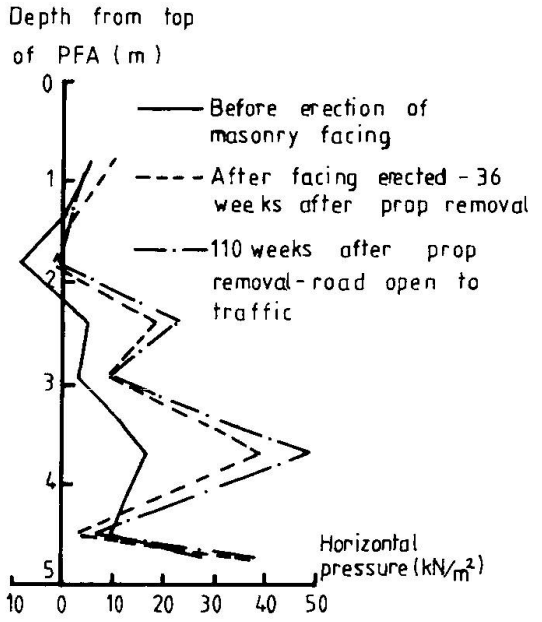

Fig. 4 Influence of facing stiffeness

3.3 Horizontal movement of the facing

Removal of the props resulted in immediate outward translation of the facing of up to 0.15% of wall height. For the Dewsbury walls the outwards displacements doubled over the next three months but the rate of movement decreased drastically. Figure 5 contains data recorded at three different elevations for various sections of walls at Dewsbury, after removal of the props.

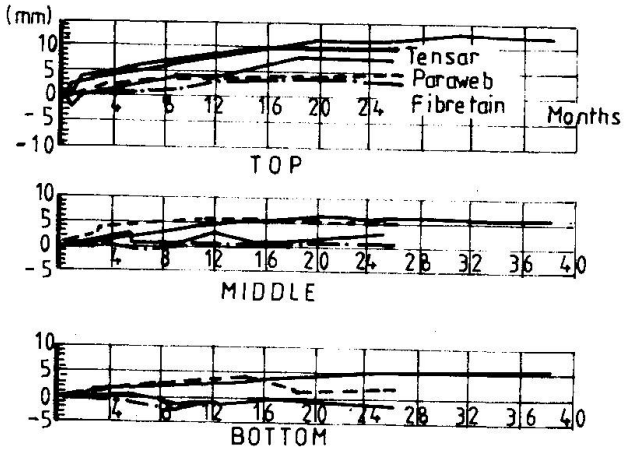

Fig. 5 Outward movement of the facing

4 CONCLUSIONS

The distribution of vertical pressure on the base of a reinforced soil block can be taken as uniform with the mean pressure equal to the overburden. PFA possess a reliable cohesion which exhibits no tendency to decrease with time or small movements of the compacted fly ash. Consequently there is no lateral pressure on the rear of the upper part of a facing which retains reinforced PFA.

5 REFERENCES

1. BE 3/78 Technical Memorandum (Bridges). Reinforced Earth Retaining Walls and Bridge Abutments, Dept. of Transport, London, 1G78.
2. JONES, C.J.F.P., JAMIESON, W., KRIPWELL, J.B. and BUSH, D.I., Reinforced Earth Trial Structure - Dewsbury Ring Road, Internal Report, 1986.
3. SARSBY, R.W., Reinforced Soil Using Pulverised Fuel Ash, 8th Danube Conference on Soil Mechanics and Foundations, Nuremberg, 1986.

Leere Seite
Blank page
Page vide

Innovative Lightweight Floor Systems for Steel Framed Buildings

Nouveaux planchers légers pour bâtiments à structures métalliques

Neue Konzepte für leichte Deckensysteme in Stahlrahmengebäuden

John R. HILLMAN
Research Assoc.
Virginia Tech
Blacksburg, VA, USA

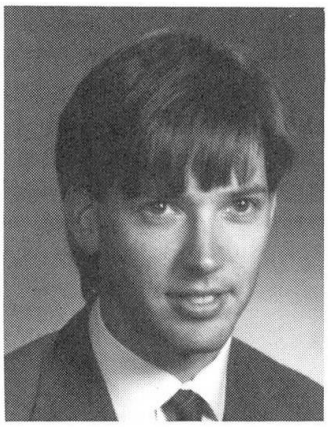

John Hillman received his Bachelor's Degree in Civil Engineering in 1986 from the University of Tennessee, Knoxville, TN, and his Master's Degree in Civil Engineering from Virginia Polytechnic Institute and State University, Blacksburg, VA, in 1990.

Thomas M. MURRAY
Prof. of Struct. Steel Design
Virginia Tech
Blacksburg, VA, USA

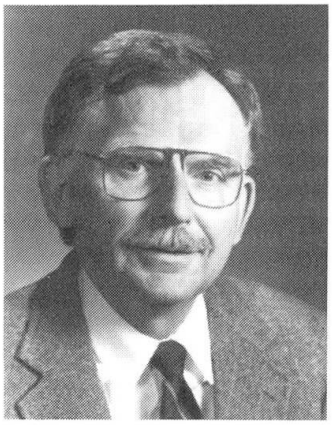

Thomas M. Murray received his Bachelor's Degree in Civil Engineering in 1962 from Iowa State University, his Master's Degree in Civil Engineering in 1966 from Lehigh University and his Ph.D. in Engineering Mechanics in 1970 from the University of Kansas. He is presently a distinguished Professor at Virginia Tech.

SUMMARY

The floor system has always been one of the heaviest components of a building structural system, and therefore comprises a significant portion of the dead load. By developing substantially lighter-weight floor systems it should be possible to reduce the entire weight of a building structural system, from the framing members to the foundations. This paper presents some innovative concepts for constructing lighter-weight floor systems using various configurations of mixed materials.

RÉSUMÉ

Le plancher a toujours été un des éléments les plus lourds du système structural d'un bâtiment et, par conséquent, il représente un part important du poids propre de la structure. En développant des planchers bien plus légers, il devrait être possible de réduire le poids total de la structure d'un bâtiment, des portiques jusqu'aux fondations. Cette communication présente quelques nouvelles idées pour la construction de planchers légers, en utilisant des configurations différentes de mélanges de matériaux.

ZUSAMMENFASSUNG

Das Deckensystem war schon immer der schwerste Teil der Baukonstruktion und macht daher einen wichtigen Teil des Eigengewichtes aus. Durch die Entwicklung von wesentlich leichteren Deckensystemen soll es möglich werden das Eigengewicht der ganzen Baukonstruktion, vom Rahmen bis zum Fundament, zu vermindern. Dieser Beitrag beschreibt neue Konzepte für leichte Deckensysteme durch Verwendung von Verbundmaterialen.

1.0 INTRODUCTION

It is a constant challenge to engineers to seek innovative methods to build lighter weight structures. Sometimes it is achieved through the development of new building materials, other times it can be accomplished by creating entirely new types of structural systems. Often lightweight structures can be more aesthetically pleasing because of their stream lined appearance. However, in general the motivating factor in building lightweight structures is to reduce the overall cost. One portion of a structure which offers tremendous potential for weight reduction is the floor system. A reduction in the dead load of this component may result in a subsequent reduction in the total weight of a building structural system. The objective of this investigation is to create or identify innovative lightweight floor systems that can effectively reduce the overall cost of steel framed building construction.

For many years the most common type of floor system used in steel framed buildings was a 102 mm thick concrete slab with the supporting beams completely encased in concrete. On top of this was a 102 mm topping slab which also contained all of the conduits and wires [1]. In all, these thick floor slabs accounted for a substantial portion of the dead load of a building.

During the early 1900's many new floor concepts were developed in an attempt to increase the fire ratings of buildings as well as reduce the dead load contributed by the floor system. Some of these include ceramic arch floor systems, the Columbian Floor System, Roebling Floor Systems, and The Rapp Fireproof Floor System [2]. Although these systems offered many advantages over thick concrete slab floors they eventually fell by the wayside. The two primary reasons for this were the dwindling supply of cinders used for the lightweight concrete fill material and the onset of steel deck floor systems [1].

The first cellular steel floor was used in a Baltimore & Ohio Railroad Co. warehouse in Pittsburgh, PA in the early 1920's. This cellular floor system was referred to as the "keystone beam", manufactured by the H.H. Robertson Co.. In early steel deck floors, the deck was the only load carrying structural element. The concrete slab was only necessary to provide a level surface and to obtain an adequate fire rating. More recent developments for the use of steel deck floor systems include steel deck that acts compositely with the slab, and composite beam action between the steel framing members and the slab through the use of shear studs. This composite beam action makes it possible for the design engineers to reduce the weight of the steel beams in the floor systems by as much as thirty percent [1].

At the present day, the most common types of floor systems used in typical steel framed buildings in the United States incorporate the use of cold-formed steel deck and concrete slabs, with or without composite beam action. Although profiled steel deck and concrete floors provide a lighter weight alternative to the thick concrete slabs of earlier years, little research has been conducted with regard to developing completely new floor systems that may result in even greater dead load reductions.

2.0 REFERENCE FLOOR SYSTEM

As a basis of comparison for the innovative light-weight floors being investigated, a series of reference floor systems were designed. In light of the advantages and the popularity of cold-formed steel decking, this configuration was chosen for all of the reference floor designs. Some of the systems were designed using hot-rolled shapes others use open web steel joists. All of the systems were designed using normal weight concrete, 22.78 kN/m^3, and two of the floors exploit composite beam action. A total of thirteen different systems were designed to allow a broader basis of comparison.

One of the primary disadvantages of lightweight floor systems is that they tend to be susceptible to annoying vibrations induced by human occupancy. The vibration characteristics of the reference floor systems were analyzed using the perceptibility criterion developed by Murray [3]. This is done by using the following inequality ($D > 1.38A_0f_1 + 2.5$), where D = required damping, A_0 = maximum initial amplitude of the floor system due to a heel-drop impact (in mm), and f_1 = first natural frequency of the floor system (in Hz). For use in the mathematical model, the heel-drop impact is approximated by a linear decreasing ramp function having a magnitude of 2.67 kN and a duration of 50 milliseconds. Based on the inequality developed by Murray, if the required damping is significantly more than 4%, then some sort of artificial damping may be necessary to make the floor system less susceptible to annoying vibrations.

All of the reference floor systems were designed using a superimposed live load of 3.35 kPa. The vibration analysis for each system only considers dead load plus a superimposed live load of 0.527 kPa. The average unit weight of the reference floor systems is 2.05 kPa, and the average required damping is 5.2%. One very obvious characteristic of all of the floor systems is that 80 to 88 percent of the total weight can be attributed to the concrete slab. As a result, it appears that the most significant weight reduction can be achieved by a reduction in the slab weight. Although lightweight concrete could be used to reduce the weight of the reference floors, normal weight concrete has been specified because it generally more available and less expensive.

3.0 FIBRE REINFORCED PLASTIC - PULTRUDED DECK

The first conceptual floor system to be discussed is a composite slab system constructed using a fibre reinforced plastic (FRP) deck with a concrete fill. The proposed deck is manufactured using the pultrusion process. Pultruded shapes are one of the most common types of FRP used in civil engineering applications and usually consists of glass fibre reinforcing with a polyester or vinylester resin. The components are combined by pulling the continuous glass rovings longitudinally through a resin bath where they are completely coated. Once coated they are pulled through a hot compaction die that cures the resin [4].

The pultruded deck consists of a series of 76.2 mm deep inverted T-beams on 76.2 mm centers. The beams are connected by intermediate flanges approximately 25.4 mm from the top flanges. A 25.4 mm concrete fill is placed on the top of the flanges (Fig. 1). The inverted T-beams and intermediate flanges are pultruded monolithically in 0.6 m to 0.9 m wide sections. The intermediate flange is located so that when composite action is considered most of the concrete is located above the neutral axis of the composite section. It was found that by assuming full composite action with the concrete, the rigidity of the section is at least doubled.

This type of deck configuration could be incorporated into a floor system by spanning the deck continuously over secondary framing members spaced at 0.9 to 2.1 m. The FRP deck itself weighs approximately 0.158 kPa. A normal weight concrete fill would add an additional 0.694 kPa. Compared to the reference floor systems this corresponds to a weight reduction of anywhere from 50% to 60%.

Despite the dramatic weight reduction this type of floor system has several disadvantages: high raw material costs, possible excessive deflections due to the low elastic moduli of the materials, poor vibration characteristics and potential fire rating concerns (which may be improved by using fire resistant resins).

4.0 STEEL GRID FLOOR SYSTEMS

Steel grid decking is another promising alternative to cold-formed steel deck/concrete slab systems. Steel grids were originally developed in the 1920's for use as a light-weight, but high strength bridge deck alternative to thick reinforced concrete slabs [5]. However, the grids manufactured for bridges would be far to heavy for use in building construction. An alternate form of steel grid floor system was developed in conjunction with this investigation (Fig.2).

The proposed system differs from present grid decks in several aspects. For example, the spacing on the primary bearing bars is increased to 457 mm rather than the usual 152 to 203 mm. The spacing on the secondary bars is also increased to 305 mm. This results in a much more open grid which in turn requires considerably fewer welds to fabricate. The primary bars used are 108 mm custom rolled I-beams. The secondary bars used are 25.4 mm by 4.76 mm rectangular bars. The secondary bars are installed such that the top of the bars are 12.7 mm from the tops of the 108 mm primary beams.

The biggest difference in the proposed deck is in the type of form pans used. Rather than install small square panels between the members of the grid, a continuous, light-gage cold-formed steel deck is placed with the ribs parallel to the 108 mm I-beams. Subsequently the profiled deck is supported both longitudinally by the top flanges of the I-beams as well as transversely by the tops of the secondary bars. The deck is installed during the fabrication process or during erection.

Finally, a 38.1 mm deep lightweight concrete slab is placed on the profiled steel deck. The entire configuration would weigh 0.895 kPa. This reduction in steel weight, along with lower fabrication costs, makes the proposed grid deck floor system feasible. This system also presents a significant reduction in the weight relative to typical floor systems.

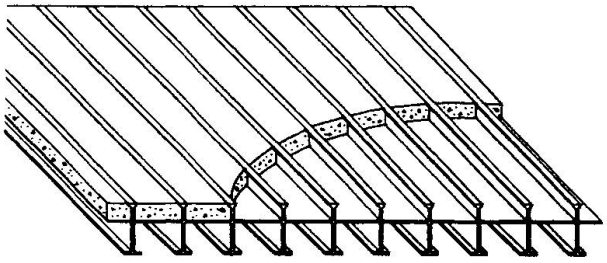

Fig. 1. (FRP) - Pultruded Deck

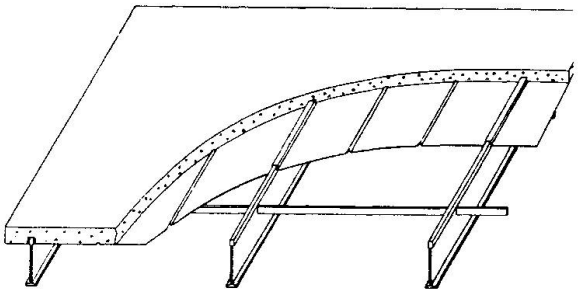

Fig. 2. Steel Grid Floor Systems

5.0 LONG-SPAN STEEL GRID

Another variation of the steel grid floor system was also investigated (Fig. 3). This system is similar to the previously discussed deck, except that the primary beams consist of a custom, hot-rolled shape that resembles an inverted T-beam rather than an I-beam. The beams are designed to be 178 mm deep with a very small top flange and very large bottom flange. These beams are then placed on 15 mm to 305 mm centers, and interconnected with 38.1x4.76 mm rectangular bars. A light gage profiled steel deck is placed continuously between the beams supported by the secondary bars. A light-weight concrete slab with a total depth of 51 mm is placed on top of the deck. Shear forces are transferred between the concrete and the steel beams by providing deformations in the top flanges of the steel beams similar to those found on typical reinforcing steel.

The primary benefit of this system is that it is able to span 9.1 m as a simply supported beam. This eliminates the need for any secondary framing members, and because the entire configuration is only 203 mm deep, it results in an overall reduction in the floor to floor height of the structure.

6.0 LONG-SPAN DECK/CONCRETE SLAB COMPOSITE FLOORS

The last floor system developed is a long-span deck and composite slab floor system. This system would consist of 190.5 mm deep, 14 gage cold-formed steel hat sections placed side by side with a shallow concrete slab poured above the top flanges (Fig. 4). The concrete itself is placed on top of a very light gage, shallow steel deck which is laid transversely across the top of the long-span deck and rigidly attached by self-tapping stand-off fasteners. In addition, the shallow profiled steel deck is designed so that shear forces can be transferred between the steel and concrete components.

The long-span deck acting compositely with the concrete slab is also capable of spanning up to 9.1 m. without the need for secondary framing members. The entire floor system is only 241 mm deep and weighs 1.436 kPa. As with the long-span steel grating, this system offers the potential for reducing the floor to floor height of a building. It may also be possible to use the cells of the deck to accommodate service requirements. These characteristics could aid in making steel framed buildings more competitive against concrete frames utilizing thin post-tensioned flat slab floors.

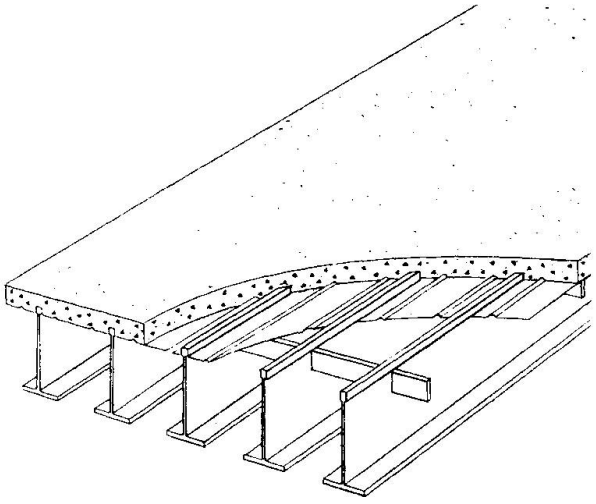

Fig. 3. Long-Span Steel Grid

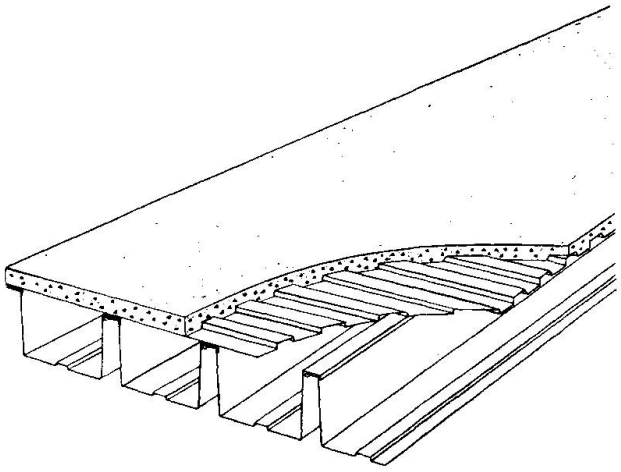

Fig. 4. Long-Span Deck/Concrete Slab

7.0 CONCLUSIONS

If strength were the only requirement, designing lightweight floor systems would be a fairly simple task. However floor systems perform a great many functions in addition to merely sustaining gravity loads without some sort of catastrophic failure. Subsequently, a host of behavioral characteristics have to be taken into consideration to successfully design and implement any innovative lightweight floor system.

Table 2, shown below, provides a quantitative comparison for some of the innovative floor systems investigated. The basis of comparison is the average reference floor system. The unit weights for the various systems include the weights of both the slab and framing components. The %SLAB value is the

percentage of the total weight attributed to the slab component. The vibration characteristics for the proposed systems have been calculated using the mathematical models presented in Technical Digest No.5 of the Steel Joist Institute [6] as well as the perceptibility criterion developed by Murray [3].

Table 2: CHARACTERISTICS OF PROPOSED SYSTEMS

SYSTEM ANALYZED (Single Bay 9.1m x 9.1m)	WEIGHT kPa	WEIGHT %SLAB	VIBRATION RESPONSE f_n (Hz)	VIBRATION RESPONSE A_o (mm)	VIBRATION RESPONSE D_{REQD} (%)
RFS AVERAGE	2.052	85.1	5.68	0.340	5.16
FRP Deck w/2% steel reinf.	0.947	73.9	8.68	0.381	7.14
Long-Span Deck/Conc. Slab	1.193	64.4	5.04	0.483	5.84
Steel Grid (18in x 12in)	1.126	79.6	5.15	0.381	5.13
Long-Span Steel Grid	1.724	80.2	4.20	0.381	4.64

As indicated in Table 2, it is possible that some of the proposed lightweight floor systems may actually perform better than the reference floors with respect to vibrations. However the results of these vibration analyses should be verified by experimental testing in order to make a truly accurate comparison.

Overall, the systems which appear to have the most potential for further development at this time are the long-span deck/concrete slab concept and the steel grid floor systems. Both of these systems offer the advantage of lighter weight compared to present methods of construction. Although they do not necessarily represent the lightest alternatives investigated, it is believed that these two floor systems may offer the best performance with respect to the various functional requirements set forth.

REFERENCES

[1] Dellaire, E.E. [1971]. "Cellular Steel Floors Mature", Civil Engineering, ASCE, 41(7), Jul, 70-74.

[2] "Sweet's": Indexed Catalog of Building Construction [1906]. The Architectural Record Co., New York, NY, 88-116.

[3] Murray, T.M. [1981]. "Acceptability Criterion for Occupant-Induce Floor Vibrations." Engineering Journal, AISC, 18(2), 62-70.

[4] Gosnell, R. [1987]. Composites and Laminates, ed.1., D.A.T.A. Inc., and The International Plastics Selector, Inc., A-1 to A-9.

[5] Gilmore, G.R. [1987]. "Steel-Grid Bridge Flooring: Recent Innovations to Modular Decking System", Modern Steel Construction, AISC, 27(5), Sept-Oct, 16-33.

[6] Galambos, T.V. [Undated]. "Vibration of Steel Joist Concrete Slab Floor Systems." Technical Digest No. 5., Steel Joist Institute, Arlington, VA.

Bamboo-Reinforced Concrete Beams

Poutres en béton armées de bambous

Betonbalken mit Bambusbewehrung

Anil SHARMA
Senior Lecturer
Univ. of the West Indies
Trinidad, West Indies

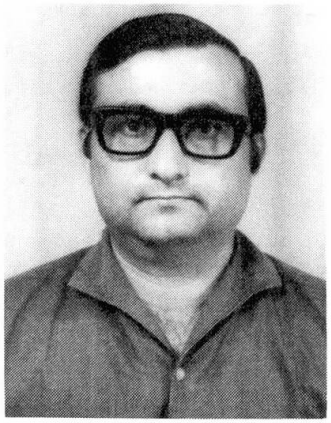

Anil Sharma, born 1942, received Ph.D. in Civil Engineering from Univ. of Rajasthan, India. Involved in teaching and research in the area of Structural Engineering for the last 25 years.

SUMMARY

An experimental investigation to examine the effectiveness of bamboo as reinforcement in reinforced concrete Tee beams is reported. In all, eight bamboo reinforced simply supported members were tested to failure to study the effect of varying percentages of longitudinal bamboo reinforcement on the ultimate strength of beams. The effectiveness of bamboo stirrups (links) as shear reinforcement was also examined. Water-repellant treatments for bamboo reinforcement are discussed. A method based on the test results is proposed for analysing such beams.

RÉSUMÉ

Cet article présente l'analyse expérimentale menée pour déterminer l'efficacité du bambou en tant qu'armature de poutres en béton armé à section en T. Huit poutres sur appuis simples armées de bambous ont été soumises à des essais de rupture pour étudier l'effet du pourcentage variable du renforcement longitudinal en bambou sur la résistance ultime de ces éléments porteurs. On examine aussi l'efficacité offerte par des étriers en bambou prévus comme armatures de cisaillement. On donne en outre un certain nombre de traitements hydrofuges des armatures en bambou. L'article propose enfin une méthode d'analyse de ces poutres en se basant sur les résultats découlant des essais.

ZUSAMMENFASSUNG

In dieser Arbeit wird über experimentelle Untersuchungen zur Anwendbarkeit von Bambus als Bewehrungsmaterial in T-förmigen Balken aus Beton berichtet. Insgesamt wurden acht mit Bambus bewehrte einfach gestützte Balken bis zum Versagen untersucht. Der Einfluß der Längsbewehrung aus Bambus in verschiedenen Prozentsätzen auf die Traglast der Balken wurde studiert. Die Anwendbarkeit von Bügeln aus Bambus als Schubbewehrung wurde auch untersucht. Wasserabstoßendmachende Behandlungsverfahren für Bambusbewehrungen werden ebenfalls besprochen. Eine Methode zur Analyse von solchen Balken mit den Ergebnissen der Untersuchungen als Grundlagen wird dargestellt.

1. INTRODUCTION

The less developed world today faces the daunting task of providing housing for the millions who now live in grossly inadequate shelters. The situation will worsen as it is estimated that the world population will increase by the year 2000 to about six billion of which more than four billion will live in these lesser developed countries. The problem of inadequate shelters is compounded by the high cost and general shortage of reinforcing steel and other suitable construction materials. Consequently research effort is now aimed at developing various types of cement concrete reinforced with locally available natural fibres or with relatively cheap man-made fibres. One such natural fibre is bamboo.

Bamboo is an ancient building material and its use so far has been more traditional than technical. It has long served many purposes but the application of materials technology to bamboo took place only in comparatively recent years [1,2]. It is yet to be fully exploited for major engineering applications. Economics and other relative factors in developing countries now require Civil engineers to apply appropriate engineering technology to utilise bamboo as effectively and economically as possible in various construction works.

This paper examines the effectiveness of bamboo reinforcement in reinforced Concrete T-beams. In all eight bamboo reinforced simply supported beams were tested to failure under four point loading. All beams were of the same cross-sectional dimensions. Collapse occurred either due to flexural and/or diagonal tension failure of the concrete in shear span. The following parametric studies were conducted:

- the effect of varying percentage of longitudinal bamboo reinforcement on the ultimate strength of beams
- effectiveness of bamboo stirrups (links) as shear reinforcement
- types of water-repellent treatment for bamboo reinforcement and their effectiveness.

Experimental test results were compared with theoretical formulas developed based on simple bending theory. The proposed formulas predict strength of bamboo reinforced beams with reasonable accuracy.

2. DETAILS OF EXPERIMENTAL WORK

The concrete was made from ordinary portland cement, natural river sand and coarse aggregate having a nominal maximum size of 10mm. The mix proportions used were (water: cement: fine aggregate: coarse aggregate) = (0.58: 1.0: 1.26: 2.11) by weight. Along with each specimen three 100mm cube specimens were also cast.

The bamboo used in this investigation belonged to the Bambusa Vulgaris which is abundantly available in the West Indies. The bamboo culms of this species were seasoned for periods varying from 60 to 78 days. The average tensile strength based on six test specimens was 145 N/mm^2. These specimens comprised of nodes and internodes. Another set of test was conducted to estimate the tensile strength between two nodes (internodal). The average tensile strength in this case was estimated to be 200 N/mm^2. Tension bamboo reinforcement was tied into two or three layers of two splints each separated vertically by short spacer splints 10mm thick with the outer sheaths of the splints facing the zone of the greatest tensile stress (Fig. 1).

The eight test specimens were divided into four groups as given in Table 1. Each group had two beams. Except group A in which the number of layers of bamboo reinforcement was two all other had three layers.

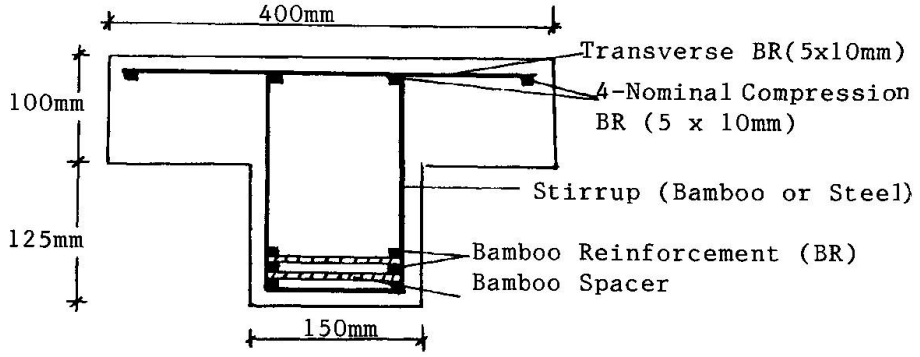

Fig. 1 Typical Cross-Section of Beam

Beam No.	Area of Reinforcement A_b (mm^2)	Percentage of Reinf.	Type of Shear Reinf.	Type of treatment of Reinf*
A2	881	2.61	Steel	WG
A3	893	2.65	Steel	BS
B4	1273	3.77	Steel	WG
B5	1302	3.86	Steel	BS
C6	1362	4.03	Bamboo	WG
C7	1361	4.03	Bamboo	BS
D8	1374	4.07	Steel	WG
D9	1367	4.05	Steel	BS

* Waterglass (WG), Bitumen + Sand (BS)
Table 1 Details of Test Beams

The reinforcement for the test specimens A3, B4, C7 and D9 were treated with two coats of bituminous paints at interval of 24 hours, dusted with sand immediately after second coat and allowed to dry for a further period of 24 hours before use. Whereas for the other beams the reinforcement was treated by plunging it into a waterglass - dipping bath for 15 mins. The density of the bath was 1.15 kg/dm^3. In the C-Series beams, 5x5mm bamboo stirrups were used at a spacing of 120mm. The stirrups consisted of two horizontal and two vertical bamboo pieces [3]. Small incisions were made at the end of the pieces, then the two ends meeting at each of the four corners were tied together by means of steel wire. Before fabrication these bamboo stirrups were pretreated as indicated in Table 1. In the rest of the test specimens high yield strength steel stirrups (630 N/mm^2) were provided. They had a nominal diameter of 3.4mm and 175mm x 100mm size (same as bamboo stirrups). The spacing of steel stirrups was 130mm.

The loading arrangement is shown diagramatically in Fig. 2a. Demec gage points on both vertical faces of the beam were provided as shown in Fig. 2b. At each increment of load the mid-span deflections and concrete strains were recorded. The load increments were applied until the beam failed.

3. ANALYSIS

The tensile strength of concrete can be reasonably estimated based on the cube strength [4] using

$$f_{tc} = 2/3 + f_{cu/15} - f_{cu}^2/2600 \quad \ldots\ldots (1)$$

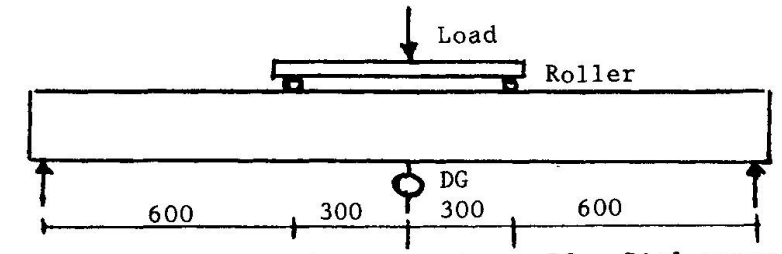

Fig. 2a Loading Arrangement DG - Dial gauge

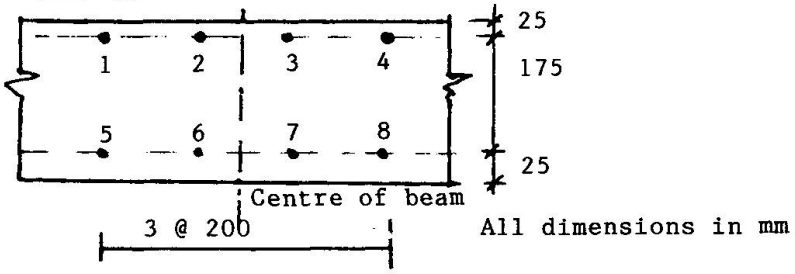

Fig. 2b Part Elevation of Test Specimen

in which f_{tc} is the tensile strength of concrete in N/mm² and f_{cu} is the cube strength in N/mm².

The cracking moment (M_{cr}) of an unreinforced concrete T-beam can be expressed as

$$M_{cr} = f_{tc} . Z \quad . . \quad (2)$$

in which Z is the section modulus of the test specimen. And the ultimate moment of resistance of beam can be calculated using BS 8110 [5]. Neglecting compression reinforcement the ultimate moment of resistance M_u is given

$$M_u = f_b . A_b . Z \quad . . . . . \quad (3)$$

in which f_b is the tensile strength of bamboo (estimated to be 145 N/mm²), A_b is the area of tension reinforcement and Z is the lever arm equal to 0.775 times the effective depth (d) of the test specimen.

The cracking or ultimate load on the beam can be calculated using equation (4):

$$P = 6M/L \quad . . . . . \quad (4)$$

The shear strength of the beam was calculated based on BS8110. Total shear strength (P_{us}) of the beam equals

$$P_{us} = (\upsilon_c + \upsilon_s)\, bd \quad . . . . . \quad (5)$$

in which b and d are the web width and effective depth of the beam respectively, υ_c is the shear strength of plain concrete and υ_s is the shear stress contributed by stirrups and is calculated using equation (6):

$$\upsilon_s = \frac{A . f}{b . S_\upsilon} \quad . . . . . \quad (6)$$

in which A is the cross-sectional area of the vertical legs of stirrup, f is the tensile strength of stirrup (bamboo-internodal strength) and S_υ is the spacing of stirrups.

4. TEST RESULTS AND DISCUSSION

4.1. Modes of Failure

The collapse of the beams was observed to have following distinct failure mode:

- Flexural Mode (Beams A2 and A3)
- Flexural and shear Mode (Beams B4 and B5)
- Shear Mode (Beams C6, C7, D8 and D9)

The flexural failure was characterized by substantial cracking emanating

from the tension face and penetrating deep into the compression zone (flange) of the beam. Whereas, shear failure (diagonal tension failure) was characterized by extensive cracking in the shear zone of the beam. The cracking was about 45° to the axis of the beam and extended from the supports to the load points.

4.2 Test Results and Comparison with Theory

The principal test results and their comparison with theory is given in Table 2. The mean P_c/P'_c is 1.135 with a standard deviation of 23.6%. The large variation could be attributed to the difficulty in ascertaining visually the initial cracks. The first four beams failed in flexure. The test results were compared with Eq.(3). The mean P_u/P'_{uf} was 1.065 with a standard deviation of 7.2%. The last four beams which were designed to fail in shear failed as predicted. The test results were compared with Eq. (5).

Beam No.	Average * Compressive Strength (N/mm^2)	Expt. Load: First crack P_c (kN)	Expt. Load: Ultimate P_u (kN)	Theoretical Strength: First crack P'_c (kN)	Theoretical Strength: Ultimate: Flexure P'_{uf} (kN)	Theoretical Strength: Ultimate: Shear P'_{us} (kN)	$\frac{P_c}{P'_c}$	$\frac{P_u}{P'_{uf}}$	$\frac{P_u}{P'_{us}}$
A2	37	17.5	62.5	13.7	60.4	-	1.28	1.03	-
A3	29	20.0	62.5	12.1	61.2	-	1.65	1.02	-
B4	41	12.5	84.0	14.7	82.0	-	0.85	1.02	-
B5	37	15.0	100.0	13.7	83.9	-	1.09	1.19	-
C6	30	12.5	50.0	12.1	-	53.6	1.03	-	0.93
C7	35	12.5	68.4	13.1	-	55.7	0.95	-	1.23
D8	29	15.0	65.0	12.1	-	54.4	1.24	-	1.19
D9	31	12.5	60.0	12.6	-	55.4	0.99	-	1.08
						Mean	1.135	1.065	1.107
						Standard Dev.	0.236	0.072	0.116

* Based on 3-100mm cubes

Table 2 Comparison of Experimental and Theoretical Results

The mean P_u/P'_{us} was 1.107 with a standard deviation of 11.6%

4.3 Effect of Percentage of Reinforcement

It was observed that an increase of bamboo reinforcement up to 3.8% increased the load carrying capacity of the beam. The load-deflection characteristics of bamboo reinforced beams (Fig. 3) are found to be similar to that of conventional steel reinforced concrete beams.

4.4 Type of Treatment

In all cases the performance of the beams treated with bitumen plus sand was better than the beams treated with waterglass. In general, the beams with former treatment gave a higher load carrying capacity.

4.5 Bamboo Stirrups

Based on the limited test data in this investigation, there are indications that steel stirrups can be replaced by bamboo stirrups. Proper care must be taken in tying the horizontal and vertical bamboo pieces. To increase the tensile strength of bamboo stirrups the pieces of bamboo should be free of nodes.

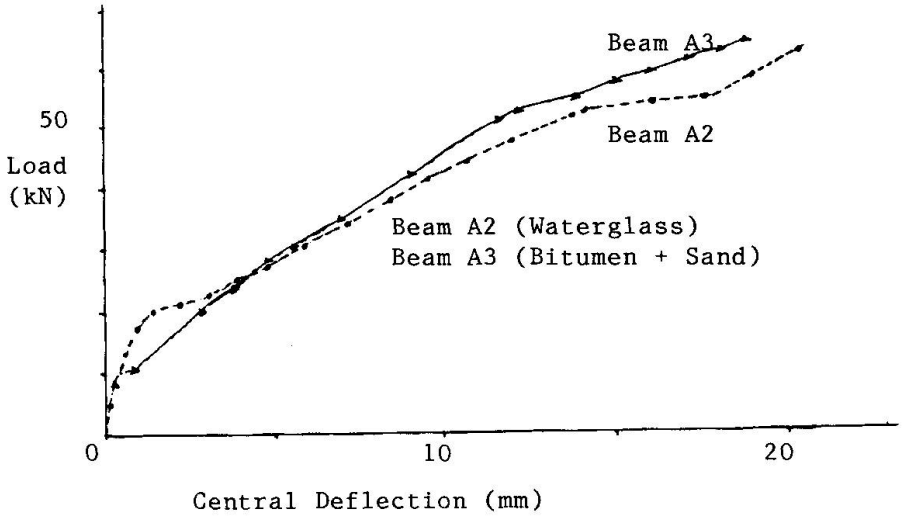

Fig. 3 Load-Deflection Curves

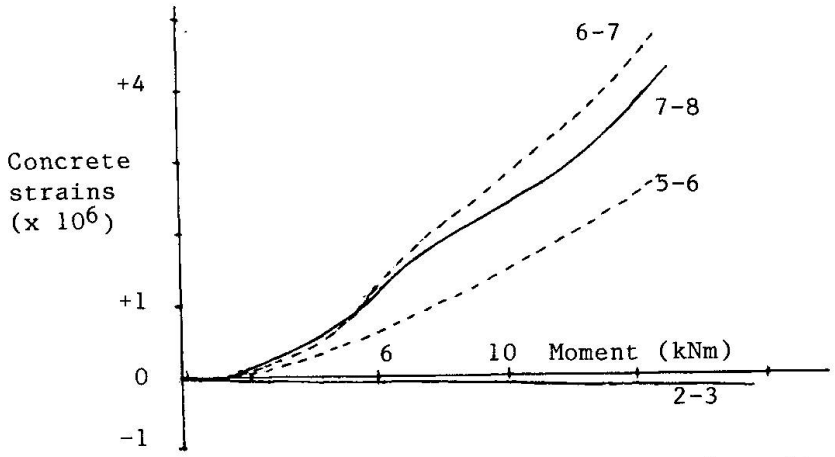

Fig. 4 Concrete strain vs Bending Moment in Beam C6

4.6 Concrete Strains

Concrete strains for a typical beam is shown in Fig. 4. The strain curves are found to be similar to the conventional steel reinforced beams.

5. CONCLUSIONS

Based on the tests reported in this investigation following conclusions can be drawn:

(a) The load carrying capacity of the bamboo reinforced concrete beams increased with increase in percentage of bamboo reinforcement. The optimum percentage range upto which the load carrying capacity increases is between 3.5 - 4.0 percent of the gross cross-sectional area of the member.

(b) 'Bitumen plus sand' water-repellant treatment was found to be suitable for bamboo reinforcement.

(c) Structural behaviour of bamboo reinforced concrete T-beams was found to be similar to that of conventional steel reinforced beams.

(d) The bamboo stirrups performed creditably well, however more tests are required before definite conclusions can be drawn.

(e) The theory proposed based on BS8110 gives reasonable estimate of the ultimate strength of bamboo reinforced concrete beams.

Developing Design Requirements for Non-Metallic Tendons

Éléments de précontrainte non métalliques

Bemessungskriterien für nicht-metallische Spannglieder

Arie GERRITSE
Civil Engineer
Hollandsche Beton Groep
Rijswijk, The Netherlands

Arie Gerritse, born in 1929 graduated in Civil Engineering at Rotterdam Technical College, the Netherlands. He is a staff member of the R & D department of Hollandsche Beton Groep (HBG).

Jürgen WERNER
Civil Engineer
Akzo nv
Wuppertal, FR Germany

Jürgen Werner born 1939 obtained his Civil Engineering degree at the Technical University of Braunschweig in 1966. He is project manager in the field of application of fibre reinforced materials in Civil Engineering.

Martin EGAS
Civil Engineer
Hollandsche Beton Groep
Rijswijk, The Netherlands

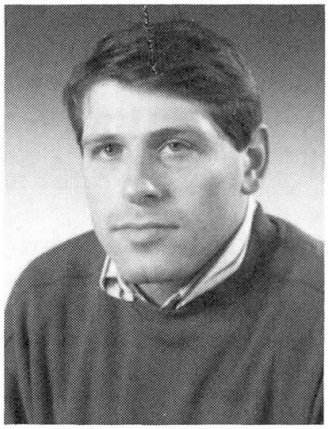

Martin Egas born in 1963 obtained his Civil Engineering degree at the Technical University of Delft, the Netherlands in 1988. He is working as a research engineer at the R & D department of HBG.

SUMMARY

The use of non-metallic tendons may involve the introduction of new or less-known problems. Specially the long-term behaviour under constant stress and in alkaline environments needs to be assessed for reliable applications of high strength polymeric fibers. A safety concept for these new materials has to take into account the abovementioned phenomena.

RÉSUMÉ

L'utilisation d'éléments de précontrainte non métalliques peut impliquer des problèmes nouveaux ou peu connus. C'est avant tout le comportement à long terme sous charge constante et en milieu alcalin qui est à examiner pour des applications fiables de fibres polymères à haute résistance. Une évaluation de la sécurité de ces nouveaux matériaux doit tenir compte de ces phénomènes.

ZUSAMMENFASSUNG

Bei der Anwendung nicht-metallischer Spannglieder können neue oder wenig bekannte Probleme auftreten. Für die zuverlässige Anwendung von hochfesten polymeren Fasern muss insbesondere das Langzeitverhalten unter konstanter Belastung in alkalischer Umgebung untersucht werden. Diese Phänomene müssen für eine Sicherheitsbeurteilung dieser neuen Materialen berücksichtigt werden.

1. Introduction

For some applications, e.g. structures in highly aggressive environment, the combination of concrete with non-metallic tendons, e.g Arapree, a prestressing tendon consisting of bonded parallel aramid fibres embedded in a epoxy resin [1], can be advantagous.
Using non-metallic tendons means that new materials are introduced through which new or less-known phenomena, due to the mechanical, physical or chemical properties of these materials, become more critical. Therefore adapted design criteria, based on the properties of the "new fibres" have to be developed.
Specially the long term behaviour under constant stress and in alkaline environment, needs to be assessed for reliable applications of high strength fiber. So it is essential to know about the:

- behaviour under sustained high stress levels (stress rupture)
- behaviour in alkaline and carbonated environment
- creep and relaxation behaviour
- fatigue behaviour
- bond with concrete

and develop a safety concept based on these data. How we approached the above for Arapree and the type of requirements we assume to be valid also for comparable materials will be explained in more detail.

2. New fibres and fibre based reinforcement for concrete

An overview of types of several high strength fibrous tensile elements recently developed for use in concrete which are already more or less commercial use is given in table 1 [2].
The range of types under development is expanding rapidly.

Table 1: High strength fibrous tensile elements

Tensile element	Type of fibre	Fibre-brand name	Type of composite	Producer
Arapree	aramid	Twaron HM	epoxy-resin impregnated parallel fibre bundles	AKZO
Bri-ten	aramid carbon	Kevlar Carbon HS	resin impregnated parallel fibre bundles	Bridon
Fibra	aramid	Kevlar '49	epoxy-resin impregnated braided rod	Mitsui Shinko-wire
Nefmac	glass aramid carbon	var.	resin impregnated mesh	Nefcom (Shimizu)
Parafil	aramid	Kevlar '49	bare parallel fibre in sheating	ICI
Polystal	glass	E-glass	polyester resin impregnated parallel fibre bundles	Bayer

In table 2 the short term mechanical properties of prestressing steel, and three representative man-made, non metallic fibre reinforced elements are given. [2]. The strength and stiffness properties of Arapree are related to the effective fibre cross-section. This relation gives a more accurate value of the characteristics than if these values are based on the gross cross-sectional area, with differing volume. percentages of resin. The available types of Arapree are therefore indicated with the number of filaments.

Arapree f 100.000 for example, is an element of 100.000 filaments, with a cross-section of aramide fibres of 11,1 mm². That gives the element a characteristic strength of 31 kN and longitudinal stiffness (EA) of 1.388 kN.

table 2: mechanical properties of some fibre based composites and (prestressing) steel

property unit	steel (FeP 1860)	Polystal (glass)	Brit-ten (carbon)	Arapree (aramid)	Unit
density	7850	2100	1580	1250	[kg/m3]
char.strength	1,6	1,67	2,4	2,8*)	[kN/mm²]
youngs-modulus	200	50	150	125*)	[kN/mm²]
ult-strain	3,5	3,3	1,65	2,4	[%]
coeff.therm.exp.	12	7	0	- 2,0	[10E-5/°K]

*) Related to the effective fibre cross-section

A comparison of the stress-strain behaviour of the fibre based composites given in table 2 and steel is given in fig. 1.
The main difference of the considered non-metallic tendons and steel is the absence of a form of plasticity. This absence of plasticity does not mean that concrete structures prestressed with high-strength fibrous tensile elements don't have a so called warning behaviour. As will be illustated later on such structures can show a high ductility.

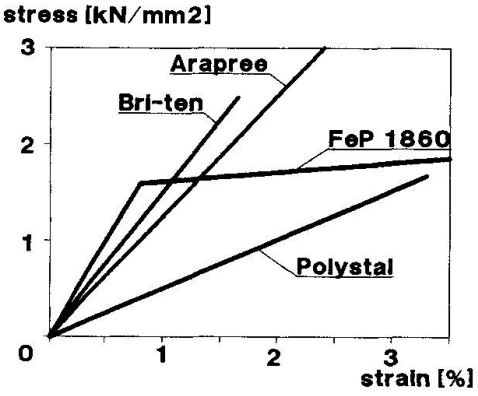

figure 1: stress-strain relation composites and steel

3. Influence of environment and time

Environment

The strength and stiffness values of non-metallic tendons are influenced by time, temperature, moisture content and acidity of the environment. As shown in fig. 2 the residual strength of Arapree after 10^6 hours (ca. 100 years) is 85% of the short-term strength [1].
Creep and relaxation are influenced by the environment. The relaxation of Arapree in an alkaline solution is approximately 20% after 10^6 hours, in a dry, neutral environment it is approximately 15%. [3].
The relaxation is hardly influenced by the stress level and temperature (less than ca. 80°C).

stress-rupture

Materials in general are susceptible to the presence of a sustained loading. Polymer materials like glass, carbon and aramid are more susceptible than steel. This so called stress-rupture behaviour can hardly be measured with steel.
The stress-rupture line in fig. 2 represents the relation between the stress-level in a aramid fibre and the average time that passes before the material fails under specific stress level (extra-polated from measurements upto 30,000 hours).

The residual strength also depends on the stress level and the loading duration.
In fig. 3 is represented the stress rupture, the residual strength of an unloaded Arapree tendon and the residual strength when a constant stress-level of 75% of the short term strength is applied. The figure shows that the residual strength of the loaded tendon follows the strength of the unloaded material, but just before the moment of stress-rupture the residual strength falls down [4].
More information about Arapree and its excellent fatigue behaviour is given in [1] and [4].

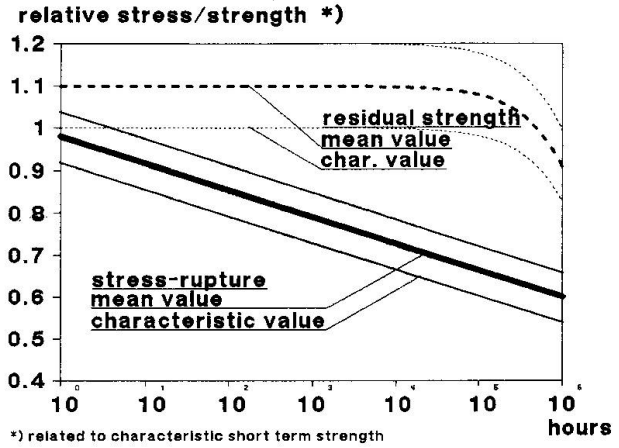

figure 2: stress-rupture behaviour (loaded Arapree) and residual strength of unloaded Arapree

4. Safety-concept

In civil engineering the effective usability of a structure must be ensured for a long period. For concrete structures a life time of 100 years (ca 10^6 hours) should be considerd.
To develop a safety concept we have to take into account at least:
- stress losses
- stress rupture
- residual strength
- enough ductility as warning for collapse.

First of all it is essential to know not only the mean strength values but also the variation of these values.
The characteristic values can be determined with this data.
A safety concept must be based on the characteristic values.

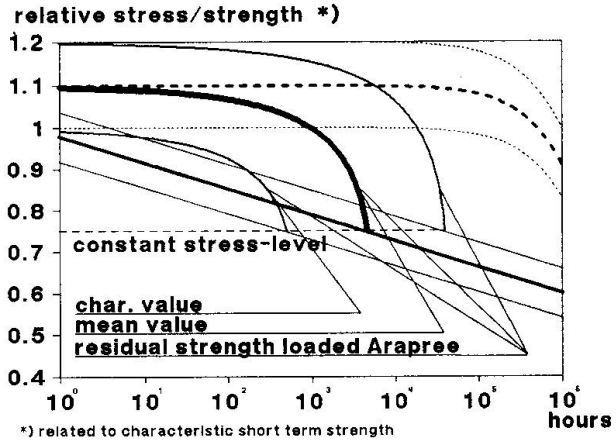

figure 3: stress-rupture and residual strength

It is clear that the stress-curve of a non-metallic tendon under sustained loading may not touch the stress-rupture curve, and a sufficient margin to the residual strength must be available. Therefore losses caused by creep and shrinkage of the concrete and relaxation of the tendon deformations and relaxation stress-rupture have to be considered.

The following formula of the stress losses has been derived:

$$\Delta\sigma_p = \{ \Delta\sigma_{p,rel,\infty} \left(1-0{,}85 \frac{\Delta\sigma_{p.cs,\infty}}{\Delta\sigma_{po}}\right)\} + \Delta\sigma_{p,cs,\infty}$$

$\Delta\sigma_p$ = final stress losses due to the relaxation of Arapree and the creep and shrinkag of the concrete

$\Delta\sigma_{p,rel,\infty}$ = final relaxation of the Arapree

$\Delta\sigma_{p,cs,\infty}$ = stress losses in Arapree due to creep and shrinkage of the concrete

$\Delta\sigma_{po}$ = initial stress in Arapree

As told before the safety of the structure in case of overloading is guaranteed because of the residual strength, which retains practically its short term unloaded strength until just before the moment of stress-rupture.
In figure 4 a maximum stress-curve with respect to losses is given. The stress rupture and the residual strength are shown with their characteristic values.

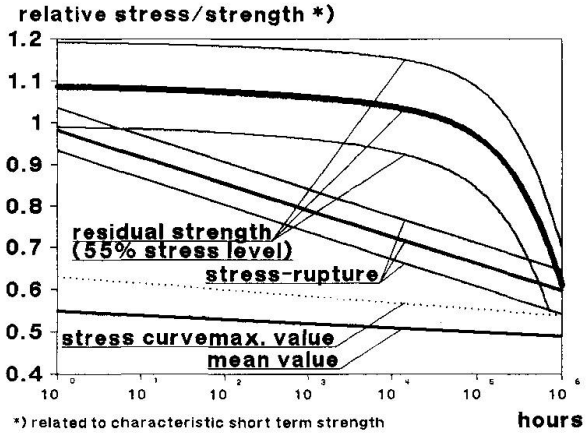

figure 4: stress curve

Although all non-metallic tendons are fully elastic elements, concrete elements prestressed or reinforced with these elements do show a high ductility because of the large strain capacity and due to cracking and deformation of the concrete. This is clearly demonstrated in the figure 5 [6] and figure 6, where the measured deflection curves are shown for two different structures. Figure 5 shows the deflection curve of a fence post prestressed with Arapree, figure 6 shows the deflection curve of an Arapree prestressed concrete panel. Like conventional prestressed concrete the warning behaviour depends on the amount and placing of the tensile elements.

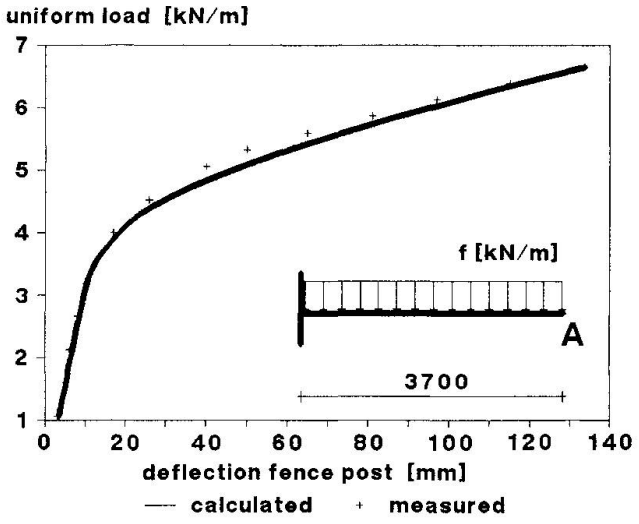

figure 5: load-deflection curve of a fence post prestressed with Arapree

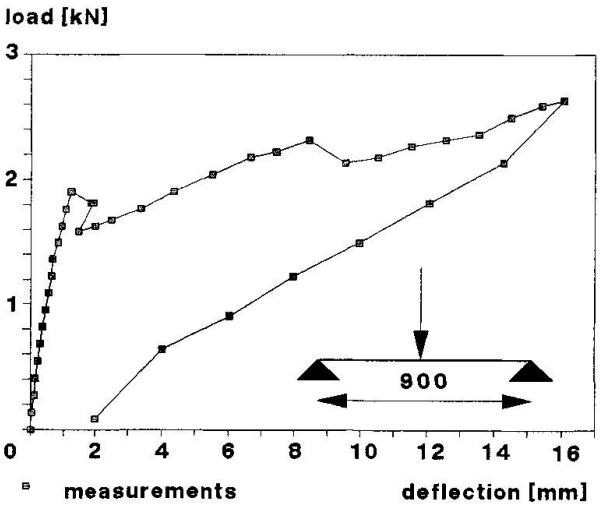

figure 6: load-deflection curve of a concrete panel prestressed with Arapree

5. Design Data

According to the safety-philosophy formulated above the following design criteria can be determined for Arapree:

- initial stress in Aramid fibre after release: $\sigma_{apo} \leq 0{,}55\ f^{*}_{atk} = 1550\ N/mm^2$
- relaxation of Arapree (deducted from tests):

$$\frac{\Delta\sigma_{p.rel,\infty}}{\sigma_{apo}} = 0{,}15 \text{ in dry environment}$$

$$\frac{\Delta\sigma_{p,rel,\infty}}{\sigma_{apo}} = 0{,}20 \text{ in wet environment}$$

*) f_{atk}: characteristic short term strength = 2800 N/mm²

- permanent loading should not cause stresses in the fibres that exceed : 1550 N/mm²
- if a stress level higher than 0,55 f_{atk} is chosen in case of a shorter life expectancy (< 100 years), the characteristic stress curve may not touch the characteristic stress rupture curve.

6. Applications:

Applications of Arapree in practice have been realised in a noise barrier, a hollow core floor slab, prestressed masonry, a fish ladder and balcony slabs [6]. More projects are under construction.

7. Conclusions:

To develop a safety concept for non-metallic tendons, one has to take into account the influence of environment, time and stress-level on the mechanical behaviour of the new materials.
Based on this properties it is possible to determine design criteria, in which is taken into account:
- stress losses due to relaxation, creep and shrinkage
- stress rupture
- residual strength

The calculated design data must be based on the characteristic values of the material properties.

References:

[1] Gerritse, A; Werner, J; Arapree the prestressing element composed of resin bonded Twaron fibres. Brochure Akzo and HBG, september 1988.
[2 Gerritse, Arie; Prestressing with Arapree; the artifical tendon; contribution to the Symposium on: New materials for prestressing and reinforcement of heavy structures, LCPC, Paris, 1988
[3] Gerritse, A; Werner, J; Groenewegen, L.A.M.; Long term properties of Arapree; Contribution to the IABSE symposium Lisbon, 1989
[4] Den Uijl, J.A.; Voorspannen met aramide vezels. Materialen 9 (1988)
[5] Christensen, R.M.; Residual strength determination in Polymer Materials, Journal of Rheology,25 (5) 1981.
[6] Reinhardt, H.W.; Werner, J.; Gerritse, A.; A New prestressing material going into practice. Contribution to FIP congres June 1990 Hamburg.

Experience with New Prestressing Materials

Expérience avec de nouveaux matériaux pour la précontrainte

Erfahrung mit neuen Spannbeton-Baustoffen

Joan R. CASS
Techn. Univ. of Catalunya
Barcelona, Spain

Angel C. APARICIO
Techn. Univ. of Catalunya
Barcelona, Spain

Recently the use of external prestressing technique became a subject of increasing interest in bridge construction. However, the long-term behaviour of external prestressing steel tendons are not yet well-known. Important corrosion problems had been already detected in cable-stayed bridges in last years. High strength fibres as an steel substitute show a satistactory short- term behaviour when tested in laboratory. However not so much is known about long-term behaviour in real construction environments. The poster deals with a full-scale application of aramide fibre as prestressing element in the agressive environment of a big city in order to continuously monitor the evolution of durability and structural properties along time.

The experimental design is a stretch (80 m. long) of a cantilever structure spanning 4 m. which has to support the upper traffic of the North Ring- Road now under construction in the city of Barcelona (Spain). This construction is a very important key in order to achieve a global solution on traffic communications involved in the celebration of the Summer Olympic Games in 1992. The prestressing element is an aromatic polyamid with a high degree of cristallinity (aramid) in a matrix of epoxy resin. Characteristic axial tensile strength is 2800 N/mm^2 and the elasticity modulus is 130 KN/mm^2. An important aspect concerning the long-term behaviour of this material is the aging phenomena under permanent prolonged load. The 80 m. experimental part is designed fully prestressed.The prestressing tendon layout is assumed straight with variable depth according to the linear variable depth of the cross section (Figure 1). Strain, displacement and pressure measurement devices are located on several elements in order to continuously monitor the long- term behaviour of prestressing fibre. In addition, five empty ducts of 10 cm in diameter are placed per element to fill-in with conventional prestressing steel tendons if the prestressing fibre does not work correctly in the future (Figure 2). Due to space problems to properly locate the ducts and long-term anchorages for the composite tendons in the cast in place solution, the prestressed cantilevers are precast elements of 1.8 m.(Total 40 elements) . The fibre is anchored by bond in concrete. According to the brittle rupture of the composite material the amount and location of reinforcing steel should be properly designed to achieve ductility requirements if the prestressing is not effective. The junction of precast elements with cast in place lateral walls is made by means of conventional prestressing bars avoiding the tensile stress in the joint (Figure 1). The cast in place reinforced concrete (20 cm) between precast elements assures the continuity of superestructure.

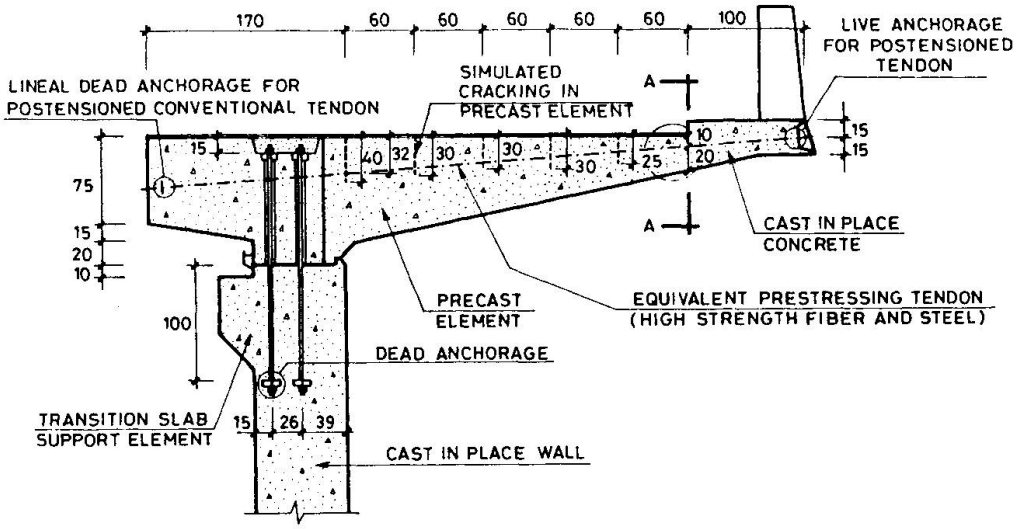

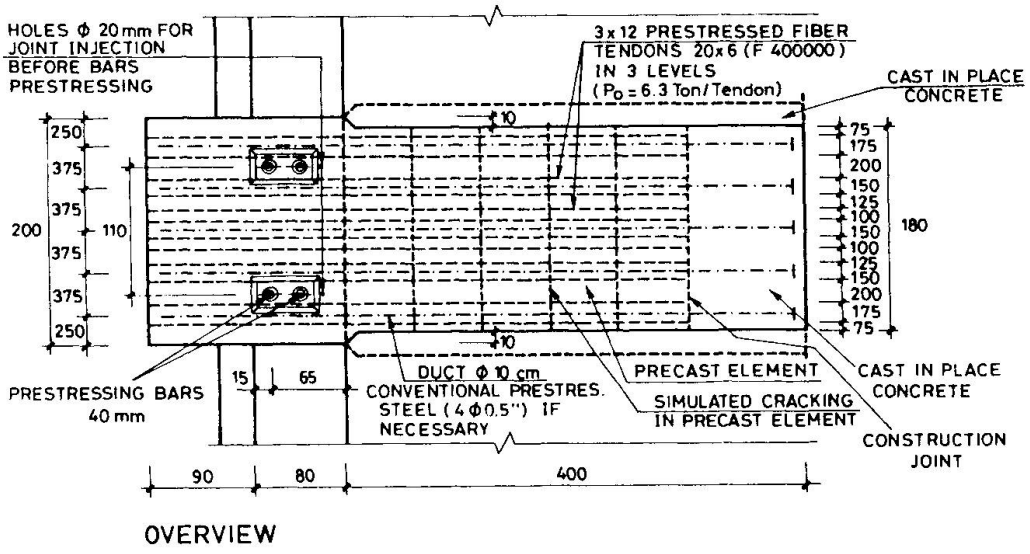

Figure 1

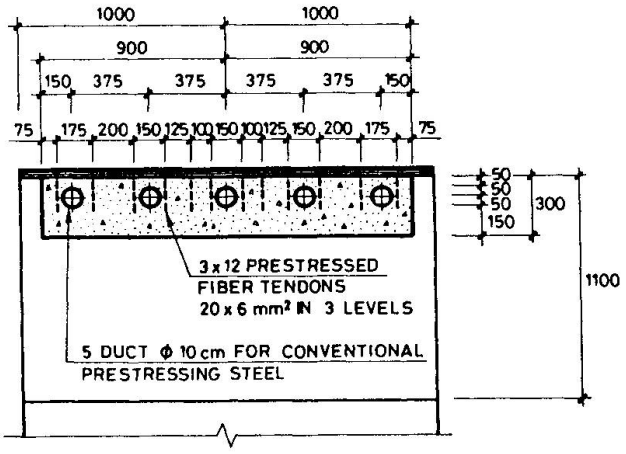

Figure 2

Structures en béton armé de fibres

Faserbewehrte Betonbauten

Fibre Reinforced Concrete Structures

X. DESTREE
Eurosteel
Bruxelles, Belgique

M. PROVOST
Bureau d'études bédrac
Bruxelles, Belgique

J.J. DEVILLERS
Bureau d'études bédrac
Bruxelles, Belgique

1. INTRODUCTION

Le béton armé de fibres (B.A.F.) connu depuis plusieurs années est appliqué dans des sols industriels en béton, des dallages portuaires, des revêtements routiers, l'industrie de préfabrication et les bétons de fondations.

Les recherches des milieus industriels et scientifiques visent à étendre à terme cette utilisation à des pièces structurelles telles que des colonnes, des voiles, ...

2. APPLICATION AUX OUVRAGES DE SUPERSTRUCTURE : COLONNES ET DALLES

L'évaluation de l'accroissement de résistance à la compression du B.A.F. en fonction de la teneur en fibres et des caractéristiques mécaniques des matériaux a été décrite dans diverses théories. Des essais d'écrasement sur cubes montrent qu'en fait cet accroissement tantôt imperceptible, tantôt significatif est fonction des matériaux, de la géométrie de l'éprouvette et des conditions de mise en oeuvre.

Nous avons procédé en 1989 à des essais comparatifs sur 2 x 3 colonnes en B.A.F. et en béton non armé sollicitées par un effort de compression agissant au bord du noyau central pour simuler des défauts de pose. Ces essais n'ont mis en évidence aucun accroissement de résistance dû à la présence des fibres. Le mode de rupture des colonnes en B.A.F. s'est avéré de type ductile contrairement au caractère brutal de la rupture des colonnes non armées. Les charges de rupture étaient à peu près équivalentes.

Une réalisation de ce type est actuellement projetée dans un grand bâtiment à Bruxelles.

Par ailleurs, suite à des essais de flexion en laboratoire, une dalle en béton armé a été exécutée dans un bâtiment en réduisant sensiblement les barres structurelles par l'emploi de B.A.F. L'examen de cette dalle en service montre un comportement exempt de toute fissure apparente.

3. APPLICATIONS AUX OUVRAGES D'INFRASTRUCTURE : PIEUX ET PAROIS

Plusieurs ouvrages de fondations spéciales (pieux, parois moulées, barettes, ...) ont été réalisés suivant le procédé SOLFIBRES qui consiste à mettre en oeuvre un B.A.F. d'acier EUROSTEEL spécifique pompé sous pression pour les pieux moulés dans le sol à l'aide de machines à tarière creuse.

Ce procédé agréé par les sociétés de contrôle technique (Socotec, Véritas, Séco, ...) est appliqué quotidiennement. A ce jour, 3.000 pieux de 10 à 35m de longueur sont en service.

Des essais comparatifs de flexion pratiqués sur pieux armés, tantôt de fibres, tantôt de barres ont mis en évidence la capacité de déformation plastique du béton armé de fibres permettant de grands déplacements et, par conséquent, une meilleure mobilisation de la réaction du sol.

Les fondations en béton armé de fibres semblent donc particulièrement adaptées aux problèmes d'efforts horizontaux, en particulier lorsqu'ils proviennent de déformations relatives au sol.

Des abaques de dimensionnement ont été dressées permettant de définir le domaine des sollicitations admissibles d'un pieu en béton armé de fibres de caractéristiques géométriques et mécaniques données.

Enfin, une recherche en cours confirme le grand intérêt du renforcement par fibres dans les applications où les sollicitations de séisme sont considérées.

4. CONCLUSION

L'emploi du B.A.F. pour des ouvrages structuraux tels que précités exige une mise en oeuvre particulièrement soignée de manière à obtenir une répartition de fibres adéquate et une conformité parfaite avec les spécifications du procédé.

Des machines d'intégration des fibres et de préparation du B.A.F. ont été développés.

En ce qui concerne le contrôle, EUROSTEEL utilise une unité mobile de contrôle du béton frais sur chantiers. Cette unité informatisée produit en 45 minutes les résultats exploitables suivants : courbe granulométrique, ouvrabilité, teneur en fines, teneur en fibres, masse volumique, rapport eau/ciment. A l'état durci, un contrôle précis de la répartition des fibres est possible par rayons X sur des carottages.

Dans ces conditions, le B.A.F. maîtrisé constitue bien souvent une solution avantageuse en raison tant de ses performances techniques qu'économiques.

Fibre végétale comme matériau de renforcement de l'adobe

Pflanzenfasern zur Bewehrung von Lehmriegelbauten

Vegetal Fibre as Reinforcing Material in Adobe Construction

C. NACARINO MONZÓN
Dr. sc. agronomiques
Univ. de la Molina
Lima, Pérou

1. Introduction

La construction en terre figure, sans aucun doute, parmi les solutions privilégiées qui permettront de résoudre l'immense problème de la croissance considerable de la population auquel sont confrontées des villes et de nombreuses régions rurales de tiers-monde.

2. Objectif

L'objet de la communication synthétise les résultats obtenus pour le cas particulier des "adobes", le rôle du renfort mécanique assuré par des fibres végétales incorporée dans une matrice de terre.

3. La matrice: préparation et essais

A cet effet on a pris trois sols disponibles provenant de la région de Gembloux. Afin de tendre vers la granulométrie idéale on a effectué des corrections en utilisant la méthode arithmétique des proportions. Les diagrammes des essais de compression et flexion montrent que le comportement est linéaire jusqu'à la rupture mais après fissuration le matériau perd toute sa structure et sa résistance devient nulle.

4. La fibre: essais effectués

On a utilisé de la paille d'orge, de riz et de froment. Les résultats montrent que la résistance à la traction et le module de déformation ne présentent aucune différence significative.

5. Le matériau terre-fibre

5.1. Adhérence terre-fibre

Les résultats permettent de conclure que l'adhérence des fibres à la terre semble assez faible et il serait judicieux de pouvoir en améliorer les performances.

5.2 Influence du dosage de fibres

On a testé 2 gammes de dosage en fibres couramment utilisées dans la pratique. Le plus faibles vont de 4 à 5 Kg de paille/m3 de terre et les plus importants de 20 à 30 kg de paille/m3. On a

essayé pour chaque catégorie la teneur moyenne ainsi qu'une valeur supérieure et une inférieure.

- La contrainte de rupture: pour les faibles dosages on peut conclure pour l'égalité de ces valeurs avec le module de rupture de la terre seule. Pour les dosages supérieurs cette égalité n'est plus respectée et il se produit même un affaiblissement des modules de rupture.

- La contrainte post-fissuration augmente avec le dosage.

- La déformation à la rupture: ce comportement est linéaire, cependant aux différentes teneurs en fibres correspondent des droites d'angulation différentes.

5.3. Influence de la longueur de fibres

Trois longueurs sont testées: 10, 15 et 20 cm.

- La contrainte de rupture: il n'y a pas de différence significative entre ces trois valeurs et la résistance de la terre seule. La paille ne rigidifie pas la matrice et la longueur de fibres n'influence pas ces valeurs.

- La déformation à la rupture: jusqu'à la fissuration de la matrice les trois cas ont le même comportement.

- Le comportement post-fissuration: la charge post-rupture varie proportionnellement à la longueur de fibres.

5.4 Influence de l'orientation des fibres

On a testé deux dosages: Vf=0.73% et Vf=2.31% avec L=15cm .

Pour le dosage Vf=0.73% l'orientation longitudinale présente les meilleurs résultats mais la situation est inverse après fissuration de la matrice.

Pour le dosage Vf=2.31% on a observé une situation similaire tant à la rupture qu'après fissuration; cependant, l'orientation planaire en tout sens donne de valeurs inférieures aux minimus recommandables.

6. Conclusions

-Le renfort apporté par les fibres n'intervient qu'après la formation des premières fissures.

-Par la similitude des modules de déformation, la paille ne rigidifie pas la terre mais agit après la rupture en maintenant ensemble les différents fragments de l'adobe.

-Les dosages de 15 à 30 gr. de fibre (0.36 et 0.73% de volume des fibres) sont les plus favorables et respectent les normes minimales de résistance.

-Le mélange à la matrice des fibres sans orientation précise est moins favorable que l'orientation parallèle à la direction principale des sollicitations.

Capacity of Truss Tension Members via High Strength Strands

Résistance d'éléments de poutre à treillis tendus à l'aide de torons à haute résistance

Tragwiderstand von Zuggliedern mit Spannlitzen hoher Festigkeit

J.J. PULLARO
Principal
Lichtenstein & Assoc.
Fiar Lawn, NJ, USA

Bala SIVAKUMAR
Project Eng.
Lichtenstein & Assoc.
Fiar Lawn, NJ, USA

The Walnut Street Bridge crossing the Tennessee River in the City of Chattanooga, Tennessee is a pin connected Camelback Pratt Truss and has the distinction of being the oldest surviving Bridge across the 2400km mile river. The Bridge was designed by a noted consulting engineer, Edwin Thatcher of Louisville, Kentucky, with construction completed in 1891. The structure replaced ferry service and helped to unite both banks of the River during the time of great economic growth in the city. The bridge is 722m in length, with a 238m iron viaduct forming one approach. Six (6) truss spans cross the river channel, three (3) spans at 64m and three (3) spans at 98m. The trusses range from 11.6m to 14.6m deep. The Roadway width is 5.5m, with two (2) 1.5m sidewalks provided. After the construction of the nearby Market Street Bridge in 1917 the bridge saw a decrease in usage. The structure was rehabilitated on various occasions including the replacement of the timber superstructure with steel stringers and an asphalt wearing surface. In 1974, in an attempt to strengthen certain eye bars, U-shaped steel bands were wrapped around the heads. The bridge was eventually closed to all traffic in 1978 due to concerns about its structural integrity.

In the 1980's there began a community spirit to rehabilitate the structure to serve as a Pedestrian Bridge and linear Park. Contributions were raised from private citizen groups and together with a grant from the Federal government and funds from the City, the project became a reality. It is expected the rehabilitated structure will be extensively used for festivals, exhibits, etc. and be a focal point for the resurgence of the river front. In the future the bridge will also be used as a crossing for a trolley system planned by the City. Extreme care in restoring as many historic details as possible would be required as the Bridge is of significant historic value and is eligible for inclusion on the National Register of Historic Places.

The task of restoring the Bridge includes many details including pier, deck and railing work. The major work however and the focus of this paper is to describe the method selected for strengthening the truss members, in particular the tension chords.

Steel eye bars make up the bottom chord and tension diagonals. The bars are in pairs and are up to 15cm x 3cm in section. A maximum of four (4) bars are used in the lower chord. The compression members including the top chord and verticals are composed of steel shapes (either angles or Z's). Existing information indicated low carbon steel was used for all tension members with an allowable design load of 1.1×10^8 Pa.

Inspection and Testing

An in-depth inspection of the trusses showed losses due to rusting and pitting at the eye bar heads to be a common condition. The inspection also revealed the presence

of numerous dimples or concave depressions of unknown origin in the head and neck of the eye bars at a large number of the lower joints. No significant losses were noted in the main body of the eye bars. Ultrasonic investigation of the eye bars did not reveal the presence of any cracks. Field metallography and chemical analysis confirmed the presence of low carbon steel. The structure was strain gauged utilizing an actual truck and results compared to theoretical values. Measured strains in the tension members were compared to computed values with the results considered consistent with actual behavior of trusses of this age.

Truss Strengthening

The maximum computed stress in the eye bars under existing dead load is 8.0×10^7 Pa. In light of the condition at the eye bar heads it was decided that the maximum allowable stress in the eye bars should be limited to the existing levels, which the trusses have safely sustained. It was also considered prudent to build in redundancy into the truss tension members since many eye bars have existing flaws that may initiate cracks in a fracture critical member.

Conventional strengthening of the truss members by adding reinforcing members was first investigated. Due to the large number of members to be reinforced and the difficulty in providing attachments to the closely packed members, this alternate was rejected. Additionally the final stresses in the eye bars would certainly be higher than the current level as the new and old members would share the applied loads.

A system of post-tensioning the trusses was then explored. The possibility of relieving the eye bars of a large portion of their existing dead load would free up capacity needed to support future live loading. In addition post-tensioning would introduce redundancy in the tension members by providing an alternate load path via the strands.

A system of straight and deflected strands was selected for the post-tensioning. The strands were placed to coincide with the bottom chords and the diagonals fanning away from the mid-span. The strands were deflected at certain lower joints by wrapping them over specially constructed saddles attached to the lower joint pins. Dead anchors secured the strands to the bearing pins and the upper joint pins. Tensioning of the strands is to be performed at the lower chord level via jacking station assemblies which are to be left in place should any adjustments be required in the future.

The strands are 1.5cm diameter Grade 270 coated prestressing strands and are installed in pairs. The post-tensioning stress introduced into the strands is 5.1×10^8 Pa or less and results in an equal reduction of force in the eye bars. The strands constitute an internal system of post-tensioning and do not affect the forces in members that are not in line with the strands. The live load stress due to pedestrian loading will be shared by the strands and the eye bars in proportion to their stiffnesses. The eye bars being much stiffer than the strands will pick up most of the live load stress. Under full live load the eye bars will experience stress no greater than 8.0×10^7 Pa. Under proposed dead load the stress in the eye bars is reduced to less than 3.45×10^7 Pa, the remainder of the dead load being in the cables.

The cost for installing the strands on twelve (12) trusses is estimated at $350,000. A total of 4880m of strands is required. Construction is to start in mid 1990 and be completed by February 1991, the 100th anniversary for the structure.

In summary, it is believed this system of installing strands to add to the load carrying capacity of tension members is a simple and economical method. Post tensioning allows for rehabilitation of structures not otherwise capable of being upgraded, as conventional methods are difficult and expensive to accomplish because of size, access and connection constraints at the pins.

Einsatz von Faserverbundwerkstoffen als Erdanker

Use of Fibre Glass Composites for Soil Anchors

Utilisation de matériaux composites renforcés de fibres pour des ancrages

Reinhard WOLFF
Strabag Bau-AG
Köln, BR Deutschland

H.-J. MIESSELER
Dipl. Ing.
Strabag Bau-AG
Köln, BR Deutschland

1. EINLEITUNG

Glasfaserverbundstäbe, wie sie als HLV-Spannglieder bereits für vorgespannte Konstruktionen Anwendung finden, lassen sich auch auf dem Gebiet der Erd- und Felsanker vorteilhaft einsetzen. Insbesondere die Möglichkeit der Integration von Sensoren schon unmittelbar während des Produktionsvorganges der Glasfaserstäbe, eröffnet die Möglichkeit der permanenten Kontrolle solcher Anker.

2. ERDANKER AUS GLASFASERVERBUNDWERKSTOFF

Die grundsätzliche Eignung von Glasfaserverbundwerkstoff als Vorspannelement, alternativ zum konventionellen Stahl, zeigen eindrucksvoll die bereits ausgeführten Brückenbauwerke wie die Straßenbrücke Ulenbergstraße in Düsseldorf und die Fußgängerbrücke zum Freizeitpark Berlin-Marienfelde.
Mit der Entwicklung von Erdankern aus Glasfaserverbundwerkstoff wird nun die Palette der Anwendungsmöglichkeiten dieses im Bauwesen doch neuartigen Materials erweitert. Folgenden Eigenschaften machen diesen Werkstoff hierfür interessant:

- der E-Modul erreicht mit 51.000 N/mm² nur ¼ desselben von Stahl, das wiederum bedeutet, daß der Einfluß des Bodenkriechens um den Faktor 4 kleiner ist
- da das Material bis zum Bruch elastisch bleibt, sind auch bei größer werdenden Verformungen des Boden durch Plastifizieren noch Rückstellkräfte im Anker vorhanden
- das geringe Eigengewicht des Stabmaterials bedeutet eine wesentliche Arbeitserleichterung insbesondere an Steilhängen und im Gebirge
- für den Korrosionschutz sind keinerlei Mehraufwendungen erforderlich
- infolge der elektromagnetischen Neutralität sind die Anker unempfindlich gegen Streuströme von Gleichstrombahnen

Der größte Vorteil gegenüber den bisher eingesetzten Erdankern aus Stahl besteht darin, daß die Glasfaserstäbe schon während der Produktion mit einem Lichtwellenleiter ausgerüstet werden können. Im eingebauten Zustand läßt sich nun das Kräfte und Verformungsspiel auf der gesamten Länge in einem solchen Erdanker von der Luftseite her permanent überwachen.

3. SENSORTECHNOLOGIE

Lichtwellenleiter, wie sie in der Nachrichtentechnik in erster Linie der Signalübermittlung dienen, zeichnen sich durch ihre hervorragende Lichtdurchlässigkeit aus. Der hierbei unerwünschte Effekt der Lichtdämpfung infolge einer mechanischen Beanspruchung wird im Falle der Bauwerksüberwachung als Sensoreigenschaft ausgenutzt. Im Gegensatz zur Nachrichtentechnik gehen die Bemühungen bei der Entwicklung des Lichtwellenleitersensors dahin, ein möglichst großes Meßsignal infolge von mechanischen Änderungen im Lichtwellenleiter zu erzeugen.
Der Gradienten-Lichtwellenleiter mit einer vom Radius des Kerns abnehmenden Brechungszahl wird im Regelfall für solche Sensoranwendungen eingesetzt. Der innere Kern wird von einem äußeren Mantel umgeben, an dem die Reflexion des Lichtes stattfindet. Er ist ebenfalls lichtdurchlässig, aber mit einer geringeren Brechungszahl. Wird ein Lichtstrahl durch einen Lichtwellenleiter geleitet treten im Bereich von Mikrokrümmungen Streuverluste auf. Dieser entstehende Lichtverlust wird meßtechnisch als Dämpfungsänderung in dB (Dezibel) angegeben. Indem der Lichtwellenleiter mit einer dünnen Drahtwendel versehen wird, macht man sich die Erkenntnis zunutze, daß Mikrokrümmungen auch infolge radialen Druckes erzeugt werden können. Bei Zug in Längsrichtung drückt die Drahtwendel ab einer bestimmten Schlaglänge radial auf den Lichtwellenleiter und erzeugt an ihm Mikrokrümmungen, die dann entsprechende Dämpfungsänderungen verursachen.

4. ERDANKERVERSUCHE

Für praktische Versuche mit diesen Glasfaserankern wurde im Jahre 1982 in Rheinbach ein Versuchsstand eingerichtet. Es handelt sich hierbei um eine gegen den Boden verankerte Verbauwand. Der hier anstehende Boden besteht aus mitteldicht gelagerten Kiesen und Sanden. Die Anker, sie waren im Mittel 10 m lang, wurden für Gebrauchslasten von 245 kN bzw. 408 kN ausgelegt. Das die Versuche begleitende Meßprogramm, überwacht und begutachtet von Prof. Nenzda, Essen, zeigte die grundsätzliche Eignung dieser neuen Ankertechnik. Als wichtigstes Ergebnis dieser Versuche zeigte sich, daß die hohe Dehnfähigkeit des Ankers einem Abfall der Spannkraft entgegenwirkt. Nach Abschluß der Versuchsserie wurden die Anker freigelegt und ebenfalls geprüft.

Ein zweiter Versuchsstand zur Durchführung von Langzeitversuchen wurde in Langenfeld eingerichtet. Die hier eingesetzten Anker bestehen aus 8 bzw. 14 Glasfaserstäben und sind für Gebrauchslasten von 240 kN bzw. 420 kN ausgelegt. Die Messungen, die sich über einen Zeitraum von nahezu 3 Jahren erstreckten, zeigten bei beiden Ankertypen einen Spannkraftverlust von ca. 4%.

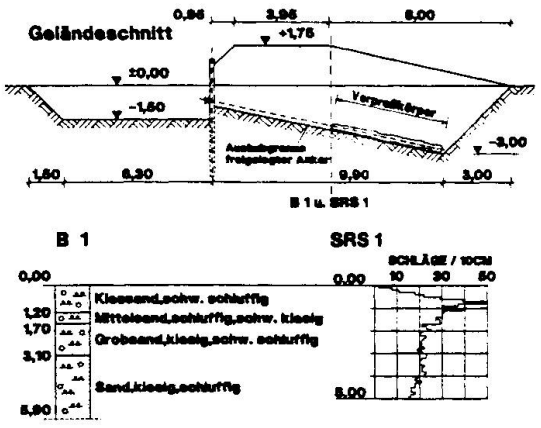

Bild 1: Verankerte Spundwand
Versuchsstand Rheinbach

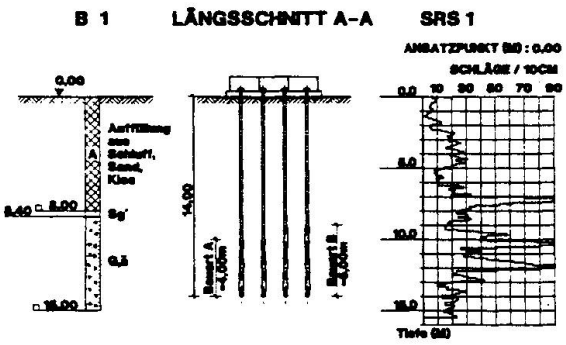

Bild 2: Langzeitversuche
Versuchsstand Langenfeld

In Situ Investigations on Soil Anchors

Examen in situ de bêches d'ancrage

In Situ Untersuchung von Grundarkern

Godfried DERVEAUX
Man. Dir.
Ingenieursbureau
Gent, Belgium

Luc TOUSSEYN
Project Mgr
Ingenieursbureau
Gent, Belgium

On the occasion of an important tunnelling project in Belgium (Liefkenshoektunnel, Antwerpen), a building excavation has been carried out with an anchored steel sheet piling. The wall anchorage is realized by means of steel soil anchors with tendons. In order to do some tests in situ, three of the steel soil anchors are replaced by GRP soil anchors. The construction is of a temporary nature (about 18 months).
The lab tests turned out to be very promising. The in situ investigations will be continued until the end of 1990. However, the first results prove to be very promising.

2. PROPERTIES OF THE ANCHORS

The soil anchors consist of 15 mm or 10 mm GRP rods made of glass fibre reinforced vinylester.

2.1. Test anchors in lab

Pull tests were carried out on two different types of anchors, i.e. :
- 1 anchor consisting of 19 x 10 mm rods;
- 1 anchor consisting of 12 x 15 mm rods.

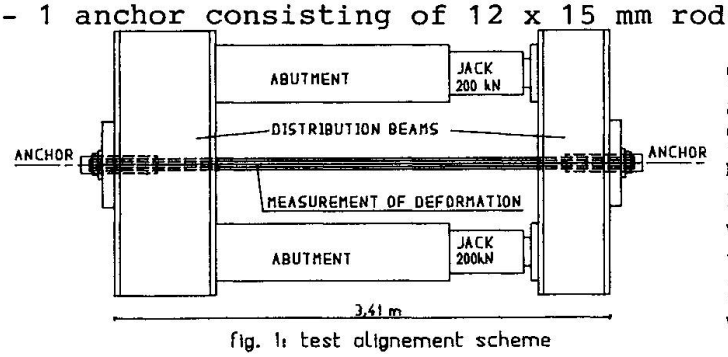

fig. 1: test alignement scheme

The rods were anchored in a purpose-made anchor head. This required a special mixture of resin and fillers. The test anchors were about 3.50 m long. In the middle of the free rod length some strain gages were applied (see fig. 1).

The tensile force was gradually increased; at a loading rate of approximately 50 kN per minute. Each loading step was followed by a pause of about three minutes. When a total load of 600 kN had been achieved, a 15 minutes' pause was introduced.

The first test has been carried out on the 12-rods system, the second test on the 19-rods system. The load-deformation diagrams are shown in fig. 2 and fig. 3.

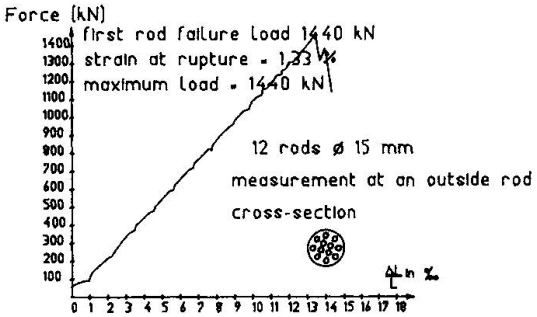

fig.2: load-deformation

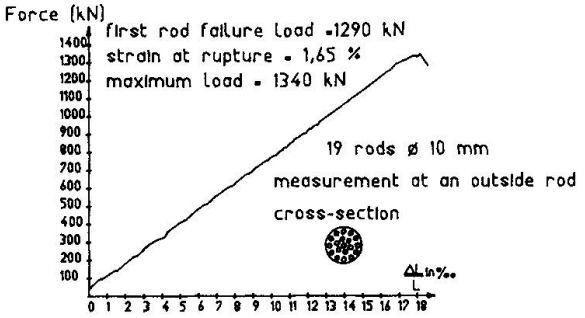

fig.3: load-deformation

2.2.Test anchors in situ

The fabricated anchors are of the same type as those described in 2.1 : - 1 anchor of 19 10-mm rods;
- 1 anchor of 12 15-mm rods;
- 1 anchor of 3 15-mm rods + 16 10-mm rods.

The anchors are to withstand a useful tensile force of 570 kN (see fig. 4). Soil anchorage is realized by means of VHP (very high pressure) grouting (see fig. 4).

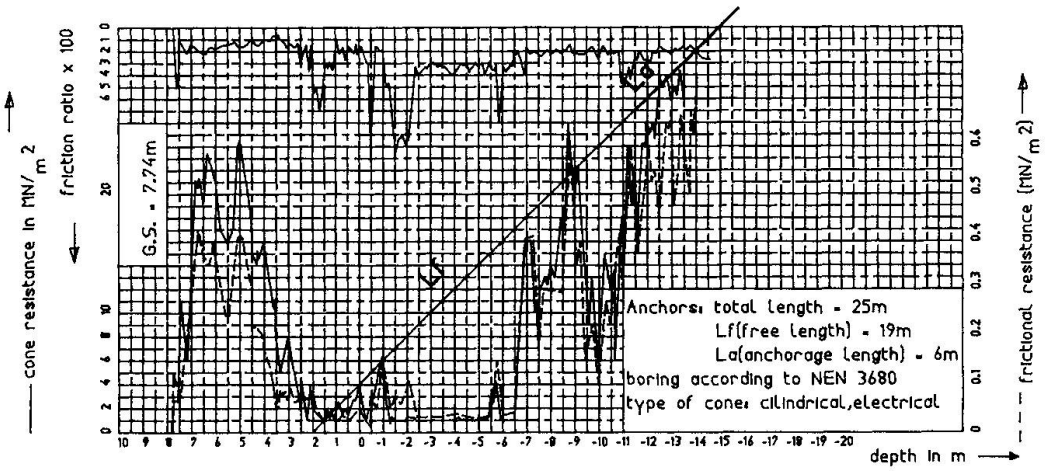

fig.4:cone penetration test with measurement of the local side friction

The anchors have been placed in the beginning of May 1989 and tightened at the end of the month. They have been tightened up to 1.5 times the service load and fixed at 1 time the service load. Early January 1990, one anchor has been checked and a remaining tensile force of 600 kN has been measured ! When increasing the force to 1,130 kN, the anchor did not fail (the theoretical maximum value is 1,200 kN). So, this first result means there has been no degradation in strength of the anchors. Further results will be available by mid 1990.

Epoxy Bonded Steel Plate Method for Repairing Deteriorated Slabs

Réparation de dalles en béton à l'aide de plaques d'acier collées à la résine époxyde

Reparatur von Stahlbetonplatten mit Epoxy-geklebten Stahlblechen

Keiichiro SONODA
Professor
Osaka City Univ.
Osaka, Japan

Shigeyuki MATSUI
Associate Professor
Osaka, Univ
Osaka, Japan

Hidenao HAYASHI
Chief Research Engineer
Hanshin Expr. Publ. Corp.
Oasaka, Japan

1. INTRODUCTION

In Japan, for repairing cracked and damaged RC decks of bridge, several methods have been developed. Among them, Epoxy Bonded Steel Plate Method is most familiar. The method is of a reinforcement by bonding a thin steel plate to the bottom surface of deteriorated deck with the aid of adhesion of epoxy resin. The repaired deck behaves like a steel plate and concrete composite slab. A main advantage of this method is that the repair work can be done without stopping a traffic service on deck. This method is executed through the following steps: (1) Holes in the bottom surface of RC deck are made and an anchor bolt is inserted into each hole. (2) A sheet of thin steel plate with a certain width is installed in the anchor bolts with keeping a clearance for epoxy resin grouting layer. (3) After all edges of steel plate are sealed with a sealing material, epoxy resin is grouted by an injection pump. The main purpose of this study is to examine reliability of the method. For sake of this, static and fatigue tests of repaired and non-repaired slabs of model composite girder bridges were carried out under vehicle loadings.

2. METHOD OF EXPERIMENT

The tests slabs supported by a twin girder bridge spanning over 3.6m have 8cm thick, main re-bars in 10cm pitch and distribution re-bars in 15cm pitch, which were modeled to an existing RC deck slab on a typical highway road bridge in Japan. A full size truck cyclically running on six composite girder bridges arranged on a circular test road was used, as shown in Photo. 1. Three steps of tests were carried out. The first was static tests by a central patch load on the slabs. The second was fatigue loading tests before repairing, in order to give some degrees of deterioration to the slabs. The third was fatigue loading tests after repairing. Through those steps, the mechanical behavior of repaired and non-repaired slabs was examined, in particular on cracking pattern, debonding of steel plate, degradation of stiffness and so on. The six test slabs named No.1 to No.6 have the same sizes and reinforcements. The load intensity of truck rear wheel in running was set to 51kN for slabs Nos.1, 3 and 5 and to 42kN for slabs Nos.2, 4 and 6. Slabs Nos.1,2,3 and 4 were repaired after a finite number of loading cycles. Slabs Nos. 5 and 6 remained non-repaired for monitoring. The higher load intensity of rear wheel applied were corresponding to about 1.5 times as large as an equivalent design load specified by the Japanese code [1].

3. RESULTS

Figure 1 shows variations of elastic deflection under the central rear wheel load, which mean the degradation of stiffness of slab. Non-repaired slab No.5 collapsed at about 160000 cycles, and slabs Nos. 1 and 3 with the same loading condition as No.5 were repaired at 17000 and 160000 cycles, respectively. While, slabs Nos.2 and 4 subjected to a lighter loading condition were repaired at earlier stages of 5000 and 17000 cycles, respectively. All test slabs except No.5 did not collapse until 600000 cycles when the tests ceased.

Photo.1 Test View

The collapse mode occurred in slab No.5 was like a punching shear mode without fracture of re-bars. By taking a view of the cross section sawn out after the tests were over, it was known that diagonal shear cracks in concrete might appear at earlier stage, but so severe debonding of steel plate to lead a shear bond failure soon was not seen yet, though only some of small parts of debonding of steel plate occurred from small cavities within epoxy resin layer, which seemed to be already made at the repair stage.

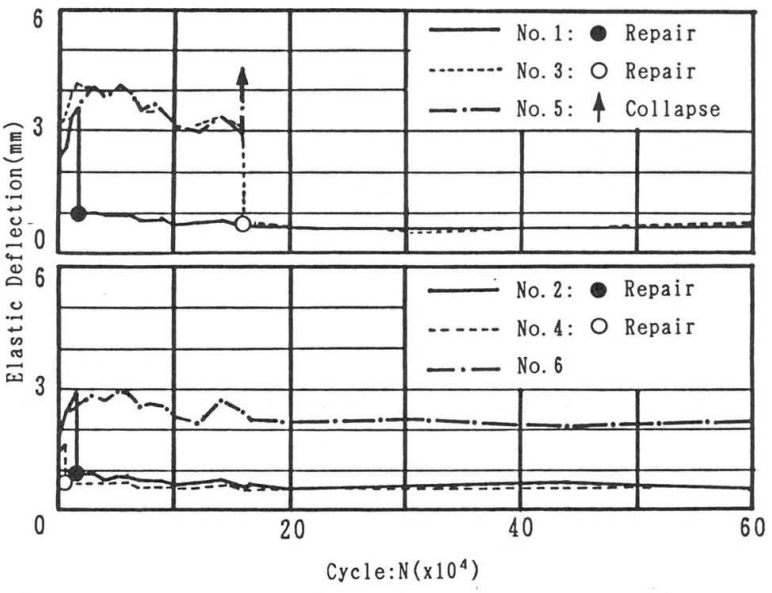

Fig.1 Relationship between Loading Cycle and Elastic Deflection at Center

4. CONCLUSION

1. Epoxy Bonded Steel Plate Method is reliable as a repair method for cracked and damaged RC slabs of bridge deck even at the stage of so severe damage as to cause diagonal shear cracks in concrete, provided that its careful work not to include any cavity in epoxy resin grouting layer is done.
2. Slabs repaired by the method behave as a full-composite slab consisting of compressive concrete and tensile steel plate.
3. Most of peeling or debonding of the steel plate are caused by initial cavities in epoxy resin grouting layer. So, careful work is required to raise reliability of the method.

REFERENCES

1. Japan Road Association, Specification for Highway Bridges. 1980.
2. SONODA, K., OKINO, M., HAYASHI, H. and KITA,H., Reliability of epoxy bonded steel plate method for repairing damaged RC slabs of bridge. Proceedings of JSCE, I-10, Oct. 1988. (in Japanese)

Load Transfer in Beams Strengthened by Means of Glued Steel Sheets

Transfert des efforts dans les poutres renforcées par des tôles d'acier collées

Kraftübertragung bei durch angeklebte Stahlbleche verstärkten Stahlbetonbalken

A. DEL RIO BUENO
Archit.
Instit. Eduardo Torroja
Madrid, Spain

J. ORTIZ HERRERA
Prof.
Politechn. Univ.
Madrid, Spain

Strengthening of R.C. beams by glueing steel sheets through thin epoxi resin layers is an usual technique that requires to analyze and solve load transfer problems between old and new part. Other way, reduced effectiveness and fragile failures phenomena may appear. The definition of an analytical model for evaluation of load transfer problems in this kind of elements requires the previous formulation of realistic and reliable constitutive laws for tangential behavior of interfaces steel-epoxi adhesive-concrete. In this sense, a good agreement with other authors experimental data can be obtained by using the expressions of **fig.1**, connecting local adhesion stresses (τ) to local slips (s). Curves resulting from their utilization are also observed in (**fig.1**).

Using proposed constitutive laws, a first 'approach' to the problem can be done by numerical simulation of 'pull-out' trials. Equilibrium and deformation compatibility conditions define a second order differential equation. Its numerical treatment provides information about interface ultimate situations: once known interface characteristics, for every steel sheet thickness, a maximum (relative) transferable load (N_{Tmax}/N_{RU}) and its corresponding maximum transfer length (L_{Tmax}) can be defined, independently of other parameters (**fig.2**). For most usual thickness in strengthening interventions, maximum transferable load is minor than ultimate tension load in the steel sheet ($N_{Tmax} < N_{RU}$). This evidences the relevance of load transfer problems.

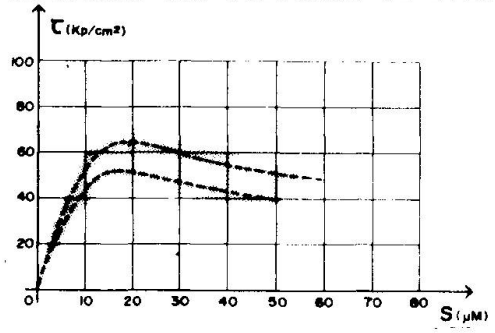

Asc $(0 \leq s \leq s_m)$: $\quad 50{,}0 \leq \tau\ (Kp/cm^2) \leq 67{,}5$

$\tau = \tau_{máx}\,[1 - [1 - \frac{s}{s_m}]^A] \quad 50{,}0 \leq \tau\ (\mu M) \leq 62{,}5$

$s_m = 18\,\mu M$

Desc $(s_m \leq s \leq s_u)$:

$\tau = \tau_{máx} \cdot e^{-B\,(s-s_m)^K}$

A = 2,00; B = 0,006; K = 1,05

FIG. 1

FIG. 2

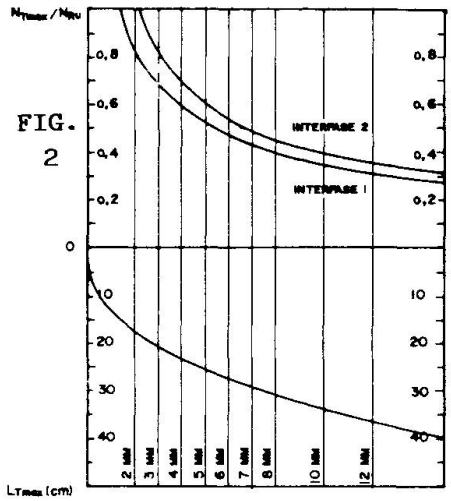

INTERFASE 1 τ_{max} = 50 k/cm², s_u = 50 μM		e_R (MM)	INTERFASE 2 τ_{max} = 67 k/cm², s_u = 60 μM	
N_{Tmax}/N_{RU}	L_{Tmax} (CM)		N_{Tmax}/N_{RU}	L_{Tmax} (CM)
0,85	18	2	1,00	17
0,68	21	3	0,80	21
0,59	24	4	0,68	23
0,52	26	5	0,61	26
0,47	29	6	0,54	28
0,43	31	7	0,50	30
0,40	33	8	0,46	32
0,36	35	10	0,41	35
0,31	37	12	0,36	37
0,27	39	15	0,31	39

A more refined study of load transfer problems in R.C. strengthened flexural elements can be based in composite girders theory. Its application provides equilibrium and deformations compatibility conditions (**fig.3**).

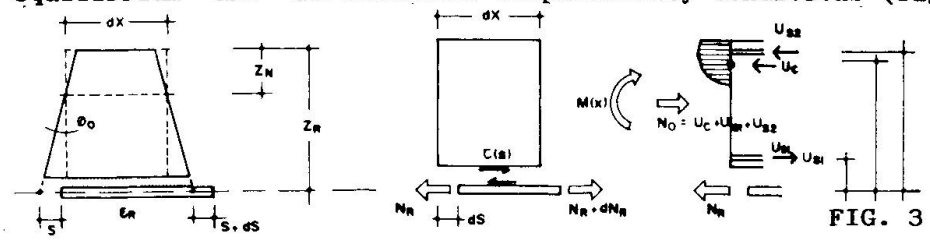

FIG. 3

(1) $\frac{dS}{dX} = \varepsilon_R - (Z_R - Z_N)\,\varphi_O$

(2.1) $\frac{dN_R}{dX} = b_R\,\tau(s)$

(2.2) $\frac{d^2N_R}{dX^2} = b_R \frac{d\tau(s)}{dS}\frac{dS}{dX}$

(3) $N_R(x) = b_m \cdot e_m \cdot \sigma_R(\varepsilon_R)$

(4) $N_R(X) = N_O(\varphi_O, Z_U, \varphi_{OP}, Z_U)$

(5) $M(X) = M_O(\varphi_O, Z_U, \varphi_{OP}, Z_U)$

The resulting five equations system (including two non-linear first order differential equations) is solved by using numerical methods. This analytical model defines for every considered situation the bond stresses and slips distribution along the interface, as well as tensile forces along the strengthening sheet. A good agreement with other authors test results has been found (**fig.4**)

Using the proposed general model, interface ultimate situations have been systematically analyzed for a big number of flexural strengthening configurations, including different sheet thickness, interface properties and geometrical and mechanical characteristics of pre-existing R.C. beam. Several conclusions related to transfer capacity of these interfaces have been obtained:

- Load transfer concentrates in reduced zones near the ends of the strengthening sheet. For interface ultimate situations, the extension of this zones of maximum transfer, approximately matches the corresponding maximum transfer length ($L_{T max}$), obtained in numerical simulation of 'pull-out' trial for the interface and sheet thickness considered.
- For interface ultimate situations, load transferred along each of these zones accords with maximum transferable load corresponding to considered interface and steel sheet thickness ($N_{T max}$).

Simultaneous consideration of previous conclusions allows the establishment of a simplified design model, able to define the necessary length of strengthening sheet to avoid load transfer mechanism collapse (**fig.5**). According to it, a double verification should be done:

FIG. 4

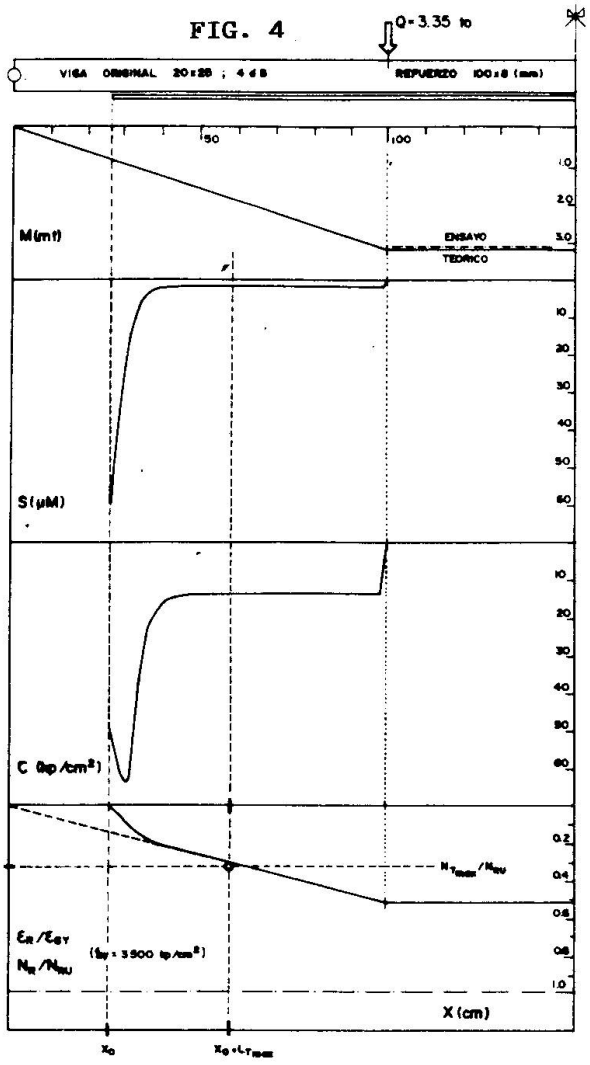

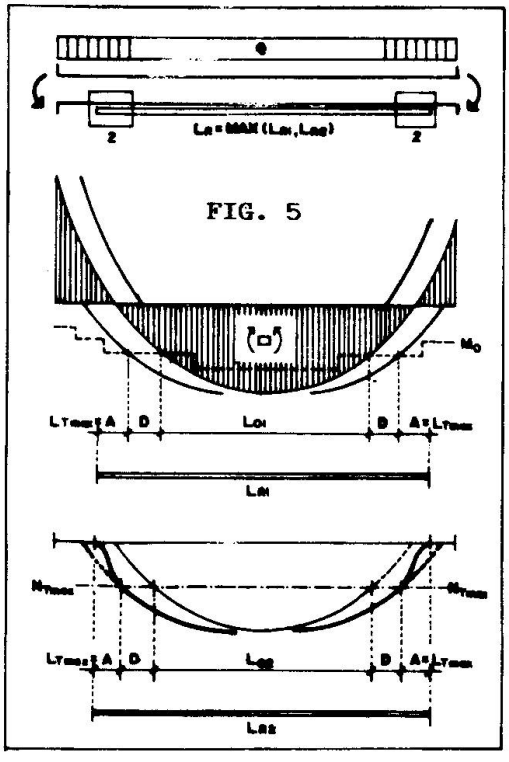

FIG. 5

- The disposition of strengthening steel sheet must be first analyzed as an ordinary Re-bar. Anchorage length should be considered equal to corresponding maximum transfer length ($L_{T max}$).
- A specific transfer check should be done that at a distance of the end of the sheet equal to corresponding maximum transfer length ($L_{T max}$), the required axial load in the sheet (admitting complete interaction with pre-existing beam) do not exceed the corresponding maximum transferable load ($N_{T max}$).

Both previous conditions define the needed extension of the strengthening sheet, and jointly with necessary analysis of critical sections of the beam, allow the complete design of this kind of strengthening interventions.